Imaging : making the invisible visible : proceedings of the symposium, 18 May 2000, Technische Universiteit Eindhoven

PROCEEDINGS

symposium

IMAGING

Making the invisible visible

Thursday 18 May 2000
Technische Universiteit Eindhoven

IEEE
Student Branch Eindhoven

Proceedings
symposium
Imaging
making the invisible visible

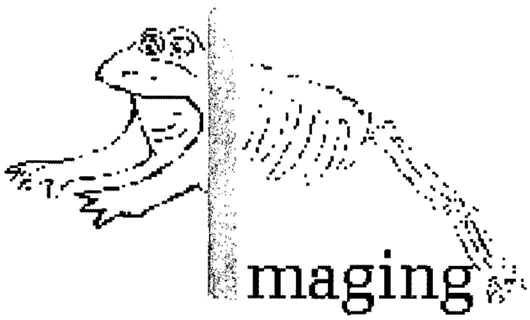

Thursday 18 May 2000
Technische Universiteit Eindhoven

years
IEEE student branch
EINDHOVEN

Preface

The rapid progress in computer technology has contributed immensely to fast growth and widespread use of Imaging techniques. It was this development that arouse our interest and made the choice for this years IEEE symposium topic easy: Imaging. After an introduction to the general concept of Imaging, the focus will be on current Imaging techniques in both the medical and the industrial field.

In the medical world, Imaging is used for research, diagnosis and surgery. The symposium presents two Imaging techniques for diagnosis: MRI and PET scan. Next to that improvements, like the conversion of current 2D to 3D images, enhancement of their resolution and provision of real time display, are presented. The opening lecture will show how these improvements are already applied in surgery for visualization of place and position of surgical tools.

The applications of the Imaging techniques in the industrial field are very diverse.

Imaging techniques for landmine detection are used to speed up the clearing of active mines, face recognition is used in security and the filled bottle inspector is used for inspection of filled bottles on small glass fragments.

To give everybody the opportunity to ask questions, the official part of the symposium will be concluded with a forum discussion. In the drink following the discussion, there is another possibility to exchange ideas with the speakers and colleague participants.

We hope all visitors and participants will enjoy the symposium as much as we enjoyed organizing it.

On behalf of the symposium committee,

Suzanne Jongen,

Chair

Program

9.00 **Reception with coffee**

9.30 **Welcome**

Dr. ir. J.B.O.S. Martens (IPO)

9.45 **Opening lecture**

Ph. D. Murat Eyuboglu (Middle East Technical University)

10.30 **Coffeebreak**

11.00 **Introduction lectures**

11.00 **"Digital Imaging and Image Processing, what it is all about."**

Dr. E.A. Hendriks (Delft University of Technology)

11.40 **"Virtual Reality in Medical Imaging-Guided Surgery"**

Dr. ir. F.A. Gerritsen (Philips Medical Systems)

12.20 **Lunch and Informationmarket**

13.30 **Parallel Sessions**

Parallel Session 1: Medical Applications

Parallel Session 2: Industrial Applications

16.10 **Forum**

17.00 **Drinks**

Program - Parallel sessions

Parallel Session 1

Medical Applications conducted by dr. ir. P.J.M. Cluitmans

13.30 "Positron Emission Tomography"

Dr. A.M.J. Paans (PET-Center, Groningen University Hospital)

14.20 "Magnetic Resonance Imaging Technique, Application and Perspective"

Dr. ir. J.M.L. Engels (Philips Medical Systems)

15.00 Coffeebreak

15.30 "New Technological Developments in 3D Medical Imaging"

Dr. ir. V. Rasche (Philips Medical Systems)

Parallel Session 2

Industrial applications conducted by dr. ir. J.B.O.S. Martens

13.30 "Sensor-fusion for anti-personnel land-mine detection"

Dr. J.G.M. Schavemaker (Electro-Optical Systems, TNO Physics and Electronics Laboratory)

14.20 "Filled Bottle Inspector"

Ir. A. v.d. Stadt (Eagle Vision Systems)

15.00 Coffeebreak

15.30 "Automatic Face Recognition"

Ir. C. Beumier (Signal and Image Center, Royal Military Academy)

Table of Contents

Preface 5
Program 6

Welcoming speech by Dr. ir. J.B.O.S. Martens 11
Opening lecture by Ph. D. Murat Eyuboglu 13
Digital Imaging and Image Processing what it is all about. 15
Virtual Reality in Medical Imaging for Image-Guided Surgery 25

Parallel Session 1 33
Positron Emission Tomography 35
New Technological Developments in 3D Medical Imaging 43
Magnetic Resonance Imaging, Technique, Application and Perspective 53

Parallel Session 2 59
Infrared processing and sensor fusion for anti-personnel land-mine detection 61
Filled Bottle Inspector FBI™ for inspection of filled bottles 73
Automatic Face Recognition 77

Sensaos: encounter the girl in the mummy 91
IEEE 99
Acknowledgements 101
Committee of recommendation 103
List of sponsors 105
The 2000 Symposium Committee 107

Welcoming speech by dr. ir. J.B.O.S. Martens

Biography

Dr. ir. J.B.O.S. Martens

Jean-Bernard Martens was born in Eeklo, Belgium, in 1956. He received the M.Sc. and Ph.D. degrees in electrical engineering from the University of Gent, in 1979 and 1983, respectively. His main research interest at the time was number theory, with applications in efficient algorithms for digital signal processing.
Since October 1984, he has been with the IPO, formerly the Institute for Perception Research, now the Institute for Human-System Interaction, of the Eindhoven University of Technology. His current research and educational interests are in computer vision and visual interaction.
This involves developing and testing new interfaces based on computer vision, image coding and processing based on mathematical models of the human visual system, and measurement and modeling of perceived image quality.

Opening lecture by Ph.D. Murat Eyuboglu

Biography

Ph. D. Murat Eyuboglu

Murat Eyuboglu received his B.Sc. and M.Sc. degrees in Electrical and Electronics Engineering from Middle East Technical University in Ankara Turkey, in 1983 and 1985, respectively. He received his Ph.D. from Sheffield University in England in 1989. Following his Ph.D., He joined the Department of Biomedical Engineering at Duke University in North-Carolina USA. Where, he was an Assistant Research Professor until 1993. In 1995-1996, He was Visiting Faculty in the Department of Radiology at University of Pennsylvania in Philadelphia - USA. Currently, He is an Associate Professor of Electrical and Electronics Engineering at Middle East Technical University.

Dr. Eyuboglu's research interest are focused on development and practical realization of new ways of Imaging, forward and inverse field problems in biomedical engineering, electrical impedance tomography and magnetic resonance imaging.

Biography

Dr. E.A. Hendriks

Emile Hendriks received his M.Sc and Ph.D. degree from the University of Utrecht in 1983 and 1987, respectively, both in physics. In 1987 he joined the electrical engineering faculty of Delft university of Technology as an assistent professor. In 1994 the became a member of the Information and Communication Theory of this faculty and since 1997 he is heading the computer vision section of this group as an associate professor. His interest is in low-level image processing, image segmentation, stereoscopic and 3D imaging, motion and disparity estimation and real time applications.

Digital Imaging and Image Processing what it is all about

Emile A. Hendriks
Information and Communication Theory Group
Faculty of Information Technology and Systems
Delft University of Technology

Abstract

Due to the rapid progress of video and computer technology, digital imaging and digital image processing has undergone a large growth in possibilities and applications in the last two decades. Nowadays digital imaging is playing a more and more important role in the broadcast world (digital television), medical world, consumer market (computer games), industry (inspection, control) and surveillance, among others.

In this introduction the basic concepts of digital imaging and image processing will be discussed. We will address the formation and representation of digital images and the different types of operations we can perform.

1 Introduction

Visual observation and interpretation plays a major role in human life. For 99% or more of the information received from our surroundings, we depend on our eyes. Since the rise of digital technology, one of the challenges is to develop a system that imitates the human visual system. Although we are far away from such a system, due to rapid progress of video and computer technology, digital imaging and digital image processing has undergone a large growth in possibilities and applications in the last two decades.

Personal computers are now powerful enough to capture and process image data. Affordable software and hardware is available for handling images, images sequences (video) and even 3D-visualization. Image processing is developing from a few specialized applications into a standard scientific tool.

Nowadays digital imaging is playing a more and more important role in the broadcast world (digital television), medical world, scientific research, consumer market (computer games), industry (inspection, control) and surveillance, among others.

In this paper we will discuss some basic concepts of digital imaging and image processing. For more detailed discussion lot of good books are available (see literature).

2 Digital Image Definitions.

An image can be seen as some measured physical quantity as a function of position.

This measured physical quality can for instance be the amount of radiation, which falls on a sensing area (e.g. X-ray, ultraviolet (UV) light, infrared (IR) light, and visible light). An example of an infrared image is shown in figure 1.

Figure 1. Example of an infrared image

In principle an image is a two dimensional (2D) projection of a three dimensional (3D) scene and therefore a function of two variables I(x,y). However with special imaging techniques like computed tomography (CT), nuclear magnetic resonance (NMR) or confocal microscopy also 3D images I(x,y,z) can be obtained. An example of a medical CT device and slices of a recorded brain and mid-ear are shown in figure 2. For the remainder of this paper we will restrict ourselves to 2D images.

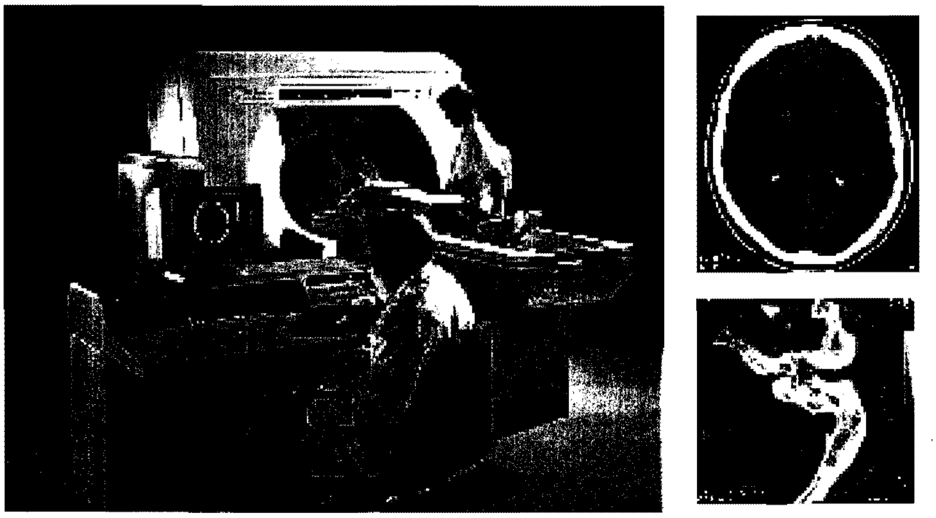

Figure 2. A medical CT device and a slice of a recorded brain and mid-ear

A digital image I(m,n) described in a 2D discrete space is derived from an analog image I(x,y) in a 2D continuous space through a sampling process that is usually referred to as digitization. The 2D continuous image I(x,y) is divided into N rows and M columns. The intersection of a row and a column is called a picture element or pixel. The discrete value assigned to a pixel I(m,n) (m = 0,1,2..M-1, n = 0,1,..N-1) is the average brightness over the area of the pixel, rounded to the nearest integer value. The process of representing the amplitude (e.g. brightness) of the 2D signal at a given coordinate as an integer value with L different gray levels is usually referred to as (amplitude) quantization. Common values encountered in digital imagery for M, N, L are given in table 1. For obvious reasons the number of columns M, the number of rows N and the number of amplitude levels is usually a power of 2. Assume that $L = 2^B$, where B is the number of bits for the binary representation of the amplitude levels, we speak of a binary image if B=1. We then distinguish only two different amplitude levels, which can be referred to, for example, as black and white. Images meant for human vision are usually 8 bit images (256 distinct levels) and are called gray level images (if no color is involved). Since human beings can only distinguish about 100 different gray levels, 8 bit it sufficient to represent all the visible details.

Parameter	Symbol	Typical Values
Columns	M	256,512,768,1024,1320
Rows	N	256,512,525,625,1024,1035
Grey Levels	L	2,64,256,1024,4096,16384

Table 1. Common values of digital image parameters

3 Image Operations

Depending on their output, operations on images can be divided into three classes: image processing, image analysis and image understanding. Image processing operations outputs another image, e.g. a sharpened image of the original. Image analysis operations outputs measurements, e.g. the area and perimeter of the objects in the image. Image understanding aims at a high-level description, e.g. a semantic description of what is visible in the image.

Image Processing

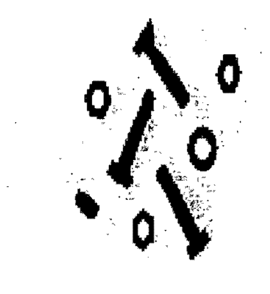

Image Analyses.

Object	Area	Parameter
1	956	197.9
2	352	38.2
3	340	37.4
4	960	213.8
5	432	98.9
6	956	209.1
7	288	73.1
8	312	33.5

Image Understanding

The image contains the face of Vincent van Gogh. His eyes, nose and left ear is visible. He has a beard and is looking downwards.

Note that graphics is more or less the opposite of image analysis: from a set of numbers, an image is generated. Image operations can be classified in a number of ways. One way to distinct them is based on the support region of the operation: point operations, local operations, object operations and global operations. Image operations can also be distinguished into linear and non-linear operations. In the following sections we will briefly describe the differences and will give some examples of their applications. For the illustration we restrict ourselves to gray value images but the idea can easily be extended to color images

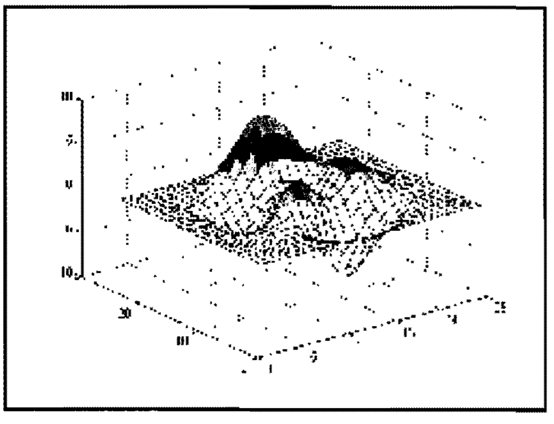

5 * sin(3w)	w^2
4.53	0.14
3.83	0.57
-1.29	1.29
-4.92	2.29
-2.88	3.57
2.49	5.14
4.98	7.00
1.73	9.14
-3.52	11.57
-4.71	14.29
-0.46	17.29
4.32	20.58

3.1 Point operations

A point operation takes a single input image into a single output image in such a way that each output pixel value only depends on its corresponding input pixel value. An example of an application is the adaptation of the range of the image grey values for better visibility of image details (stretching, see figure 3a and 3b).

3.2 Local operations

A local operation takes a certain neighborhood of input pixels of which the gray values define the gray value of the output pixel. This neighborhood can be any form or size, but is the same for every input pixel. Often an odd-sized rectangle is used (3x3, 5x5, 7x7, etc.). An example of a local operation is the Prewitt edge detector (see figure 3c). It calculates the summed differences in horizontal en vertical direction of a 3x3 neighborhood.

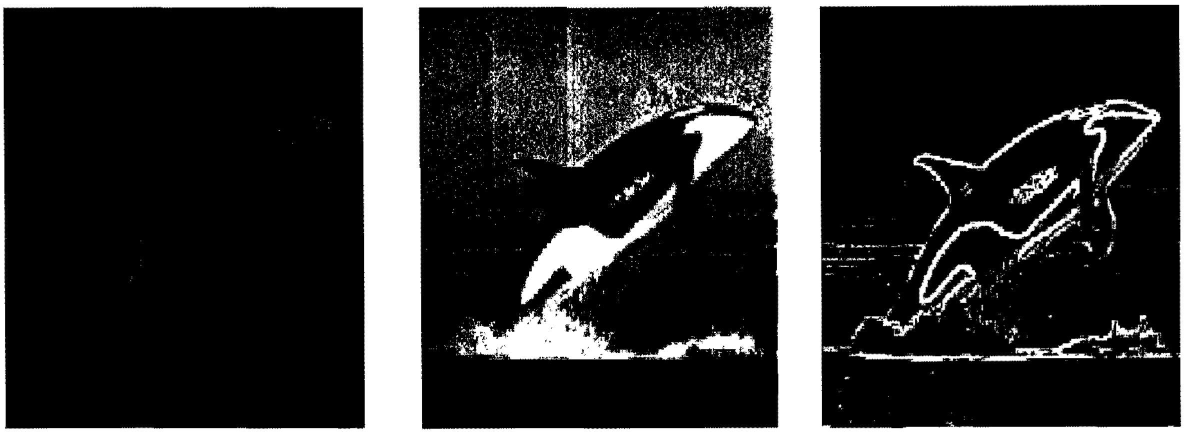

Figure 3. (a) Original image with low contrast (b) more details are visible after stretching (point operation) (c) Prewitt edge detection (local operation)

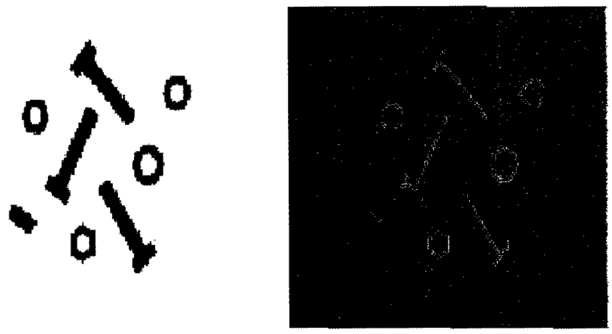

Figure 4. Skeleton detection of nuts and bolts

3.3 Object operations

Object operations are often used in image analysis. After having detected the objects in an image, the position and/or gray values of the object pixels determine the output value. Straightforward examples are area measurement or skeleton detection (see figure 4)

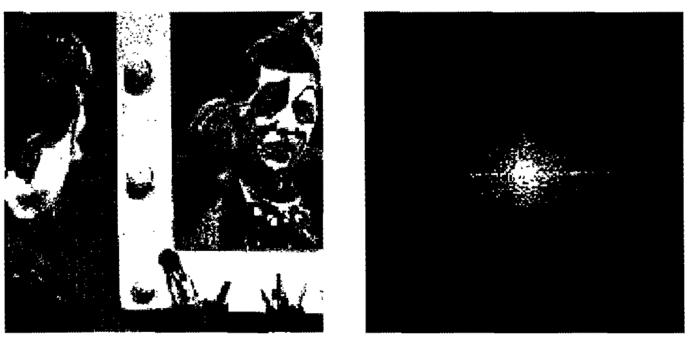

Figure 5. Image and its Fourier transform

3.4 Global operations

If the value of each output pixel depends on all input pixels the operation is said to be global. A wellknown global operation is the Fourier transform. A Fourier transform of an image decomposes the information in the image into spatial frequencies (see figure 5). Any change in an input pixel value will affect all output values

3.5 Linear image operations

If the output of an operation, performed on a linear combination of input images, is the same as the linear combination of the outputs of the operation on the individual input images, then the operation is said to be linear. For linear operations powerful mathematical tools are available, like Fourier analysis, which can be used for images as well. Under certain constraints linear image operations can be implemented as a (digital) convolution, also called convolution filtering. The output value for each pixel is equal to a weighted sum of neighboring pixels. The weights are usually represented in matrix form. An example is the uniform filter or averaging filter in which case all the weights are equal and sum up to 1 (see figure 6b).

3.6 Non-linear image operations

Every image operation for which the linearity property does not hold is said to be a non-linear image operation. Examples are the median filter (taking the median value of a certain neighborhood) or the max filter (taking the maximum value of a certain neighborhood). Median filtering can be applied for instance for removing impulse noise (see figure 6c).

$$\begin{pmatrix} \frac{1}{25} & \frac{1}{25} & \frac{1}{25} & \frac{1}{25} & \frac{1}{25} \\ \frac{1}{25} & \frac{1}{25} & \frac{1}{25} & \frac{1}{25} & \frac{1}{25} \\ \frac{1}{25} & \frac{1}{25} & \frac{1}{25} & \frac{1}{25} & \frac{1}{25} \\ \frac{1}{25} & \frac{1}{25} & \frac{1}{25} & \frac{1}{25} & \frac{1}{25} \\ \frac{1}{25} & \frac{1}{25} & \frac{1}{25} & \frac{1}{25} & \frac{1}{25} \end{pmatrix}$$

Figure 6. (a) Image corrupted by impulse noise (b) output after 5x5 uniform filtering (c) output after 3x3 median filtering

4. Imaging System

In figure 6 a typical architecture of an imaging system is depicted. The scene to be recorded is projected onto a sensor. The parameters that control this are governed by the image formation block and include lenses, light conditions, etc. The sensor takes care of the conversion of the physical quantity into numbers, the sampling process and the quantization. The output is raw image data in some format. Usually a preprocessing step is necessary to compensate for undesired sensor and image formation properties (e.g. non-linear relationship between physical quantity to be measured and image values, distortion due to non-ideal lenses, etc.). Depending on the application different routes can be followed.

4.1 Image enhancement

If the images are meant for visual inspection or just to look at, image enhancement can be applied. The goal of it is to let the images look nicer for optimal visual perception. This includes for example image sharpening and noise removal. It is well known that humans prefer images in which the contours of objects are enhanced (see example image processing).

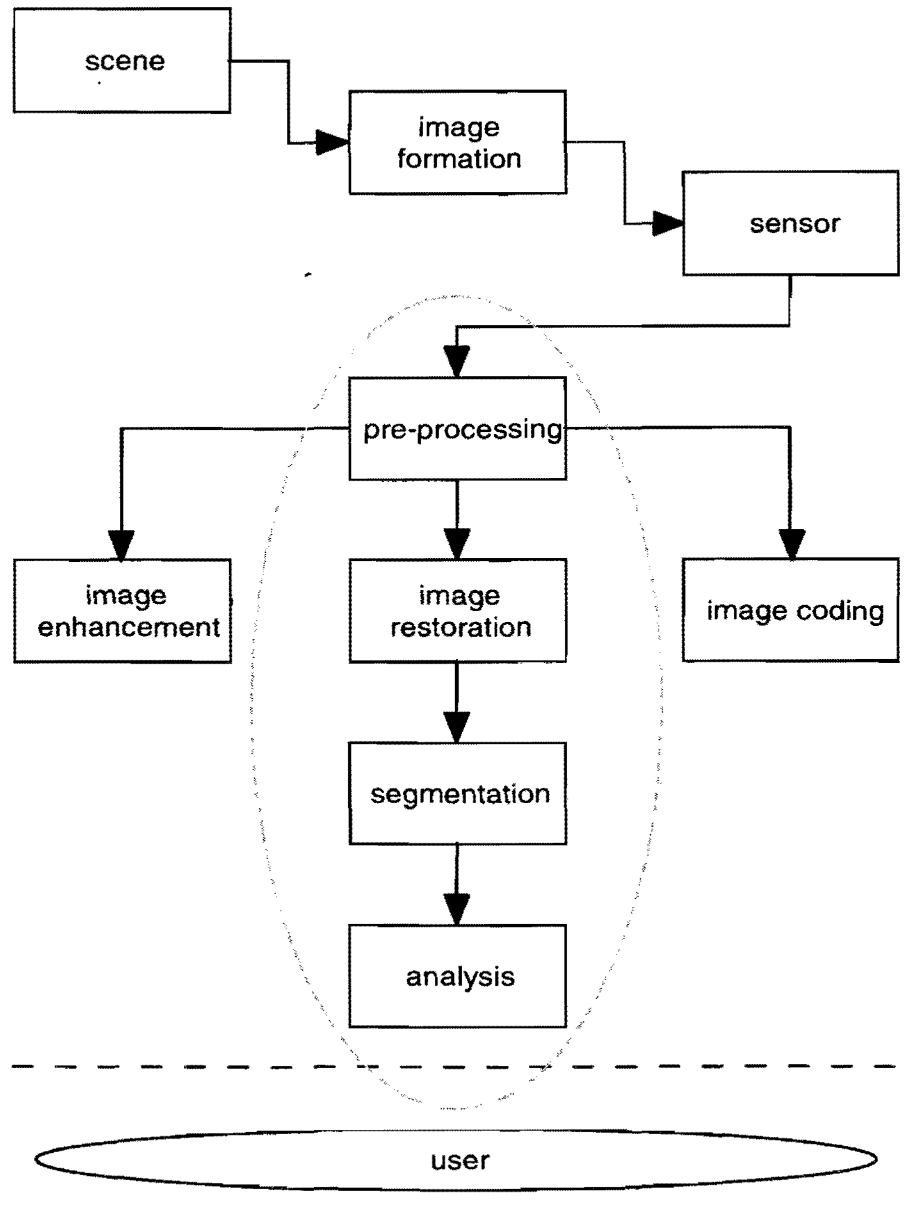

Figure 6. Image system architecture

Figure 7. Image system architecture

4.2 Image coding

For storing or transmitting digital images usually a coding (compression) step is necessary. Digital images contain a lot of data. A standard CCIR601 YUV 4:2:2 digital video image is built up of 720*576 pixels, each pixel containing 8 bits for the luminance information and 8 bits for the chrominance information. Having 25 full images per second implies that only 40 seconds of video can be stored on a 650 MB CD-ROM in uncompressed form. Using coding techniques like MPEG2 this can be increased with a factor of 25 without loosing any visual quality. If a decrease of quality is allowed (e.g. reduction of spatial and/or temporal resolution) then a complete movie can be stored. Real-time transmission over a network, even over high bandwidth ATM links, is not possible without coding.

4.3 Image Restoration

No image formation system is perfect due to inherent physical limitations. Therefore images are not a one-to-one representation of the underlying physical quantity. The images are degraded because of noise, motion of objects, blurring introduced by the optical system, etc. The correction for this known or unknown image degradation is called restoration. Image restoration plays a role in scientific applications, medical applications but also industrial applications. If a robot is to be steered by a visual system then his decisions should be made as much as possible on the real physical data (e.g. distances to objects). Therefore the first step is to retrieve the original information as good as possible before it is being analyzed.

4.4 Image Segmentation

The kind of analysis strongly depends on the application but mostly a segmentation step is involved, that's is, segmenting the image into, for the application, meaningful objects. This is by no means a trivial task. For human beings it is easy to distinguish the individual mushrooms in the image of figure 8a. To do it automatically, e.g. for a robot-picking machine, is much more complex. In figure 8b an example is shown of a segmented image into objects using a simple thresholding technique. The pixels are classified into foreground and background, based on their gray value. The foreground pixels are then grouped into object based on their connectivity. As can be seen some mushrooms are separated, but most of them are grouped and seen as one object. To solve this more intelligent and complex segmentation algorithms have to be applied.

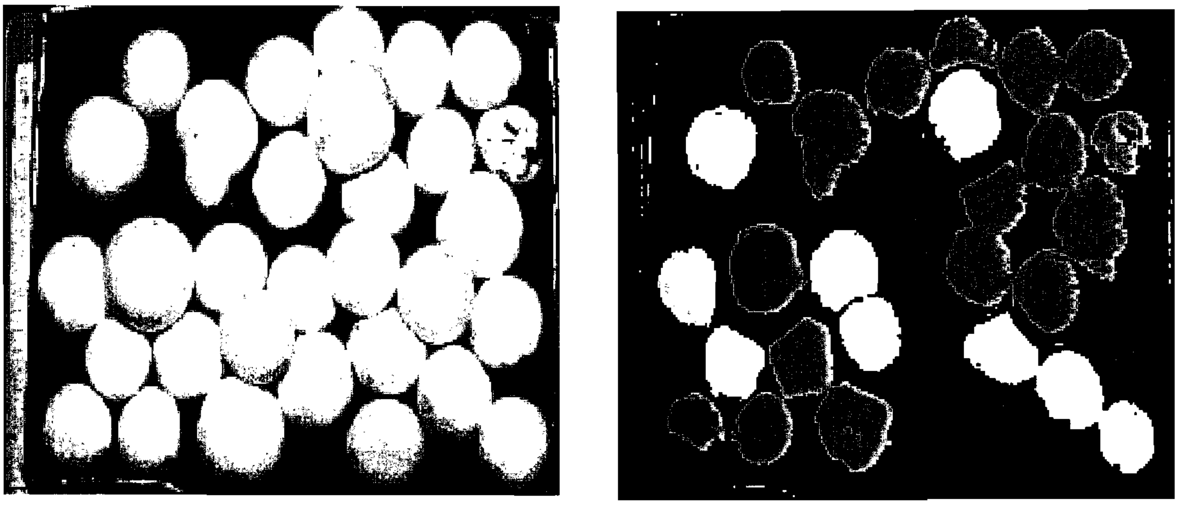

Figure 8. (a) Image of mushrooms (b) labeled image. in which each object has a different gray value

4.5 Image analysis

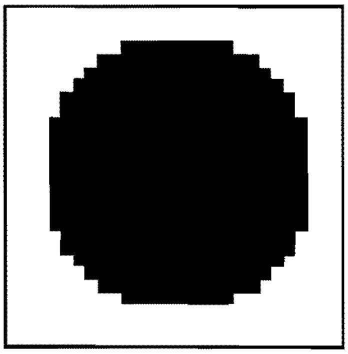

Figure 9. Binary image of a circle with radius of 10.

Having obtained a segmentation of the image the detected objects can be analyzed. For instance in a fruit sorting machine the size and shape of the of the individual objects (apples, oranges, etc) are measured before they are sorted. The size (area) can be easily measured by just counting the number of pixels that belong to the object. The shape of the object can be defined and thus measured in different ways. One way to represent the shape is to calculate the ratio of the perimeter and area. An estimator for the perimeter is the number of pixels that belongs to the border of the object. Counting the number of edge pixel of the circle in figure 9 gives us 53 as an estimation of the perimeter, which is lower than the real length 66. If a more accurate estimation of the length is needed one have to use more sophisticated estimators that take into account the different role of horizontal/vertical neighboring edge pixels and diagonal neighboring edge pixels. If for each horizontal/vertical step 1 is taken and for each diagonal step 1.4 than the estimated perimeter is 59

5 Outlook

Digital imaging and digital image processing is a rapidly growing field in the last twenty years and has a lot of applications in different areas.

In this paper the basic concepts of digital imaging and digital image processing are discussed and some examples are given. The objective is to give the reader some notion of commonly used terminology and some basic understanding of how an imaging system works and what kind of operations can be performed. For more detailed discussion of application of these concepts the reader is referred to the other contributions in this proceedings.

6 References

R.C. Gonzales and P. Wintz (1992). *Digital Image Processing.* Addison-Wesley.

A. Rosenfeld and A.C. Kak (1982). *Digital Picture Processing.* Academic Press.

A.K. Jain (1989). *Fundamentals of Digital Image Processing.* Prentice Hall.

K.R. Castleman, *Digital Image Processing, Prentice Hall,* 1996

B. Jahne. *Digital Image Processing, Springer,* 1997

V.K. Madisetti, D.B. Williams. *The Digital Signal Processing Handbook, Chapter 51, Image Processing Fundamentals (I.T.Young, J.J. Gerbrands and L. van Vliet),* CRC Press, 1998

Biography

Dr. ir. F.A. Gerritsen

Frans A. Gerritsen was born in 1953 in Balikpapan (Borneo, Indonesia). He has been working in the field of image processing since 1975. He obtained his Ph.D. degree in Applied Physics from Delft University of Technology in 1982 on the subject "Design and Implementation of the Delft Image Processor DIP-1", a pipelined array processor tuned for image processing. Between April 1981 and 1984 he worked at the NLR National Aerospace Laboratory in Amsterdam in the fields of Digital Cartography, Remote Sensing and F-16 Mission Planning. In April 1984 Frans joined Philips Medical Systems (PMS), where he worked in the fields of Magnetic Resonance system architecture and reconstruction software. In 1986-91 he was one of the pioneers laying the groundwork for what later became the EasyVision family of clinical viewing/analysis workstations. Since 1991 he is the chief of the EasyVision Advanced Development group. At PMS this group is responsible for working with affiliated contract research and clinical application sites to develop and validate innovative and robust prototypes of future EasyVision products.

In the period 1992-1994 Frans was responsible for managing the contribution of PMS to the EC-sponsored COVIRA project, with R&D in the field of computer vision technology in radiological workstations. In the period 1996-1998 he was project manager for the EC-sponsored EASI project, with R&D in the field of surgery planning and intra-operative navigation for minimally invasive neurosurgery and aortic surgery.

Frans is a member of the board of the Dutch Society for Pattern Recognition and Image Processing (NVPHBV) and editor of its web-based newsletter.

Virtual Reality in Medical Imaging for Image-Guided Surgery

Frans A. Gerritsen
EasyVision Advanced Development
PHILIPS Medical Systems Nederland B.V.
Frans.Gerritsen@Philips.com
http://home.planet.nl/~frans.gerritsen

(For the pictures vide the website quoted on page 31)

Abstract

This presentation discusses relatively recent advances in the use of techniques from medical imaging and simulation to facilitate minimally invasive surgery. The descriptions in this paper are based on original work done in the EC-sponsored EASI-project (European Applications in Surgical Interventions). During the presentation at the symposium also more recent advances by others are explained for tutorial purposes.

With medical imaging equipment one can generate images of the inside of the body. The images can be used for diagnosis, but also for planning and simulation of radio-therapy, surgery and other types of interventions, as well as for guidance and navigation while intervening according to the pre-operative plan. Several registration techniques are available to transfer the pre-operative virtual plan onto the real patient on the operating table, so that planned positions, orientations and sizes can be found back. The position and orientation of surgical tools are measured so that they can be overlaid interactively onto images, showing the tools to the surgeon in relation to the patient's anatomy and pathology. Such guidance greatly facilitates minimally invasive surgery, it improves surgical accuracy and speed, it reduces surgical risks, and it improves the surgeon's confidence.

A further step is the integration of intra-operative imaging (e.g. with microscopy, endoscopy, ultrasound, X-ray, CT and MR) to update pre-operative images for changes which have occurred, either as a result of surgery itself, or because of flexible anatomy.

For microsurgery where a very high precision is needed, it is advantageous to augment the surgeon's dexterity with the help of telemanipulators, to minify movements, to filter any remaining micro-tremor, and to limit the force (or degrees of freedom) of surgical instruments. Simulation of surgery is gaining acceptance for training of surgeons in the non-destructive use of laparoscopic and endoscopic surgical tools.

1 Introduction

During the last few decades various three-dimensional medical imaging techniques have become available, such as Computed Tomography (CT) and Magnetic Resonance (MR) imaging, with which various parts of the human body can be accurately depicted. The resulting images can be used as an aid in diagnosing pathology and for planning of medical treatment.

Conventionally, diagnosis is performed in a visual way: clinicians compare what is seen in patient images with knowledge of anatomy and pathology. Planning of treatment is performed similarly. Prior to surgery, surgeons use the images to mentally project the three-dimensional patient's anatomy and they determine the surgical plan on the basis of this.

In recent years, advances in computer technology and a significant increase in the accuracy of imaging have made it possible to develop systems that can assist and augment the clinician much better in the full path of diagnosis, planning and treatment.

In the European Applications in Surgical Interventions (EASI) project, research, development and clinical evaluation in the area of image-guided surgery were performed. The project focused on two application areas: image-guided neurosurgery of the brain (EASI-Neuro) and image-guided vascular surgery of abdominal aortic aneurysms (EASI-Vascular). The goal was to improve the effectiveness and quality of surgery and to reduce the overall cost of treatment.

EASI-Neuro concerned surgical procedures such as the retrieval of brain biopsies for tissue analysis, resection of brain tumours, endoscopic ventricular surgery and the treatment of neurovascular aneurysms. Advanced tools were developed for planning, visualization and tracking, while using the EasyGuide™ intra-operative navigator and EasyVision clinical workstation as starting platforms.

EASI-Vascular was concerned with image-guided treatment of abdominal aortic aneurysms (AAAs), a life-threatening dilation of the abdominal aorta. Rupture of an AAA leads to instant death in the majority of the cases. Conventionally, these aneurysms are treated with open surgery via the abdomen. Relatively recently, a minimally-invasive technique has been introduced for the endovascular placement of an aortic prosthesis via the femoral arteries. The EASI-Vascular project focused on planning of the dimensions (length and diameter) of the prosthesis from pre-operatively acquired 3D CT images and on image-guided prosthesis placement.

2 Project Approach

First, the needs of the clinical users were analysed with respect to the various steps involved in image-guided surgery (pre-operative imaging, pre-operative planning and intra-operative navigation). For the applications of interest, the desired improvements and possible new surgical procedures were formulated in a clinical specification.

From the clinical specification, a functional specification was derived in which each of the required functions and its required performance was specified in detail. This functional specification was translated into a technical specification in which the hardware and software tools to be developed were specified.

Based on the technical specification, prototype image-guided surgery planning and navigation systems (called demonstrators) were built and installed at clinical sites for clinical validation. On the basis of results of the ongoing clinical validation the demonstrators were continuously improved.

3 Neurosurgery

The clinical procedures addressed in EASI-Neuro are craniotomy (opening of the skull for e.g. tumour resection), biopsy (the retrieval of small brain tissue samples), insertion of shunt catheters into the ventricles (draining of CSF) and endoscopic surgery. For all of these procedures the clinical users want to accurately plan the procedure on the basis of pre-operatively scanned CT or MR images. This may involve segmentation and visualization of critical structures such as blood vessels, tumours, ventricles, gyri and sulci. Furthermore, the users want to accurately follow the pre-operative plan during surgery while getting feedback about any deviations from the plan.

3.1 Basic platforms for EASI-Neuro

The EasyVision CT/MR pre-operative planning station and the EasyGuide™ intra-operative navigator were used as starting platforms. New software and hardware tools were added to improve functionality, resulting in the EASI-Neuro demonstrator.

3.2 Developed tools for EASI-Neuro

Tools were developed for correction of scanner-induced distortions in CT/MR images, for planning and guidance in frameless stereotactic biopsy, for craniotomy and path planning in tumour resection, and for image-guided endoscopic surgery.

3.3 Geometric correction

The first step in image-guided neurosurgery is pre-operative CT or MR imaging. Geometric distortions may be present in the images due to, for example, imprecisely reported table speeds or gantry tilts (CT) or imperfect magnetic fields (MR). Such scanner-induced distortions may influence the accuracy of image-guided navigation. Special phantoms were designed for measuring distortions in CT and MR images and methods were developed for correcting the images (any patient-induced MR distortions are not corrected for).

Use of these phantoms on scanners of various manufacturers revealed that distortions of several mm are no exception, both for CT and MR. We are evaluating how much the overall navigational accuracy can be improved by correcting for such scanner distortions.

3.4 Frameless stereotactic biopsy

When diagnostic imaging indicates the possible presence of a tumour, often a biopsy is retrieved. This is conventionally done by using a stereotactic frame. In the operating theatre, the base of a reference frame is attached to the patient. The patient is then transferred to the radiological department for CT or MR scanning. After scanning, the patient is brought back to the operating theatre, where the arc is mounted to the base. The needle's insertion point, orientation and insertion depth are measured from the scanned images and are transferred onto the arc of the stereotactic frame. Then a needle is inserted and the biopsies are taken.

The conventional frame-based stereotactic procedure is patient unfriendly, time consuming and sub-optimal for hospital logistics. We therefore developed a frameless procedure that is described below.

The patient is first scanned (CT/MR) with fiducials markers attached to the skin and is then transferred to the operating theatre. There, the EasyGuide™ navigator is used to register the patient to the pre-operative images. The biopsy entry and target points are planned with a special biopsy planner tool, which allows evaluation of the path from entry to target. The needle is positioned and oriented according to the planned path by using a special biopsy needle guide which is mounted in a surgical arm attached to operating table or Mayfield clamp.

The alignment software in the biopsy planner tool helps the user to find the correct position and orientation quickly and accurately. The surgeon first puts the tip of the biopsy needle guide on the planned path (+ marker). The surgeon then aligns the guide's orientation with the planned path (x marker). The alignment matches the defined path position and orientation when both the + and x markers are shown at the image center position, indicated by the crosshair. The positions of the markers are calculated in the biopsy needle guide coordinate system, which establishes a natural feedback: left, right, up, down on the screen is also left, right up down for the biopsy needle guide.

As the needle is tracked, the progress of the needle insertion can be shown in relation to the pre-operative images. The surgeon can simulate the retrieval of a biopsy by moving the guide's depth stop as if a needle was inserted. The pre-operative images are shown at the needle tip position. When all is satisfactory the real needle can be inserted into the guide and the biopsies can be retrieved.

Clinical studies have shown that the procedure can be performed in a very short amount of time (about 40 minutes in the OR) with accuracy better than 2 mm.

3.5 Craniotomy and path planning for neurosurgery

We developed a craniotomy planner tool for tumour resection that allows the surgeon to accurately determine the tumour position (the target), to compare alternative positions and shapes/sizes of the craniotomy (the entry point) and to verify the path from the entry point to the tumour.

This tool uses advanced segmentation techniques to discriminate the tumour and surrounding critical structures (e.g. major blood vessels and gyri and sulci of healthy brain tissue) and advanced visualization techniques to show what is encountered on the path.

The pre-operative plan can be transferred onto the patient by using the tracked pointer of the EasyGuide™ navigator. During surgery, deviations from the plan can be visualized on the navigator display.

3.6 Endoscopic procedures for EASI-Neuro

A mountable pointer has been developed to enable tracking of the position and orientation of the endoscope during endoscopic surgery of the ventricular system. The pointer can be placed at any position on the working cannula of the endoscope. The geometry of the endoscope-pointer combination can be learned with a specially developed tool. The EasyGuide™ navigator displays the orientation and position of the endoscope on the pre-operative images. Special tools have been developed to grab and display video images from the endoscope.

3.7 Clinical validation results for EASI-Neuro

Advanced tools were developed for planning of a craniotomy and a surgical path to a selected location in the brain and for planning and performing frameless brain biopsy.

The surgical plan is based on CT/MR images that have been acquired pre-operatively. These images may contain geometric distortion which influence the obtainable surgical accuracy. Tools were therefore developed to measure and remove scanner-induced distortions.

Finally, tools were developed to enable tracking of various surgical instruments (pointers, endoscope, catheters).

The tools were thoroughly validated at National Hospital London, where they were used in 404 operative procedures. The 11 clinical users highly appreciated the tools: for instance 96% of the users was of the opinion that usage of tools has significant advantages over conventional techniques.

Especially the tools for frameless biopsy were highly appreciated. A true frameless procedure could be performed in less than 40 minutes with an accuracy of about 1.5-2.0 mm, which compares favourably with conventional frame-based methods.

4 Vascular surgery

4.1 User needs for EASI-Vascular

EASI-Vascular concentrates on the treatment of aneurysms of the abdominal aorta. An abdominal aorta aneurysm is a life-threatening weakness of the aorta wall which results in a swelling and possible rupture of the aorta. The attention in this project is focused on the Transfemoral Endovascular Aneurysm Management (TEAM) procedure, which is a relatively recent technique to reinforce abdominal aneurysms by placing a endoprosthesis (often Y-shaped) inside the aorta while passing through a small insertion in the femoral artery. The prosthesis is hooked from inside the aorta into its wall. For patients satisfying certain selection criteria, the minimally-invasive TEAM procedure can replace the rather invasive conventional procedure in which the abdomen is completely opened to replace the aorta by a prosthesis.

A careful pre-operative planning is necessary to see whether the patient satisfies the selection criteria, to evaluate the suitability of the access trajectory and to determine the dimensions of the required endoprosthesis. We have also evaluated whether intra-operative surgical guidance could improve the accuracy of positioning the prosthesis as planned.

4.2 Basic platform for EASI-Vascular

Contrary to EASI-Neuro, EASI-Vascular had no navigation products that could serve as a starting platform. The demonstrator was therefore developed based on an EasyVision CT/MR clinical workstation with additional hardware and experimental software.

4.3 Pre-operative planning for EASI-Vascular

To evaluate the access trajectory and attachment sites, a (semi-) automatic algorithm was developed that segments and tracks lumen and thrombus in CTA images from the insertion point in the groin up to the renal arteries. The algorithm automatically calculates the diameter of the aorta along the central lumen line and determines the diameter of the best-fitting endoprosthesis.

4.4 Intra-operative navigation for EASI-Vascular

To aid the clinical user in the placement of the endoprosthesis, a navigation system has been developed that registers intra-operative fluoroscopic X-ray images with pre-operative CTA images.

This allows the visualisation in the intra-operative X-ray images of structures which are clearly visible in the CTA images (such as the lumen), but which are not visible in the X-ray images.

Briefly summarized, the registration method operates as follows. A vertebra is segmented from the 3D CTA images. A projection of this vertebra is constructed and automatically registered to the corresponding vertebra in an intra-operative 2D X-ray image. The registration is performed by using a similarity measure based on pattern intensity. This similarity measure performs better than other measures, such as the normalised cross-correlation and mutual information.

The registration only remains valid as long as the patient has not moved with respect to the X-ray imaging system. Therefore an automatic motion detection method was implemented. In clinical practice, such motion occurs regularly, due to both intentional and unintentional repositioning of the operating table and/or the X-ray device. When motion has been detected, the registration is declared invalid and the registration algorithm is restarted.

4.5 Clinical validation results for EASI-Vascular

A method was developed for image-guided placement of an abdominal aortic prosthesis. The prosthesis is inserted through a small incision in the femoral artery. Intra-operative guidance is supplied on the basis of registering intra-operative 2D fluoroscopic X-ray images to pre-operatively scanned 3D CT images. After registration, information that was retrieved from the CT data and that is not clearly visible in the X-ray (e.g. the aorta) can be overlaid on the X-ray.

In the last phase of the project, attention was shifted towards planning: determination of patient eligibility and sizing of the patient-specific prosthesis. Tools were developed for automatic segmentation of the lumen in the aorta and for automatic estimation of the prosthesis dimensions. A preliminary clinical validation showed that the dimensions can be accurately estimated. The EASI-Vascular demonstrator has been clinically validated at the Utrecht University Hospital (AZU). Up to now the system has been evaluated in 11 procedures (of circa 20 in total since July 1996). Discussions with the surgeons have repeatedly led to important redesigns. Therefore quantitative results are not present in the same abundance as they are in the EASI-Neuro part of the project.

The vascular surgeons are very pleased with the planning tools for pre-operative assessment of patient eligibility, for measurement of the dimensions of the required prosthesis, and for planning its attachment site. The vascular surgeons' enthusiasm for intra-operative guidance is much less. From a technical viewpoint, the developed intra-operative guidance method proved to function well in practice. Intra-operative localization (based on matching intra-operative X-ray to pre-operative CT) was realized with an accuracy of circa 1 mm in the directions parallel to the plane of the X-ray projection, and circa 2-3 mm in the perpendicular direction. However, the accuracy specified by the surgeon was 1 mm in all directions, for accurate determination of position and orientation of the tip of the endoprosthesis. This could not be reached with only a single direction of X-ray projection. Further improvement of the localization performance can be reached by using two or more directions of X-ray imaging.

However, if one relies on similarities between the pre-operative imaging and the intra-operative situation, then it is not sufficient to only improve the intra-operative localization accuracy. For instance, when the aorta's shape changes, and/or when its relation to the vertebrae changes significantly, the resulting lack of similarity severely reduces the usefulness of the pre-operative images.

5 Conclusions and future plans

In the course of the EASI project, advanced methods and tools were developed and validated for planning and performing image-guided surgery on the basis of pre-operatively acquired imagery.

Future research, development and clinical co-operations will focus on further increasing the accuracy of surgery, by combining intra-operative images (CT, MR, US, Video) with pre-operative images.

The competition in this field is heavy and the market has not taken off as quickly as was estimated several years ago. In order to limit the development costs, several companies merged their image-guided surgery activities in the Surgical Navigation Network (SNN). Philips joined SNN in October 1998. The aim of SNN is to come to an open-standard, multi-vendor, modular, plug-and-play image-guided surgery platform.

Philips Medical Systems introduces the achievements of the EASI project and other related work as much as possible into SNN.

PMS is currently focusing more attention to the combination of intra-operative imaging (e.g. mobile CT, interactive MR, X-ray, ultrasound and video) and image-guided navigation.

6 Acknowledgements

The innovations mentioned here are based on previous and current work of many colleagues at Philips Medical Systems in Best (EasyVision Advanced Development, EasyVision and EasyGuide Application and Engineering groups, MR Clinical Science, CT Clinical Science), Philips Forschungslabor Hamburg (PFL-H), Laboratoires d'Electronique Philips (LEP), AZU & Utrecht University, University Twente, Guy's Hospital London, National Hospital London, Katholieke Universiteit Leuven and the University of Minnesota.

The following persons made major contributions to the work that is summarized here: Jan Blankensteijn, Hubrecht de Bliek, Marco Bosma, Marcel Breeuwer, Ivo Broeders, Willem van de Brug, Hans Buurman, Thorsten Buzug, David deCuhna, Thomas Deschamps, Paul Desmedt, Neil Dorward, Arnold Dijkstra, Bert Eikelboom, Louis van Es, Carola Fassnacht, Ron Gaston, Paul Gieles, David Hawkes, Derek Hill, Johan de Jong, Neil Kitchen, Michael Kuhn, Steven Lobregt, Cristian Lorenz, Jean-Michel Létang, Peter Luyten, Frederik Maes, Willem Mali, Alastair Martin, Calvin Maurer, Peter Luyten, Sherif Makram-Ebeid, Graeme Penney, Paul Porskamp, Roland Proksa, Colin Renshaw, Jörg Sabczynski, Georg Schmitz, Jaap Smit, Paul Suetens, Jeroen Terwisscha van Scheltinga, David Thomas, Roel Truyen, Charles Truwit, Joop van Vaals, Dirk Vandermeulen, Binti Velani, Max Viergever, Kees Visser, Ted Vuurberg, Jürgen Weese, Onno Wink, John Wadley, Jason Zhao and Waldemar Zylka.

EASI project partners

PhilipsMedical Systems Nederland B.V. (NL)
National Hospital London (UK)
Utrecht University Medical Centre / Image Sciences Institute (NL)
Katholieke Universiteit Leuven(B)
Guy's, King's & St. Thomas' Schools of Medicine (UK)
Philips Research Laboratory Hamburg(D)

EASI project web site: http://home.planet.nl/~frans.gerritsen/EASI/EASI.html

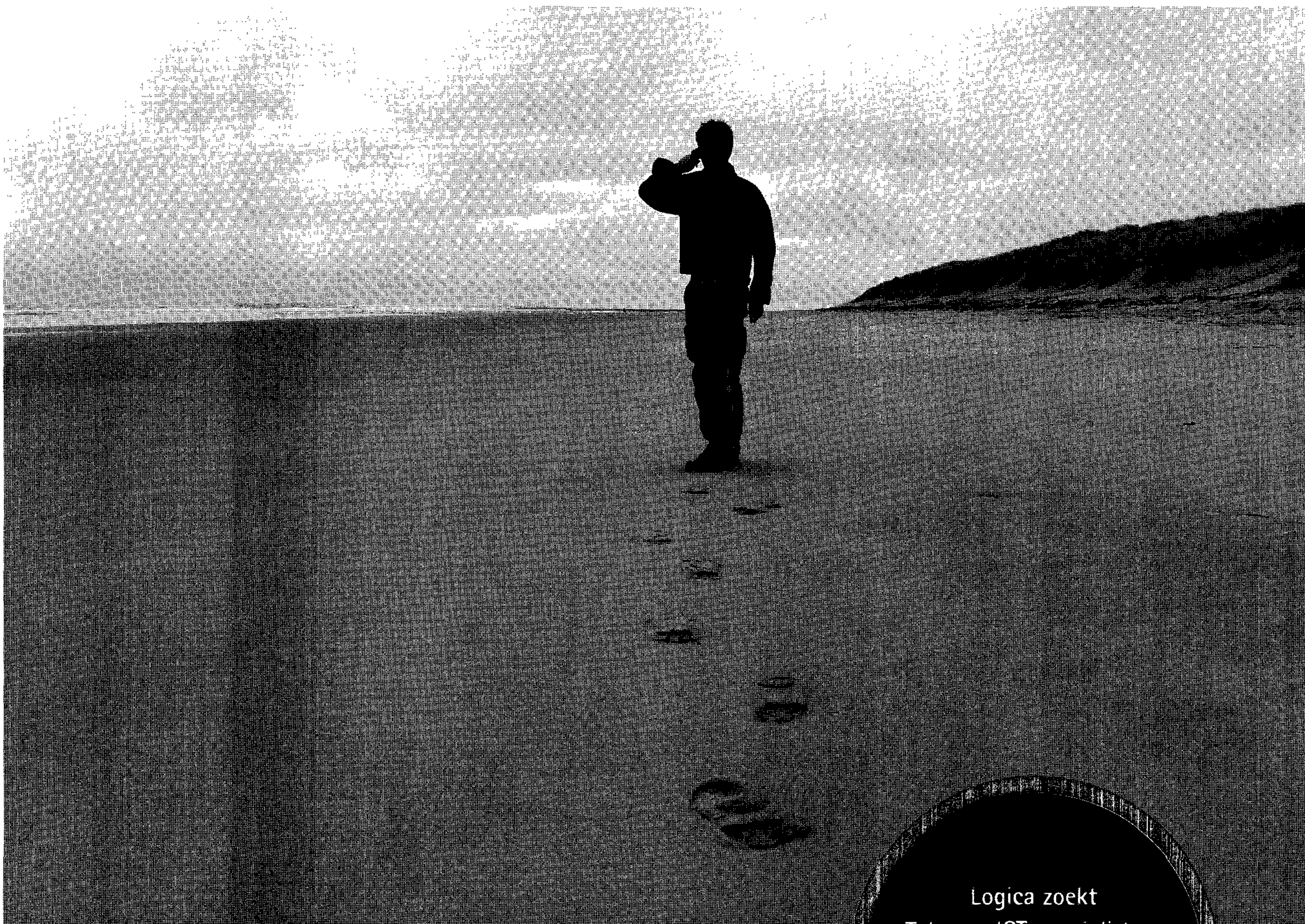

Parallel Session 1

Medical Applications conducted by dr. ir. P.J.M. Cluitmans

Biography

Dr. A.M.J. Paans

Dr. A.M.J. Paans (1944) studied experimental physics at the University of Utrecht. After this study (1970) he worked in the field of nuclear physics instrumentation and experimental nuclear physics at the Kernfysisch Versneller Instituut (KVI) in Groningen. From end 1974 until 1987 he worked in the field of nuclear medicine and was involved in the development of the production of radionuclides for Positron Emission Tomography (PET) and the development of positron cameras as a staff member of the Department of Nuclear Medicine. These developments in PET were made possible by the facilities of the Department of Organic Chemistry and the KVI jointly. His thesis "Imaging in nuclear medicine with cyclotron generated radionuclides" was in the overlapping field between nuclear physics and nuclear medicine. He is co-founder of the first PET-center in The Netherlands in 1987. With the actual realisation of this center at the beginning of 1991 he is responsible for all physical aspects of PET within this center which is joint venture of the Groningen University Hospital and the Groningen University.

Positron Emission Tomography

Dr. A.M.J. Paans
PET-center, Groningen University Hospital
A.M.J.Paans@pet.azg.nl

Abstract

Positron Emission Tomography (PET) is a method for determining biochemical and physiological processes in vivo in a quantitative way by using radiopharmaceuticals labeled with positron emitting radionuclides as ^{11}C, ^{13}N, ^{15}O and ^{18}F and by measuring the annihilation radiation using a coincidence technique. This includes also the measurement of the pharmacokinetics of labeled drugs and the measurement of the effects of drugs on metabolism. These functional measurements allow the establishment of deviations of normal metabolism and also insight in biological processes responsible for diseases can be obtained. The effects of therapy on metabolism can be evaluated in an non-invasive way.

Since the short-lived character of the radionuclides requires an in house production facility (cyclotron) with the necessary chemical facilities, PET is multidisciplinary research environment. In a PET-center the fields of nuclear physics/technology, organic(-radio)-chemistry, pharmacy and medicine are coupled into one cooperative team.

1 General overview

The idea of in vivo measurement of biological and/or biochemical processes was already envisaged in the 1930's when the first artificially produced radionuclides of the biological important elements carbon, nitrogen and oxygen were discovered with help of the then recently developed linear accelerator and cyclotron. These radionuclides decay by pure positron emission. When a positron recombines with an electron the positron-electron pair will annihilate resulting in two 511 keV g-quanta emitted under a relative angle of 180° which are then measured in coincidence. This idea of PET could only be realized when the inorganic scintillation detectors for the detection of g-radiation, the electronics for coincidence measurements and the computer capacity for image reconstruction became available. For this reason Positron Emission Tomography (PET) is a rather recent development in functional in vivo imaging.

PET employs mainly short-lived positron emitting radiopharmaceuticals. The radionuclides employed most widely are: ^{11}C ($t_{1/2}$ = 20 min), ^{13}N ($t_{1/2}$ = 10 min), ^{15}O ($t_{1/2}$ = 2 min) and ^{18}F ($t_{1/2}$ = 110 min). These are all neutron deficient radionuclides. Carbon, oxygen, nitrogen and hydrogen are the elements of life and the building stones of nearly every molecule of biological importance. However, for hydrogen no positron emitting neutron deficient is possible. For this reason a fluorine isotope is often used as a replacement for a hydrogen atom in a molecule. Due to these short half-lives the radionuclides have to be produced in house, preferably with a small, dedicated cyclotron. Since the chemical form of the produced radionuclides can only be simple, input from organic- and radiochemistry is essential for synthesis of the desired complex molecule [1]. Input from pharmacy is required for the final formulation and pharmacokinetic studies and medical input is evident and required for application. Longer lived positron emitting radionuclides are sometimes commercially available or obtainable from research facilities with larger accelerators. Some examples of longer liver positron emitting radionuclides of use in medicine are ^{52}Fe ($t_{1/2}$ = 8.3 h), ^{55}Co ($t_{1/2}$ =17.5 h) and ^{124}I ($t_{1/2}$ = 4.2 d). Sometimes also positron emitting radionuclides can be obtained from a generator system. Examples are ^{82}Rb ($t_{1/2}$ = 76 s) from ^{82}Sr ($t_{1/2}$ = 25.5 d) and ^{68}Ga ($t_{1/2}$ = 68 m) from ^{68}Ge ($t_{1/2}$ = 288 d). Although all these radionuclides are used, the isotopes of the biological most important elements receive most attention.

At the moment small dedicated cyclotrons are a commercially available product. These accelerators are one or two particle machines with fixed energies. At the moment mostly negative-ion machine are being installed because of their relative simple extraction system and high extraction efficiency. They are installed complete with the targetry for making the four above mentioned short-lived radionuclides in Curie amounts. Also the chemistry for some simple chemical products is incorporated. Sometimes more complex syntheses are also available from the cyclotron manufacturer or a specialized company. The radiopharmaceuticals become available via dedicated, automated systems or via programmable robotic systems. Other radiopharmaceuticals have to be set up individually in each PET center.

The state of the art positron camera is a complex radiation detection technology product combined with a relative large computing power for data acquisition and image reconstruction [2]. The basic detector in a modern PET camera is a bismuthgermanate (BGO) detector block divided in 8x8 subdetectors read out by 4 photomultiplier tubes (PMT). By adding and subtracting the individual signals of the PMT's the scintillating subdetector in the BGO block can be identified. Around 70 blocks will form a ring and 4 of these rings can added to get an axial field of view of approximately 15-16 cm. In this way 63 planes are imaged simultaneously with a spatial resolution of 4-5 mm FWHM, see fig. 1. Septa are placed between the adjacent subdetector rings in order to reduce the amount of scattered radiation. These septa can also be retracted creating a much higher sensitivity in the so called 3-D mode at the cost of a larger scatter fraction. With the present generation of positron camera's the singles count rates that can be managed are in the order of over 50,000,000 counts per second resulting in coincidence count rates of over 500,000 per second. Hardware and software for data acquisition, image reconstruction and for image manipulation is available. Positron cameras are able to measure the radioactivity in absolute terms, Bq/pixel, which is an unique feature. This is possible because the coincidence technique allows for the correction of the attenuation of radiation inside the body of the individual patient. This correction is accomplished by making an individual "transmission image" with an external positron emitting source. This individual transmission image can also been used for the individual correction for scattered radiation present in the image after a 3D-acquisition. This external source is built into the camera and can be extended from its well shielded storage box when necessary. To translate the measured radioactivity distribution into functional or physiological parameters compartimental models have been developed for radiopharmaceuticals with known metabolite profiles. Although only a few measurable quantities, i.e. tissue and plasma concentration (the latter by taking blood samples), are available, it is still possible to calculate e.g. the glucose consumption by employing a dynamic data acquisition protocol in combination with a compartimental model [3]. It is also possible to make a whole body scan by translating the patient through the PET camera. By projection the transverse section images a whole body overview can be made.

A PET center is the combined relevant knowledge of chemistry, medicine, pharmacy and physics and a PET center is staffed by all these disciplines in a good cooperating team.

2 Possibilities of PET in research and patient care

The clinical applications of PET are in the fields of cardiology, neurology and oncology. In the cardiology the measurement of the myocardial blood under rest and stress conditions with ^{13}N-ammonia and the energy consumption with ^{18}FDG (^{18}F-fluorodeoxylucose) is a standard examination in order to disciminate between ischemic and infarcted tissue. In the neurology the cerebral blood flow and/or the energy consumption of the brain is the standard examination, see fig. 2. In the oncology PET is used for the detection of tumors and to measure the effect of therapy on the tumor metabolism.

^{13}N-ammonia is used for the measurement of the myocardial bloodflow. To study the viablity of the heart it is used in combination with ^{18}FDG. The combination of ammonia rest, ammonia stress and metabolism study deliver a much too large number of images to evaluate individually. For this reason software to re-orient the images perpendicular to the long axis of the heart followed by a translation of the data into quantitative parameters of bloodlfow and glucose consumption per heart region has been developed.

Bloodflow and metabolism are than visualized per examination in a so called polar map. It also possible to use the electro-cardiac signals to make a gated cardiac study. From this data it is possible to generate images of the beating heart and if from these images the wall of the left ventricle can be detected, the wall motion can be quantified.

The clinical and research programs in the fields of neurosciences in Groningen are directed to glucose metabolism (^{18}FDG), protein synthesis rate (PSR) with ^{11}C-tyrosine [4] and bloodflow with $H_2{}^{15}O$ [5]. The improvement in resolution can be seen in fig. 1 where the glucose metabolism of the brain is shown for the different generations of PET scanners. For oncological studies both ^{18}FDG as well as L-[1-^{11}C]tyrosine are available. Software voor for the translation of measured radioactivity into glucose-consumption (^{18}FDG) and protein synthesis rate of ^{11}C-tyrosine have been developed. The D_2 receptor in the human brain can be studied with ^{18}F-DOPA or ^{11}C-raclopride and is of importance in the case of Parkinson's disease. Measurement of the regional cerebral bloodflow (rCBF) with $H_2{}^{15}O$ is of great importance to discover the functional anatomy in fields like cognitive neuroscience, linguistics, selective attention and to measure the effect of drugs on the rCBF in different categories of patients.

For the study of tumor metabolism ^{18}FDG is often used but other possibilities in the form of amino acids do exist. Also the effect of therapy on the tumor metabolisme can be quantified by measuring before and after therapy. By performing the second study already during the therapy may be also a prognostic statement can be made. For oncological brain studies the use of an amino acid can be favourable due to the better signal to noise ratio which can be obtained with respect to the glucose metabolism study. It is also possible to generate "whole-body" images by projecting a number of consecutive transverse images into a planar image.

3 New developments

The cyclotron as available now for PET centers is adapted to requirements for the production the four most important radionuclides. This results in a technically more simple machine which has also incorporated the targetry for the most important radionuclides. Automation and computer control is integrated into the design. For the day-to-day operation no separate operating team is required, the cyclotron can be operated by the technical chemical staff. The present developments tend into a few directions, but reduction in costs by a reduction in maximum beam energy is a general goal for the marketing of cyclotrons for clinical PET-centers. Since the production capacity for the four important radionuclides should remain target technology becomes more important. Changing to a superconducting magnet would decrease the size and weight. Advantage is the smaller size of the vault but a more complex technology is introduced. Some cyclotron manufacturers also provide local movable shielding of concrete and lead, fitting tightly around the accelerator, resulting in lower total mass of the shielding. Also developments in linear accelerators (linacs) and in Radio Frequency Quadrupole accelerators (RFQ's) for the production especially of the four PET radionuclides, are taking place. However, it still has to be shown what is the best cost effective solution.

The radiation detectors used in positron cameras at the moment are made of BGO in most cases but also NaI or BaF_2 has been used or still is in use. Although BGO and BaF_2 have a high stopping power for 511 keV and a number of other favourable properties, the light yield of NaI is also favourable. The ideal detector for a positron camera should have a time resolution of approximately 10 ps and this combined with other properties like high stopping power, high Z, non-hygroscopic etc.. This extreme fast timing would allow for the measurement of the place of annihilation within a few millimeters by means of the time-of-flight (TOF) measurement. With the present detectors only the line on which the annihilation took place is being determined. The filtered back-projection reconstruction technique in combination with block structure of the detectors makes a spatial resolution of 4-5 mm FWHM standard. Recently LSO (lutetium-orthosilicate) has been discovered as a scintillator [6]. LSO combines the good properties of BGO with high light yield (75% of the yield of NaI) and is also rather fast (40 ns). A disadvantage is the presence of natural radioactive isotope of lutetium but, since a coincidence technique is employed, this will not influence the image formation. The higher light yield will improve the energy resolution and by this decrease the scatter fraction. At the moment small LSO PET-scanners are being built for small animals (rats and mice) and a spatial resolution of 2 mm FWHM has been achieved in these systems. Based on this experience one can expect that in the future whole-body systems with this spatial resolution will become available.

The fundamental limit in the spatial resolution is of course the range of the positron itself. At the mean positron energy, 40% of the maximum energy, the range of the positron varies from 1.1 mm for ^{11}C via 2.5 mm for ^{15}O to 5.9 mm for ^{82}Rb. At the moment interplane septa are used to limit the opening angle of each individual plane. This reduction of opening angle is necessary to keep the amount of scattered 511 keV g-quanta within reasonable bounds. By removing these septa the efficiency of the whole system increases with a large factor but the fraction of scattered radiation will also increase. This is due to the rather bad energy resolution, 25% at 511 keV, of the BGO block detectors used. Nevertheless a lot of efforts has been invested in the development of systems without septa and in the development of correction algorithms for scatter, yielding a three dimensional imaging system [7].

The fact that the annihilation of positron and electron does not take place at zero momentum is proven by the fact that there is a finite angular width of 0.5° FWHM in the angular distribution about the mean angle of 180°. With a detector ring diameter of roughly 80 cm and an improving spatial resolution this parameter is becoming more important as a limitation in the spatial resolution.

4 PET and other imaging modalities

The most common imaging technique in medicine uses X-rays. In its most simple form a density projection is generated by holding the subject of interest between the X-ray tube and a photographic plate. The advanced form can be found in a CT-scanner in which a rotating X-ray source and detectors make a transverse section image. Again sort of a density map is generated although extraction of the exact density will not be possible, and is also not necessary for diagnostic use, due to the broad energy spectrum of the generated X-rays. Due to the large difference in density between bones and tissue the bones can be visualized perfectly while small differences in tissue density will be more difficult to visualize. The use of contrast agents, like fluids with high densities and high Z-components, can change the difference in density and by this the interpretation of the images dramatically.

The Nuclear Magnetic Resonance (NMR) technique is in use to visualize the protons (bound to water) in the human body. Homogeneous magnetic fields up to 2 T are in use in medical NMR scanners, nowadays abbreviated to MRI (Magnetic Resonance Imaging). In order to have a short imaging time, gradient fields with frequency decoding are used. The strength of the NMR signal is proportional to the difference in population of the spin-up and spin-down state. Under normal conditions at room temperature the ratio between spin-up and spin-down is rather close to unity. The NMR technique is a rather insensitive technique [8] for this reason but which is successful because of the high water concentration in the human body. Also paramagnetic contrast agents like Gd-DTPA are used to increase the contrast. Both, the X-ray and the MRI technique, supply anatomical information.

With NMR also information on the structure of molecules can be obtained, as is done in the chemistry. This also possible in the human body but limited to the brain and to molecular structures which have a concentration of 0.1 mM or more as a rule of the thumb. The limitation to brain tissue is because the signals from water and fatty tissues have to be suppressed and these concentrations are rather low in the brain in contrast to e.g. the thorax.

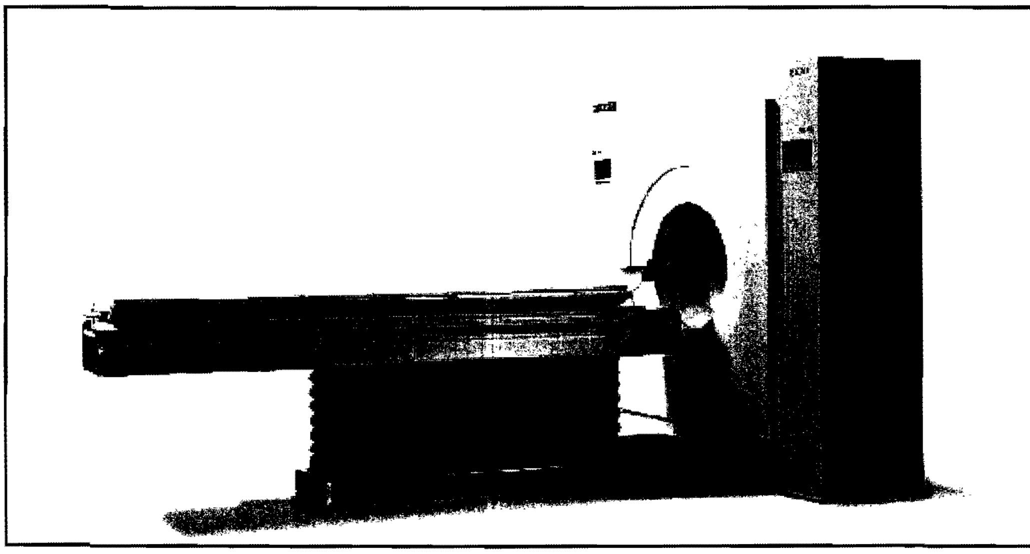

Figure 1. The Siemens/CTI Ecat Exact HR+ positron camera. 4 rings with BGO block detectors resulting in 63 planes over an axial length of 15.2 cm. 2D- and 3D-acquisition mode (Courtesy Siemens/CTI).

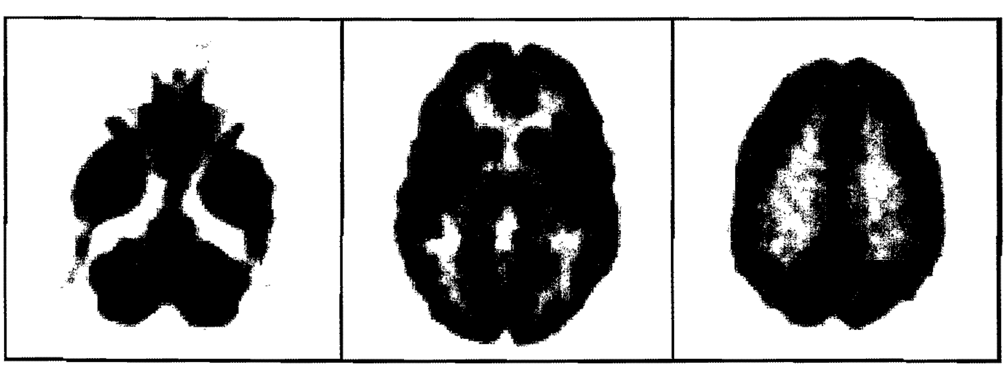

Figure 2. The glucose consumption in the human brain as measured with ^{18}FDG on Siemens Exact HR+ PET camera. Images of three different levels in the brain are shown (Courtesy Siemens/CTI).

By using radionuclides bound to different molecular structures functional emission imaging became available in the 1950's. It is functional imaging because the chemical structure and the human metabolism determine the faith of the molecule in vivo. PET is the ultimate form of nuclear medicine. Because the nuclear reactions for the production of positron emitting radionuclides are of the type (p,n) or (p,a) in most cases, the element produced is different from the target element. By this type of reactions the amount produced in weight is extremely low (1 Ci of ^{11}C has a weight of 1.2 ng) while the amount of radioactivity is considerable (1 Ci of ^{11}C can routinely be made and a patient dose is 10 mCi). This so called specific activity (TBq/mg) is of importance e.g. for receptor research and makes it possible to call it "tracer" experiments.

Since the PET method supplies functional information the combination with X-ray and NMR techniques, CT and MRI, would yield an identification of the functional anatomy. In order to make this combination the images of the different disciplines should be available in a transparant way and image resize and re-orientation techniques should be available to match the images from the different modalities. At the moment there are no general applicable routines available to perform this kind of matching operations. In a number of PET centers the combination of PET-, CT- and NMR-images is subject of interest. In some institutions also the comparison and transformation of PET images to a stereotactic brain atlas have been performed [5]. The head and brain are the first structure/organ of choise to evaluate the "multi-modality" matching for obvious reasons.

References

1.Vaalburg W, Paans AMJ, *Radionuclides Production II*, ed Helus F,. CRC Press, Boca-Raton, USA, 1983, 47.

2.Phelps ME and Cherry SR, Clinical Positron Imaging 1, 31 (1998).

3.Phelps ME, Huang SC, Hoffman EJ, Selin C, Sokoloff L, Kuhl DE, Ann Neur 6, 371 (1979).

4.Willemsen ATM, van Waarde A, Paans AMJ, Pruim J, Luurtsema G, Go KG and Vaalburg W, J Nucl Med 36, 411 (1995).

5.Frackowiak RSJ, Friston KJ, Frith CD, Dolan R, Maziotta JC, Human Brain Function, Academic Press, San Diego, 1997.

6.Casey ME, Eriksson L, Schmand M, Andreaco MS, Paulus M, Dahlbom R, Nutt R, IEEE Trans NS 44, 1109 (1997).

7.Watson CC, Newport D, Casey M, IEEE Trans NS 44, 90 (1997).

8.Paans AMJ, Vaalburg W, Woldring MG, Eur J Nucl Med 11, 73 (1985).

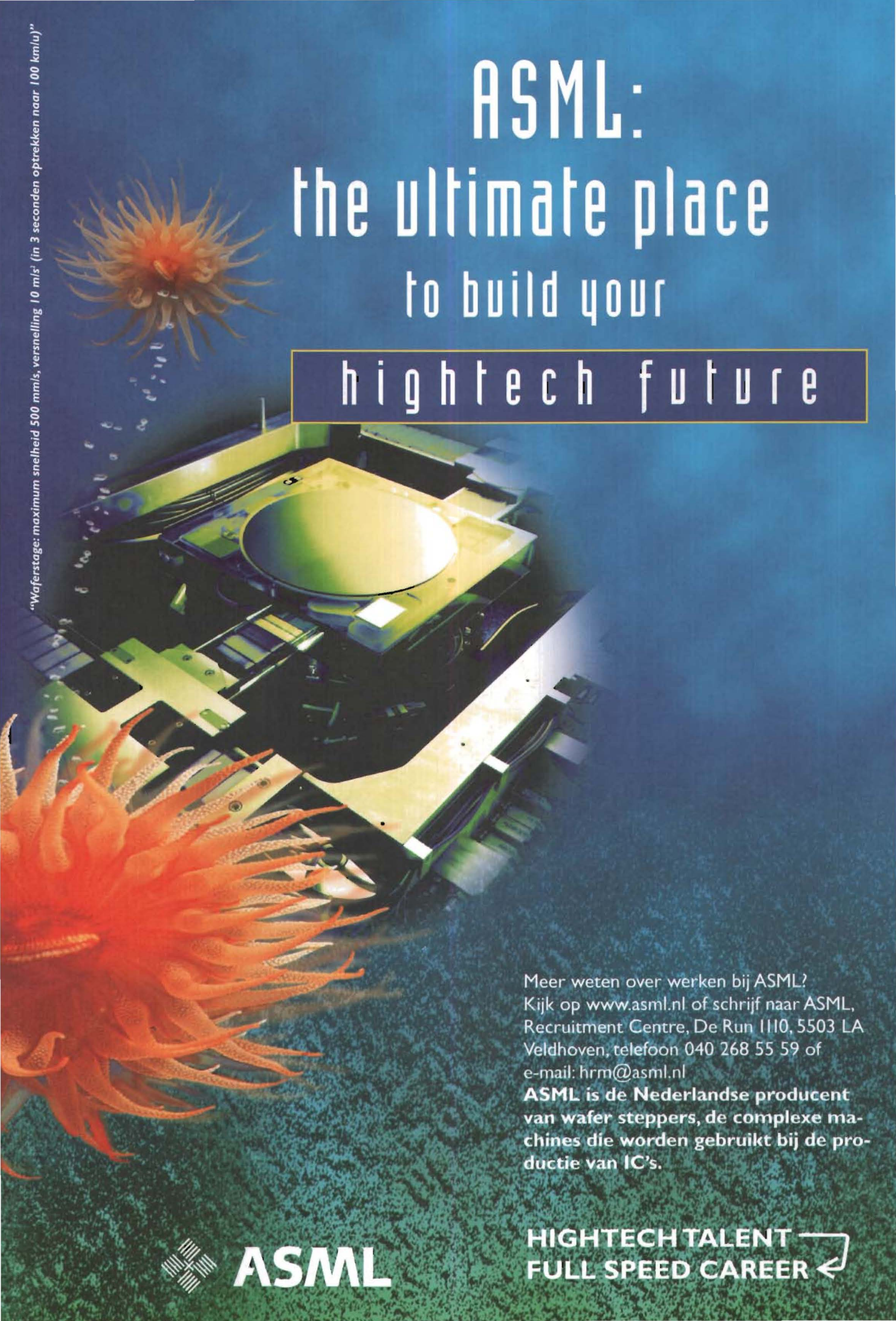

"Waferstage: maximum snelheid 500 mm/s, versnelling 10 m/s² (in 3 seconden optrekken naar 100 km/u)"
ASML:
the ultimate place
to build your
hightech future
Meer weten over werken bij ASML?
Kijk op www.asml.nl of schrijf naar ASML, Recruitment Centre, De Run 1110, 5503 LA Veldhoven, telefoon 040 268 55 59 of e-mail: hrm@asml.nl
ASML is de Nederlandse producent van wafer steppers, de complexe machines die worden gebruikt bij de productie van IC's.
ASML
HIGHTECH TALENT
FULL SPEED CAREER

Biography

Dr. ir. V. Rasche

Volker Rasche was born in 1963 in Bad Oeynhausen, Germany. He received his Master's degree in Physics from the University of Bielefeld. He joined the Philips Research Laboratory Hamburg in 1991 to evaluate fast Magnetic Resonance Imaging techniques for interactive real-time scanning. In 1995 he received his PHD degree from the University of Bielefeld for his work on real-time projection reconstruction MRI.
Currently, his work is focused on research aspects for 3D rotational X-ray imaging.

New Technological Developments in 3D Medical Imaging

Volker Rasche
Philips Research Laboratories
Division Technical Systems
Roentgenstrasse 24-26
D-22335 Hamburg

1 General

In non-nuclear medical imaging magnetic resonance imaging (MRI), computer tomography (CT), Ultrasound (US), and recently introduced 3D Rotational X-Ray Imaging (3D-RX) are techniques capable of providing 3D information of the human subjects. The field of non-nuclear medical imaging is currently undergoing some major changes, the three most important of them being a transition from a couple of 2D slices to true 3D imaging preferably at high isotropic resolution, the extraction of physiological information instead of pure anatomy, and the trend to realize real-time image acquisition and display.

High-resolution 3D imaging becomes increasingly relevant as diagnosis, treatment planning and interventional procedures will grow together in the future. There are several exciting new technological developments in 3D medical imaging providing the capabilities for sub-mm^3 volume acquisitions utilizing Rotational X-Ray Imaging, Computer Tomography, Magnetic Resonance Imaging, and Ultrasound.

Additionally to the increased spatial resolution, the access and preferably automatic extraction of physiological information will become more and more mandatory since the high-resolution volumetric scans will provide thousands of images and the physician must be supported by additional information for efficient diagnosis.

Real-time imaging is a must for certain applications such as the guidance of interventional procedures and the acquisition of functional information especially in the field of heart imaging.

The application of the various modalities will depend on their versatility but also on their price, ranging from relatively low for Ultrasound to very high for Magnetic Resonance Imaging using open magnet structures. This presentation gives some insights into these developments and will addresses the state-of-the-art of the different techniques.

2 3D-RX

In 3D Rotational X-Ray Imaging (3D-RX) conventional high-end C-Arm type X-Ray systems such as shown in Figure 1 are utilized for volume reconstruction. The required information is obtained by taking two-dimensional X-ray projections of the investigated subject during rotating the tube-detector assembly. Data reception is performed with a so-called image intensifier (II) converting the trapped X-ray photons into light with an integrated electron optic for signal amplification. Utilizing standard C-arm X-ray systems for volume reconstruction was so far limited by the projection orientation-dependant distortions of the projection data introduced by the interaction of the electron beam with the earth-magnetic field. Recently, however, new calibration and image reconstruction methods were introduced allowing the application of these conventional C-arm type X-ray systems for the reconstruction of volumes with high isotropic spatial resolution as shown in Figures 2,3. Up to now the application of this technique is limited to objects providing high-contrast relative to the background such as contrast agent-filled vascular structures or bones. Currently, 3D-RX is predominantly applied for the visualization of complex vascular structures in the neuro-radiological field.

The major challenge in 3D-RX is the extension of the technique to objects providing lower contrast by utilizing new detector concepts and new acquisition strategies.

3 Computer Tomography

In Computer Tomography (CT) a so-called gantry containing the X-ray tube and the normally one-dimensional X-ray detector is rotated around the subject within a second. CT is currently undergoing a major change from the one-dimensional single array detectors to two-dimensional multi-array detectors. Furthermore a significant interest in shorter gantry rotation times down to 500ms has arisen. The benefit of sub-second multi-array scanning lies in the fact that large volumes can be covered rapidly since multiple slice data can be acquired within one rotation of the gantry, thus allowing for complete lung or abdominal scans as well as cardiac imaging within a single breath-hold (see Figures 4,5). Furthermore, the sub-second acquisition times may be utilized for fluoroscopic CT providing almost real-time imaging capabilities.

The major challenges are in the detector technology and its cost management, and in the reconstruction algorithms, which have to be based on cone-beam rather than fan-beam geometry. The latter poses problems with respect to both the algorithms as well as the computing power requirements.

4 Magnetic Resonance Imaging

In Magnetic Resonance Imaging technological advances have recently opened capabilities in the area of interactive, real-time imaging and cardiovascular imaging. Real-time imaging requires ultrafast image acquisition protocols and video-rate reconstruction hardware. Interactive imaging is based on a system architecture with real-time feedback loop to allow for on-line adjustment of contrast and slice orientation. Main application areas of real-time MRI arise in the field of cardiovascular imaging and for the guidance of interventional procedures.

For cardiac MRI, the ambition is to offer a so-called one-stop-shop approach to cardiac diagnosis, thus combining several diagnostic steps (myocardial perfusion (see Figure 9), heart wall motion, coronary artery imaging) which currently are performed in different imaging modalities (including nuclear medicine and X-Ray angiography). MRI currently appears to be the only modality being capable of providing all the required diagnostic information.

For interventional procedures MRI is predominantly applied for the planning of surgical procedures based on high-resolution volume imaging. Recently, MRI has been introduced for the guidance of ablations either by cooling or heating, and some initial steps have been taken to apply MRI for the guidance of intravascular procedures (see Figure 8) such as stent placement and dilatations.

The major challenges in MRI are in the field of dedicated magnet designs especially so-called open magnets, the development of application specific acquisition techniques, further reduction of the image acquisition times while maintaining the signal-to-noise ratio, and the investigation of technologies providing MR-visible interventional devices and the ability to automatically track these during imaging.

5 Ultrasound

Ultrasound imaging is advancing rapidly. New concepts such as harmonic imaging utilizing the harmonic components of the backscattered signal instead of the base frequency has significantly increased the field of application of US especially in the cardiovascular arena. In combination with the recently introduced US contrast agents US appears to be the second candidate for acting as the one-stop-shop modality in cardio imaging with the exception that coronary arteries can currently not be foreseen to be assessable by this techniques. The major advantage of US appears to be its capability of providing 3D-data in real-time utilizing novel scan heads for direct acquisition of 3D data, its interactive nature, its capability of easily assessing flow (see Figure 11), and its cost advantage. Improved image quality is expected from real-time spatial compound imaging in which multiple views are combined in a geometrically correct manner to reduce specle.

The major challenges in the field of US will arise in further miniaturizing the entire equipment, the development of dedicated two-dimensional scan heads for providing real-time 3D images at an acceptable image quality level, and the further investigation of techniques providing quantitative physiological data.

6 Common

A common challenge for all modalities is the paradigm change from defining scan parameters such as slice thickness and orientation prior to scan to defining these parameters during the visualization and the integration of physiological and anatomical information. The resulting large data-sets (see Figures 4, 7) will on the one hand force further developments in the field of 3D volume visualization and on the other hand require further investigations of user-interaction concepts. Virtual fly-throughs through hose-like structures (see Figure 6) such as vessels, the so-called virtual endoscopy is expected to become a valuable diagnostic tool. Since the final goal will be to acquire this information in real-time as well as to perform a real-time visualization a further challenge will be the development of faster, possibly dedicated computer platforms.

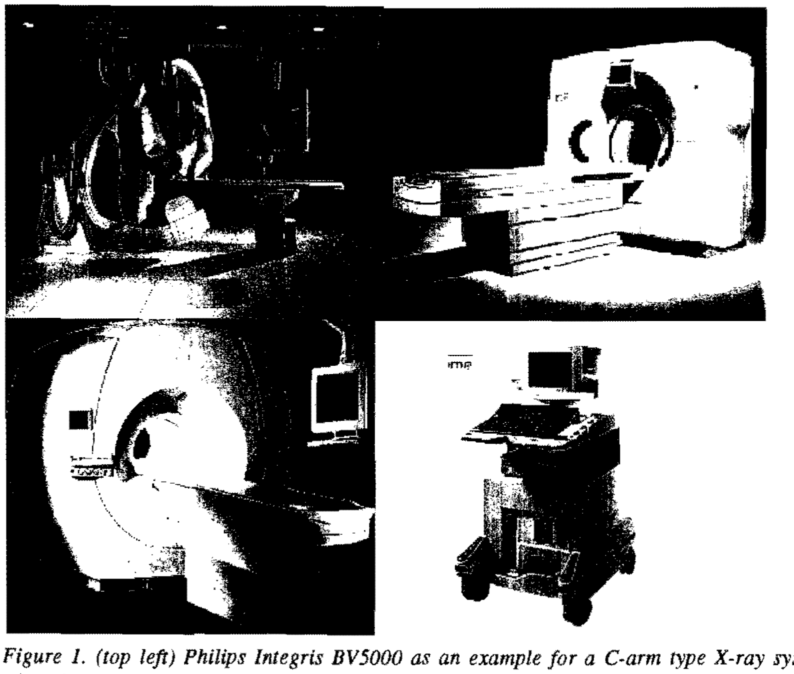

Figure 1. (top left) Philips Integris BV5000 as an example for a C-arm type X-ray system being capable of performing 3D-RA; (top right) PMS CT Vision Secura as a typical example for a CT scanner; (bottom left) PMS Gyroscan Intera as a typical example of a state-of-the-art MRI system; (bottom right) PMS ATL HDI 5000 as a typical high-end Ultrasound imager.

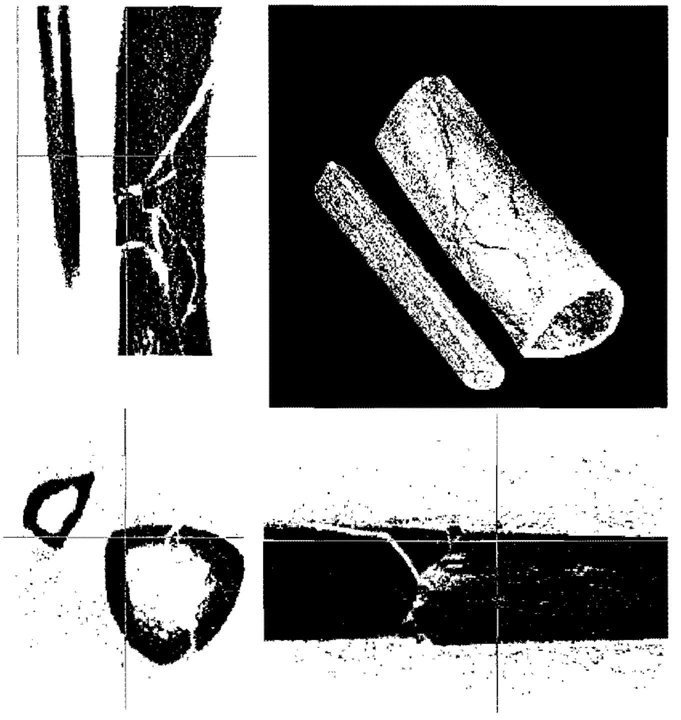

Figure 2. Example of a complex shin-bone fracture obtained by 3D-RX. Orthogonal slices (left, bottom) as well as the volume visualization (top right) clearly show the complexity of the fracture.

Figure 3. Complex arterial venous malformation in the head acquired by 3D-RA at an isotropic spatial resolution of $250\mu^3$.

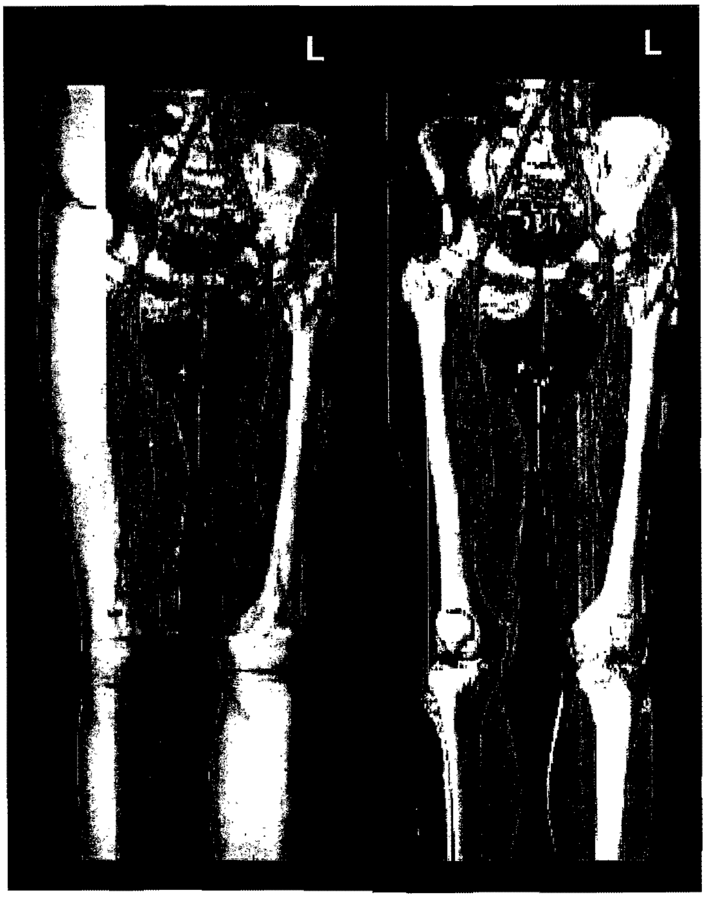

Figure 4. Composite of bone, blood, and soft tissue information with (left) and without (right) superimposed surface information. The underlying data were acquired by CT.

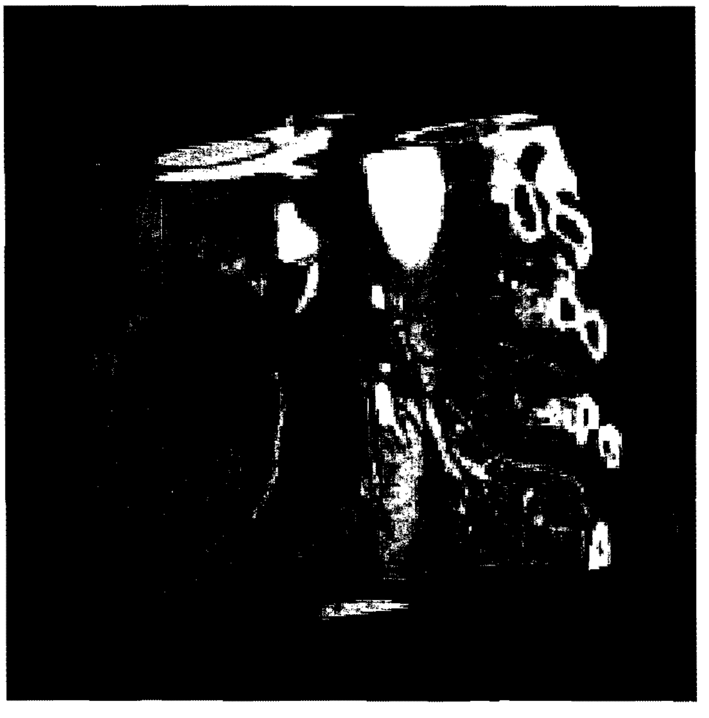

Figure 5. 3D visualization of the human heart and the main coronary arteries acquired by a 0.5s gantry rotation multi-line CT system. Data is courtesy of Siemens Medical Systems.

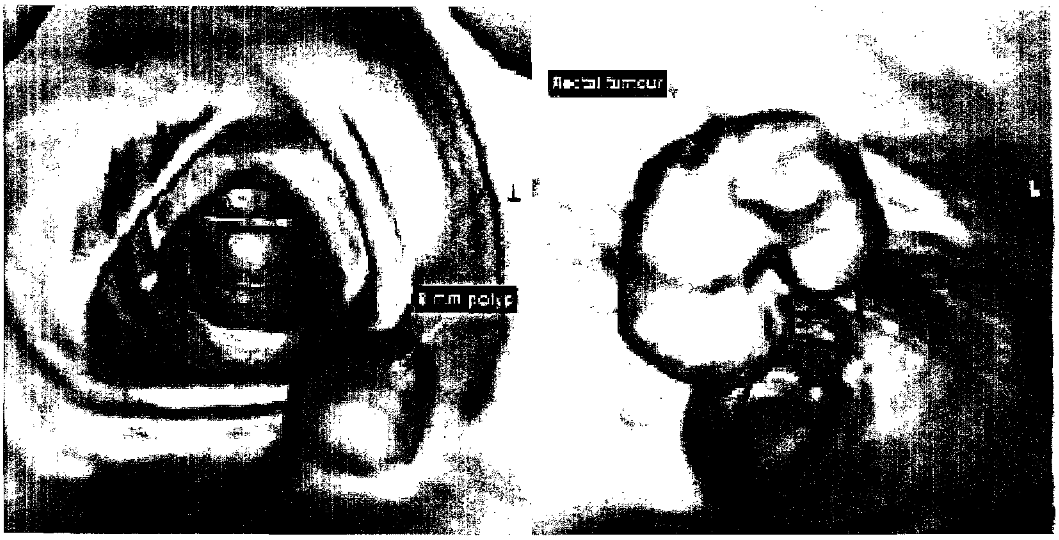

Figure 6. Virtual fly-through through the colon clearly showing a polyp (left) and the shape of a tumor (right).

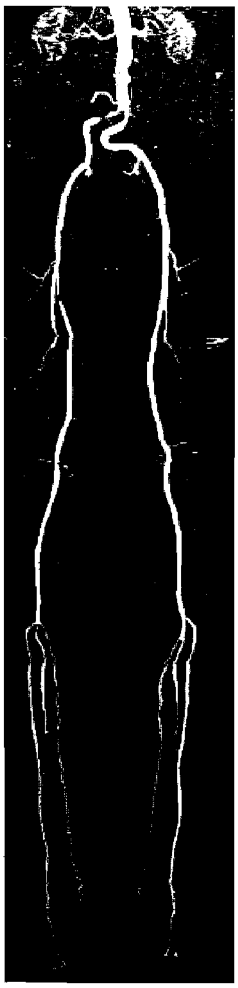
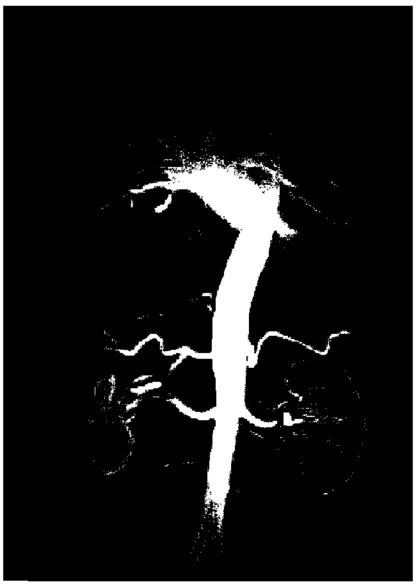


Figure 7. Volume visualization of the entire vascular tree of the abdominal aorta and the lower extremities (left), the entire aorta including the renal vascular structures (middle), and the aorta including the pulmonary vessels (right). The images were obtained by MRI.

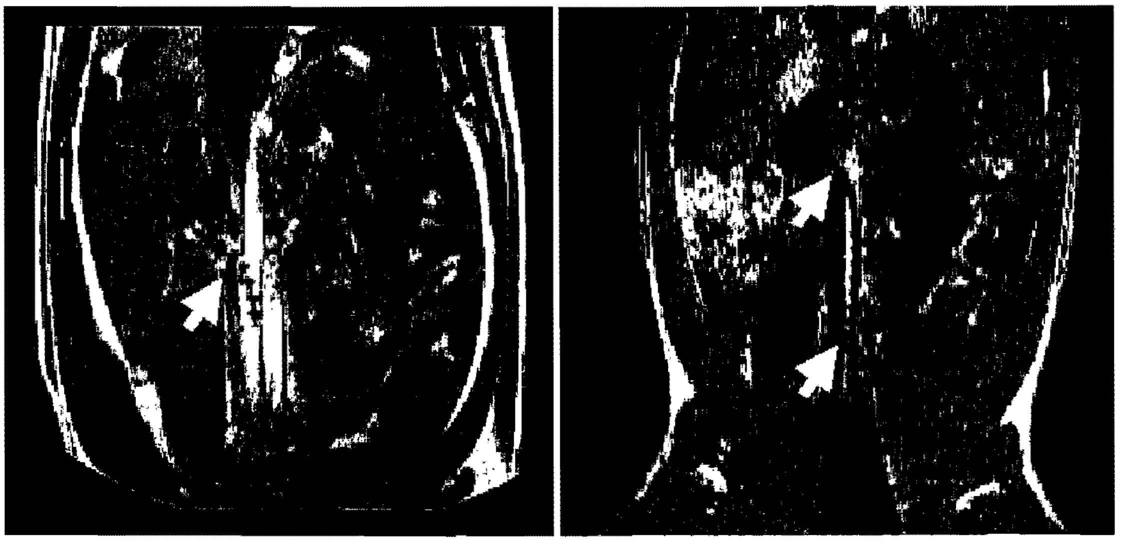

Figure 8. Guidance of intravascular procedures by MRI. Both images show an MR visible catheter (see arrows) which was feed into the renal arteries via the aorta.

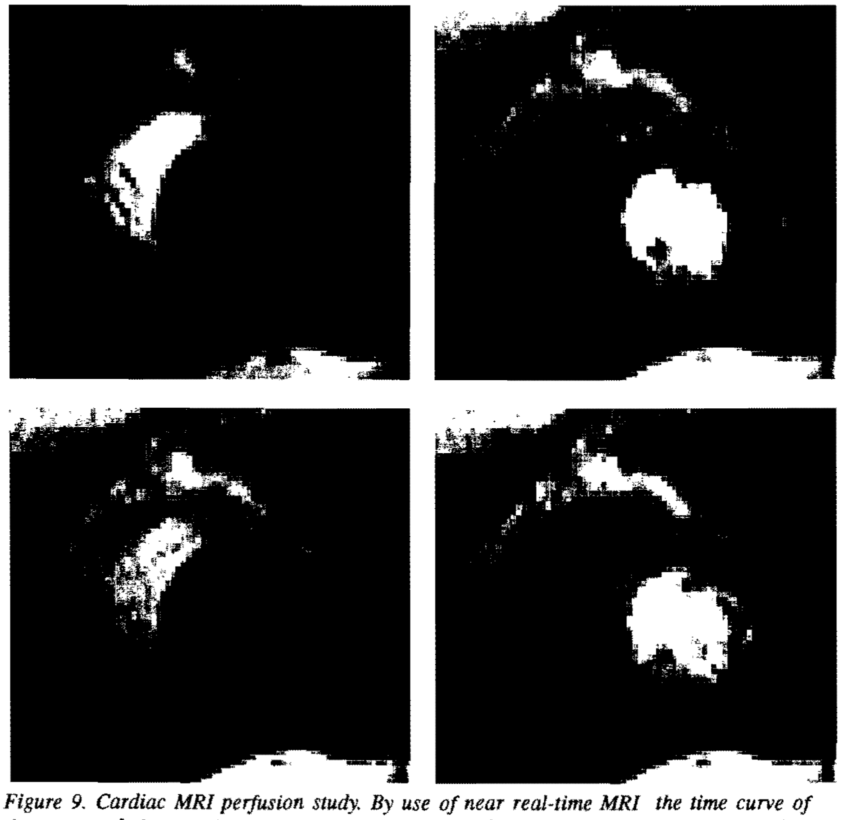

Figure 9. Cardiac MRI perfusion study. By use of near real-time MRI the time curve of the contrast bolus starting in the right ventricle (top left), followed by the left ventricle (top right), the myocardium of the left ventricle (bottom left), and the second pass of the contrast medium through the left ventricle (bottom right) can be clearly visualized.

Figure 10. 3D image of a fetal face obtained by US

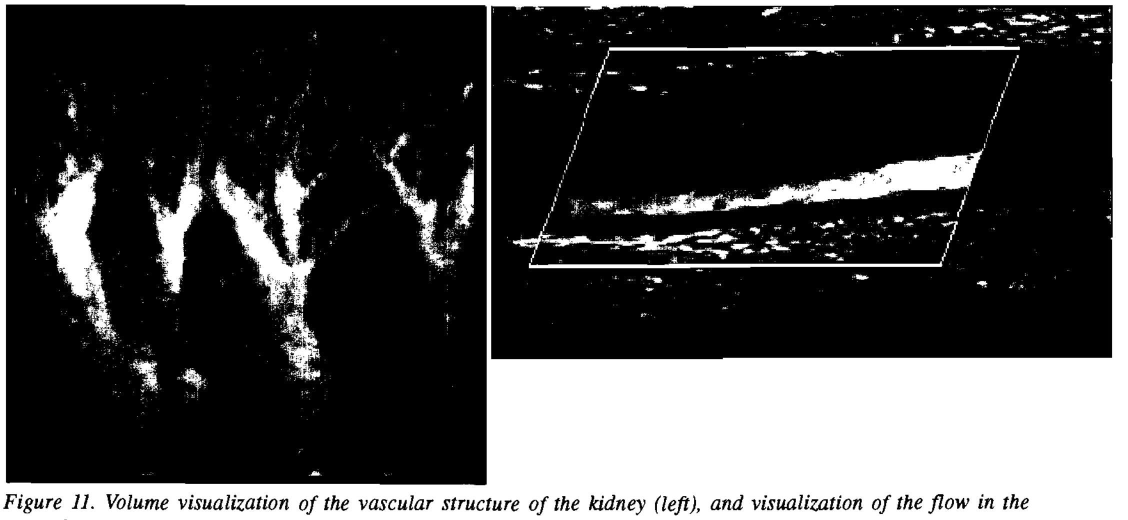

Figure 11. Volume visualization of the vascular structure of the kidney (left), and visualization of the flow in the carotid artery clearly showing a dissection.

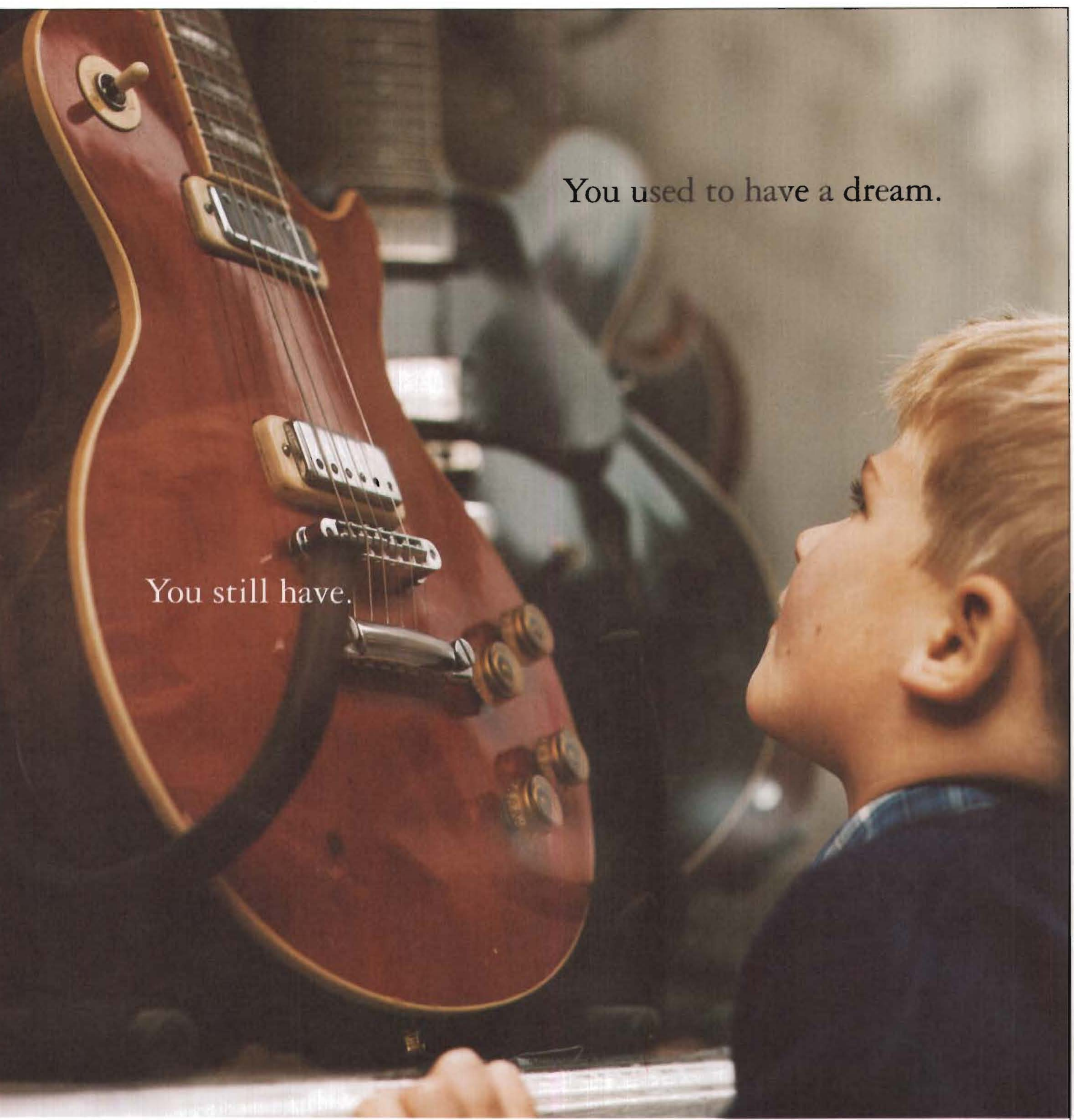
You used to have a dream.
You still have.

Biography

Dr. ir. J.M.L. Engels

Dr. J.M.L. Engels was born in Amsterdam in 1948 and lived and studied in Amsterdam till 1970. After the HBS-b exam at the Ignatius College he studied experimental physics at the University of Amsterdam. Served in the Dutch army for 1.5 year and subsequemtly moved to Eindhoven to start working at the Philips Research Laboratories in Waalre. At the Nat Lab an experimental study was done to measure the drift velocity of excess electrons in liquid Methane and Argon which resulted in a thesis and promotion at the Technical University of Delft. From the Research laboratory of Philips his career was continued at Philips Medical Systems as groupleader for the development and manufacturing of medical sensors for patient monitoring. Since the Medical Electronics activity was sold to Honeywell in 1981, he continued to work for Honeywell & Philips Medical Electronics till 1984. From then and up till know he worked again at Philips medical Systems in the development of MRI scanners at served many different positions. He started as groupleader and Clinical Scientist responsible for the Technical Application of MRI in academic hospitals. Subsequently, moved with his family to the USA to work in a hospital environment on the clinical MRI scanner for a period of 2 years. He founded the Frits Philips Research Center at Emory University in Atlanta. After his return to the Netherland he became groupleader and later on departmental manager in the MRI development organization. As such he has been responsible for the development of MR Methods (the scanning technique), the system design group, the Scan SW department and at this moment is responsible for the (pre)development of RF coils.

Magnetic Resonance Imaging, Technique, Application and Perspective

Dr. J. M. L. Engels
Manager MR Coils
Philips Medical Systems
Best, The Netherlands
Hans.Engels@Philips.com

1 Introduction

The growth of Magnetic Resonance Imaging (MRI) as a diagnostic modality in the hospital has been explosive in the past 17 years and is still going strong. MRI was a totally new modality for the physicians, not based on any form of x-ray scanning or Ultra Sound scanning, as a new imaging modality with totally different contrasts and views of the human body. MRI offered new capabilities to the physicians, especially the imaging of soft tissue, and is at this moment already completely accepted in the clinical routine practice. Most applications are still in the area of neuroradiology and to some extent in orthopaedics, body imaging and breast imaging. Newer application area's, e.g. cardiac imaging and interventional imaging, are being developed and undoubtedly will become routine practice some time from now. Also Magnetic Resonance Spectroscopy (MRS) is introduced in the clinical practice, but the routine application of this technique is still not wide spread.

Philips has been involved in the development of MRI and MRS from the beginning. At first at the research laboratories in Waalre (1972) and later at Philips Medical Systems. The first image of the brains of a human being (a colleague) was made in 1980. The first clinical MR scanner was installed in Leiden (AZL) in 1983. The system was built using a 0.15T magnet. Shortly after this installation the first systems at 0.5T were introduced, applying superconducting whole body magnets. Since then developments went on resulting in scanners based on magnets at different magnet field strengths, mainly 1.0T and 1.5T, which at this moment are the most wide spread type of systems used in the hospital. Research already went on at even higher field strength: 4T. All these magnets where superconducting cylindrical magnets, thus having a horizontal magnetic field. New developments introduced much shorter superconducting cylindrical magnets, still at the same high magnetic field strength. The shorter magnets are much friendlier for the patient, since the patient no longer will get the claustrophobic feeling when entered in the bore of the magnet.

Since a few years a new class of systems have been introduced. These are the open C-shaped magnets, which have a vertical magnetic field. These systems were running at lower magnetic field strength, 0.2T till 0.4T, although in the past few month also open systems at higher field strength, 0.7T till 1.0T, are introduced or at least are announced. The open C-shaped systems have the advantage of openness for the patient (the patient no longer is positioned in the bore of the cylinder, but is positioned between the poles of the magnet). The importance of patient comfort is so high that even the disadvantage of the lower magnetic field (and thus the reduced image quality or increased scan time) is accepted. Also the range of types of cylindrical superconducting systems is expanded. It is now expected that there will also be enough interest in routine clinical scanning with superconductive systems at 3T (about 30 of these scanners are already operational in the academic university hospitals). Finally, the research is at this moment experimenting with systems at a magnetic fields as high as 8T!

The development of new MRI systems is not only based on the introduction of new types of magnets. Also the development of the other major components of the system, the magnetic gradient field, the RF antennas, the data acquisition HW but also the basic computer, the capabilities of the acquisition SW and the SW for image handling and image processing show strong progress.

2 The Technique

The MRI technology is based on the well-known technique from physics, Nuclear Magnetic Resonance (NMR). For obvious reasons the N from Nuclear was omitted, but all started with the classic Spin Echo (SE) and Inversion Recovery (IR) NMR techniques. Newer was the addition of position and phase encoding via the application of switched gradient magnetic fields and gradient echo techniques (Field Echo FE), which formed the basis of the MRI imaging technique. MR images have contrasts based on the differences in relaxation times and density of the protons in the different tissues. The amount of signal in the echo is largely determined by the values of the T1 (spin-spin relaxation time) and the T2 (spin-lattice relaxation time). T1 and T2 are different depending on the chemical environment of the protons, the tissue or organ it is part of and whether the organ is healthy or not. The amount of image contrast and signal amplitude is also determined by facts such as: are the protons stationary or moving (blood, CNS fluid), what is the type of motion (diffusion, perfusion), is the tumour benign or malign, by possible chemical shift and susceptibility, is the functioning of the organ ok, etc.

The development of new types of magnets (as referred to in the introduction) resulted in new application areas. For instance the open magnets resulted in application of more interactive and interventional studies. The development of new data acquisition techniques, expansions of the SE and IR technique, resulted in an avalanche of new acronyms, such as Turbo Spin Echo (TSE), Turbo Field Echo (TFE), Echo Planar Imaging (EPI), Gradient Spin Echo (GRASE), etc. Mostly these newer techniques result in faster data acquisition or in optimised contrast for a specific type of study. They allow also a full rang of new applications expanding the capabilities of MRI scanners. Partly due to the introduction of these new measurement schemes, applications such as ‘functional imaging’ and cardiology became possible. A very important aspect of the data acquisition schemes, the MR methods of scanning, is compensation for motion. The ultimate challenge is the imaging of the moving heart. Current techniques allow data acquisition synchronisation with the heart beat and respiratory motion, but also navigation of the data acquisition to compensate for position changes during the scan. This made it possible to scan the coronary arteries of the heart.

Other developments are related to the gradient system producing the local magnetic gradient field essential for the localisation of the signal and thus for the image composition. For the cylindrical magnets, the gradient coils are also large cylinders, which fit the whole patient. It produces gradient fields in all three orthogonal directions. Thanks to this capability, it is possible for MRI to acquire images in all (even oblique or double oblique) planes, at all positions of the patient. MRI is therefore capable of scanning from head till toe and applications of all anatomy can be found in the literature. In view of the required switching times and signal amplitudes of the gradient system, this part of the systems is almost as expensive as the magnet. The past ten years the capabilities of the gradient systems expressed in terms of T/m/s are much improved. It is mostly the combination of the new scanning techniques with the new gradient system, which speeded up the MRI data acquisition. Virtually, there is no scan time limitation any more, i.e. images can be acquired in times as short as a few milliseconds. Since there are no motions faster then these milliseconds in our body, the limit has been reached (of course at the expense of image resolution and Signal to Noise Ratio of the image).

Finally, also the RF antennas referred to as the RF Coils, have improved considerably. The RF Coils have two functions in the systems. First it is used to emit the RF energy in order to excite the protons at the exact frequency of their rotation in the magnetic field (the Larmor frequency). Subsequently, the same RF coil or another dedicated RF coil is used to acquire the RF data (the echo signal) emitted by the protons in the tissue. The excitation is mostly done with a whole body transmission coil, where the challenge is to produce a homogeneous exception field in the area of interest in the body. New developments for this transmit coil are in the area of coil design and high power handling. For the receive RF coils the development is more found in the optimisation of the coil design for the anatomy studied. In the basic system, the whole body transmission coil can also be used for reception of the signal. Obviously, more signal can be obtained with dedicated receive RF coils positioned near the anatomy studied. As a result a whole range of optional receive only RF coils is available (Head coil, Knee coil, cardiac coil, abdomen coil, etc). Integration of electronics in the coils (preamplifiers, malfunction circuitry, coil element selection), multi element coils (linear, quadrature, phased array) are the areas where further improvement is to be expected. Especially, the combination of electronic and mechanic requirements, together with the fact that these RF coils are to be positioned on the patient and are shaped optimally for the anatomy to be scanned makes the development and production of these RF coils an interesting part of the MRI development activity.

All these HW and MR scanning methods related developments allow many different types of scans on the system and open up a lot of new application areas. A very important aspect hereby is the amount of data that becomes available and the presentation of this data to the physicians. First of all the acquired original data in the frequency domain must be reconstructed in order to create images from this data. The reconstruction basically is the Fourier Transformation of the spectral data into time and position related data, which is represented as the images of each scan. Reconstruction speed is very important. The images must be presented in the viewing station almost immediately after the scan (such that the next scan can be based on the results of the previous scan). With all the new HW capabilities, the amount of data (i.e. the number of images per scan, the image resolution, the specific information in the images) grows steadily and creates an on-going competition between the reconstruction development team and the data acquisition team. Furthermore the information in the images searched for, may become visible only after data processing of these images (subtraction of images, manipulation of 3D data sets, filtering, etc.), so also processing time becomes critical.

3 Application areas

The acceptance of MRI by the medical world and the large number of different application areas are a guarantee for the continuity of MRI in the hospital environment. In the early days MRI was mainly applied for neuroradiology (head and spine studies) since it offered optimal contrast as compared to the existing (X-ray, CT) techniques and could visualise areas which could not be imaged earlier (Ultra Sound). In addition, the fact that the head or spine could be fixated easily was very important since in those days the examination still could take up many, many minutes (the patient is obviously not allowed to move during the scanning time). The development of data synchronisation techniques (cardiac triggering, respiratory motion gating) and the capability to compensate for patient motion (cardiac and respiratory motion, flowing blood or spinal fluid) and the modern speed of the data acquisition (selectable between minutes, seconds and even milliseconds) allows applications in many other areas. Patient movement is still a problem but this is small as compared to the problems in the early days. In fact also MRI techniques were developed specifically making use of the fact that some protons are not stationary in the human body. The most concrete application is the study of angiography, whereby the flowing protons in the blood create extra contrast in the image (in fact all signals from the stationary protons in the tissue is suppressed and only the angiogram remains).

In addition to the HW and SW developments which enlarge the capabilities of the MRI scanner and in spite of the fact that the protons in the human body create enough signal and signal contrast, the introduction of contrast agents cannot be stopped anymore. Many different types of contrast agents are available, contrast agents which highlight the blood (blood pool agents), which visualise the functioning of organs and which distinguish between healthy and or sick tissue. The effect of the contrast agents can be a further reduction of the scanning time (due to the increased signal to noise) or a more specific diagnosis of the functioning of organs. Up till now the contrast agents for MRI are very patient friendly and do not pose an extra risk on the MRI study.

An important development for MRI is the study of the human heart, whereby the imaging of the coronary arteries is the ultimate goal. For the coronary arteries all challenges come together. The heart is the fastest moving organ in the body. It does not come back to the same position after every heart beat. The required resolution for the coronary arteries is less then 1mm. Frequently, the patient is very ill and not very co-operative (cannot be instructed to hold his breadth for a short period, has obstructed blood flow, irregular heart beat, etc.). Current techniques applying so-called navigator echoes are capable of correcting for displacements. We are now capable of imaging the coronary arteries of healthy volunteers in a few minutes time. A large number of academic hospitals are closely working together with the industry to further improve the technique. The co-operation with the hospitals is essential since this type of studies on healthy volunteers (our colleagues) are not representative anymore for patient studies and obviously, also the application of contrast agents is a barrier for volunteer studies. It is expected that cardiac studies including imaging of the coronary arteries will become routine practice one or two years from now.

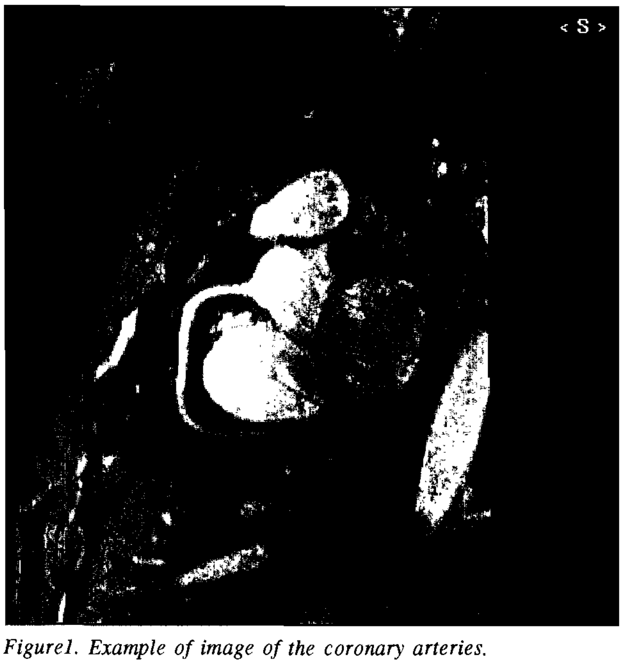

Figure1. Example of image of the coronary arteries.

4 Perspective

Already a few years ago, the application of MRI for functional imaging of the brain became possible and since then is being studied in the academic hospitals. Specific scan techniques are sensitive for the oxygenation and the blood circulation in the active parts of the brain and thus can visualise the activity of the brain. Using the eyes highlight the visual cortex, moving your hands can visualise the motor cortex, etc. For certain surgical procedures it is very important to know which part of the brain is still functioning well and should not be touched during the surgical procedure.

The realisation of very fast scan techniques together with the capability to present the result of the scan almost immediately, opens new application areas such as interactive MRI scanning. The physician can follow in real time the correct positioning of a needle for biopsy or catheter for surgery or medicaments injection and can be sure that it is not touching the critical tissue or takes the biopsy from the correct tissue. New techniques to visualise the tip of the needle or catheter are being developed. Another area will be the use of MRI during an interventional surgical procedure. Again the physician can see real time what he is doing, whether he has removed all the affected tissue. The success of this direct feedback to the physician has already proven to be very beneficial for the patient. Especially, the design of the more open C-arm type of magnets or the shorter cylindrical magnets allows these interactive studies.

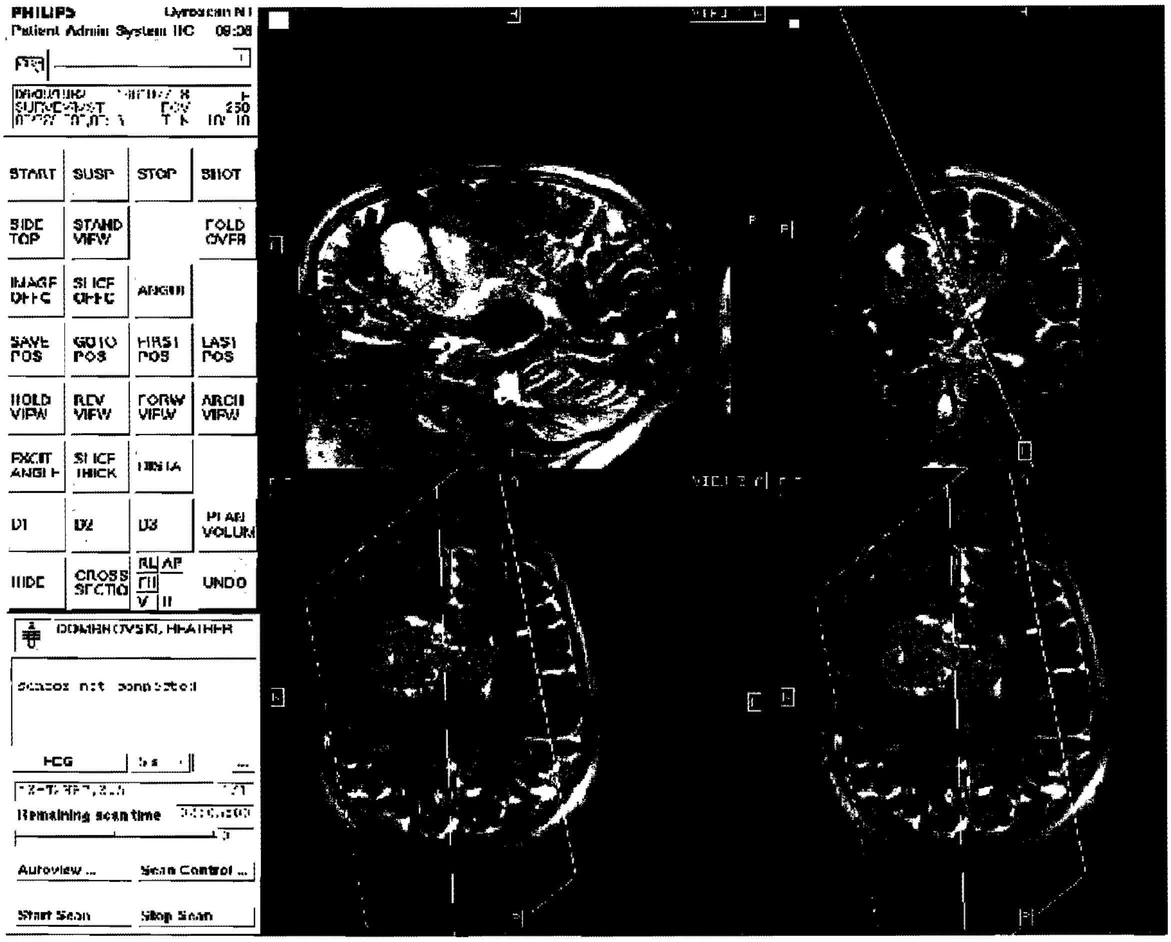

Figure 2. Illustration of interactive MRI (single shot TSE scan in 0.66sec).

Clearly, the development of MRI scanners has not come to an end. Although the N from Nuclear is preferably avoided for medical diagnosis of the patients, NMR still is a very challenging technique for physicists, electrical engineers, SW and technical engineers to bring innovation into practice.

Twinning

Twinning is een business accelerator die investeert in veelbelovende innovatieve ICT start-ups en de groei van deze start-ups versnelt door middel van de Twinning formule: toegevoegde waarde leveren op cruciale succesfactoren, zodat de startende ondernemer een korte time-to-market heeft. Snelheid, lef en ondernemerschap vormen de basis van het succes van zowel Twinning als de Twinning companies. Twinning heeft inmiddels in 40 start-ups geparticipeerd.

Voor meer informatie over Twinning kunt u terecht:

www.twinning.com

of bij Twinning te Eindhoven 040 - 239 0500

Parallel Session 2

Industrial applications conducted by dr. ir. J.B.O.S. Martens

Biography

Dr. J.G.M. Schavemaker

John Schavemaker received his M.Sc. degree in computer science from the University of Amsterdam, The Netherlands, in 1994. His thesis was entitled Segmentation in morphological scale-space. In 1999, he received his Ph.D. degree from the Delft University of Technology, The Netherlands, for a thesis on document interpretation applied to public-utility maps. He currently works at the TNO Physics and Electronics Laboratory. His research interests include image processing, document processing, and computer vision.

Infrared processing and sensor fusion for anti-personnel land-mine detection

John Schavemaker, Frank Cremer, Klamer Schutte and Eric den Breejen
Electro-Optical Systems, TNO Physics and Electronics Laboratory
P.O. Box 96864, 2509 JG The Hague, The Netherlands
phone: +31 70 374 0860, fax: +31 70 374 0654, Schavemaker@fel.tno.nl

Abstract
In this paper we present the results of infrared processing and sensor fusion obtained within the European research project GEODE (Ground Explosive Ordnance DEtection system) that strives for the realization of a vehicle-mounted, multi-sensor, anti-personnel land-mine detection system for humanitarian demining. The system has three sensor types: an infrared camera, a ground penetrating radar and a metal detector. The output of the sensors is processed to produce confidence values on a virtual grid covering the test bed. A confidence value expresses a confidence or belief in a mine detection on a certain position. The grid with confidence values is the input for the decision-level sensor fusion and provides a co-registration of the sensors. We describe the methods TNO-FEL developed for the processing of infrared (3-5 μm) data to produce confidence values. We show results of experiments with infrared processing and sensor fusion on real sensor data. The performance of the processing and fusion are measured with the SCOOP evaluation method that yields a less biased probability of false alarm by taking into account the spatial arrangement of false alarms.

Keywords: AP land-mine detection, infrared processing, sensor fusion, performance evaluation.

1 Introduction
The existence of (abandoned) land mines in a large number of post-war areas forms a major threat to human lives in these areas. The majority of these minefields is currently cleared by manual prodding, which is a very slow and tedious process and which cannot circumvent that the number of active mines is still worldwide increasing. As such, the detection of land mines by any (technical) means is an important research issue.

Current research focuses on the improvement of existent sensors [6] and the combination of multiple sensors (i.e. sensor fusion) to land-mine detection [2, 3, 8, 4, 1, 12]. The use of one sensor is generally believed to be insufficient for land-mine detection meeting the requirements of humanitarian demining for the reason that a single sensor has a false-alarm rate which is too high or a detection rate which is too low. The aim of sensor fusion is to make higher probabilities of detection (P(d)) possible with a lower probability of false alarms (P(fa)). In order to combine or fuse sensors, the sensor readings of the different sensors must be converted to a common grid and common confidence values. We show the processing steps taken for the infrared camera.

2 Data Acquisition
The experiments are based on data acquisition at the test lane of THOMSON-CSF DETEXIS, Paris, France (see also [8]). This test lane measures 25 by 1 square meter and contains 26 mines that are either buried or laid on the surface. For more information about the mines, see [10]. Additionally, the lane contains six false-alarm objects. Tables 1 and 2 give details on the mines and false-alarm objects.

Object	Name	x [m]	y [m]	Metal	Size	Depth
1	MAUS 1	0.50	0.25	low	large	surface
2	Mle 59	0.75	1.13	no	small	slightly buried
3	Mle 72A	0.25	1.75	low	small	surface
4	VS 1.6	0.50	2.63	low	large	buried
5	PFM 1	0.75	2.88	high	large	surface
6	*Foot print*	0.25	3.88	no	large	surface
7	*Cartridge case*	0.50	4.50	high	small	slightly buried
8	MK 2	0.25	5.38	high	small	buried
9	Piquet 62	0.75	6.25	no	small	surface
10	Mortar 60	0.50	7.25	high	large	buried
11	MD 82B (M14)	0.25	7.63	low	small	suface
12	*Cylindric print*	0.50	8.50	no	large	surface
13	Trip wire	0.75	9.50	high	small	surface
14	PRB 409	0.50	10.38	low	large	slightly buried
15	Mle 51	0.75	11.50	no	small	surface
16	Mle 72A	0.25	12.50	low	small	surface
17	TS 50	0.50	13.50	low	large	slightly buried
18	Mle 59	0.25	14.50	no	small	surface

Table 1. Objects *1 18* in the bare agricultural area in the test lane (continued on Table 2). The items in italics are false-alarm objects.

The test lane is divided into three parts with different types of terrain. The first part is bare agricultural ground, the second part is a vegetation area, and the third part is bare sand. The agricultural part is 15 meter long, the vegetation part five meter, and the sand area is also five meter long. For the measurements, the sensors were one by one attached to a trolley and moved over the test lane. The applied sensors were a dual-frequency metal detector of Förster, a mid wavelength band (3-5 μm) infrared camera and ground penetrating radar of Emrad. To perform decision-level sensor fusion, the raw sensor data is processed and mapped to obtain decision-level data on a reference grid. The sensor processing results in confidence levels on a grid with grid cells of 2.5 × 2.5 cm. This grid cell size ensurexs that there are even multiple cells over the smallest land mine.

Images of the infrared camera in the wavelength band 3-5 μm were recorded and pre-processed by Marconi Communications. The mines in these images have a higher apparent temperature (and thus a higher intensity in the image) then their surrounding.

3 Performance evaluation

For a comparison of performance, Receiver-Operator Characteristics (ROC) curves are used. In a ROC curve, the detection rate is plotted as a function of the false-alarm rate. The detection rate is defined as the fraction of the detected mines. The number of false alarms per unit area is calculated using the SCOOP (Split Clusters On Oversized Patches) [8] evaluation method. The name SCOOP refers to the scoop size area that need to be checked by the mine-clearance personnel, it is typically set to an area of 20 by 20 cm^2.

Object	Name	x [m]	y [m]	Metal	Size	Depth
19	PMN	0.75	15.50	high	large	surface
20	TS 50	0.50	16.50	low	large	slightly buried
21	*Stone*	0.75	17.25	no	large	buried
22	Coca cola can	0.25	17.75	high	large	slightly buried
23	Trip wire	0.75	18.13	high	large	surface
24	VS 69	0.25	18.50	high	large	surface
25	VS 2.2	0.75	19.25	low	large	buried
26	HEC3A1	0.50	19.50	low	small	surface
27	Mle 51	0.25	20.38	no	small	slightly buried
28	Mle 51	0.75	21.25	no	small	slightly buried
29	*Chewing gum paper*	0.25	21.75	low	small	buried
30	*BLU 62*	0.75	22.50	high	small	slightly buried
31	*Mle 59*	0.25	23.38	no	small	slightly buried
32	*PMN*	0.75	24.25	high	large	surface

Table 2. Objects in the test lane (continued from Table 1). Objects *19 26* are in the vegetation area and objects *27 32* are in the bare sand area. The items in italics are false-alarm objects.

The flowchart of the SCOOP evaluation method is shown in Figure 1. The grid cells which have a confidence value above a threshold are clustered. Every cluster is treated differently depending on whether it contains one or more mines. If a cluster does not contain any mines, it is counted as a number of false alarms equal to the number of scoops it contains. Clusters with one or more mines that are larger in area than the product of the number of mines and the scoop size also contribute to the number of false alarms. In this case, the number of false alarms is set equal to the cluster area divided by the scoop size minus the number of mines. The method is repeated for different threshold values to obtain a number of ROC points. The SCOOP evaluation method results in a percentage of detected mines as a function of the number of false alarms per unit area. This kind of performance measure is requested by the demining experts as an indication of the reduction in workload. It takes into account that more time is needed to reject false alarms occupying large areas (multiple 'scoops') than false alarms occupying small areas.

4 Infrared image processing methods

In this section we describe two methods for mine detection using infrared data. The processing methods described here made the infrared camera the best sensor of the GEODE sensor platform, as shown in the experiments section. The methods rely on the principle that the mines have a higher (apparent) temperature than their surrounding. This is reflected in a higher intensity in the infrared image. In Figure 2(a) the infrared image data is shown for the GEODE test lane. One can clearly distinguish some of the mines listed in Tables 1 and 2 (the origin is in the bottom left corner). Note that depending on the demining scenario (type of soil, time of day) the mines can also have a lower apparent temperature. In that case, one has to use negative contrast.

As there is a correlation between apparent temperature and mines an obvious choice for the conversion of sensor data to confidence levels is to use the raw infrared data as confidence levels. Because the spatial resolution of the infrared camera does not match the resolution imposed by the 2.5 × 2.5 cm grid cells for sensor fusion, the infrared data must be resampled. The ROC for mine detection using an infrared camera can then be calculated using the above-mentioned SCOOP algorithm, the result is shown in Figure 4(b). The ROC expresses mine detection as a function of false alarms for different global thresholds on the grid with confidence levels, i.e. infrared image data.

However, global thresholding does not take into account the changing surroundings of mines. For instance, the vegetation area of the test lane is much colder than the agricultural and bare sand area and global thresholding cannot account for that. As such, our proposed methods apply local contrast enhancement to make them invariant for the local background intensity. Furthermore, global thresholding would not reduce the number and size of false alarms. Our proposed methods perform false-alarm reduction by selecting blobs on morphological and size attributes. In order to do so, some a priori knowledge on the scoop size is used.

In the following sections we describe our proposed methods. The methods result in some different operating points (a certain detection rate with a certain number of false alarms) on the ROC.

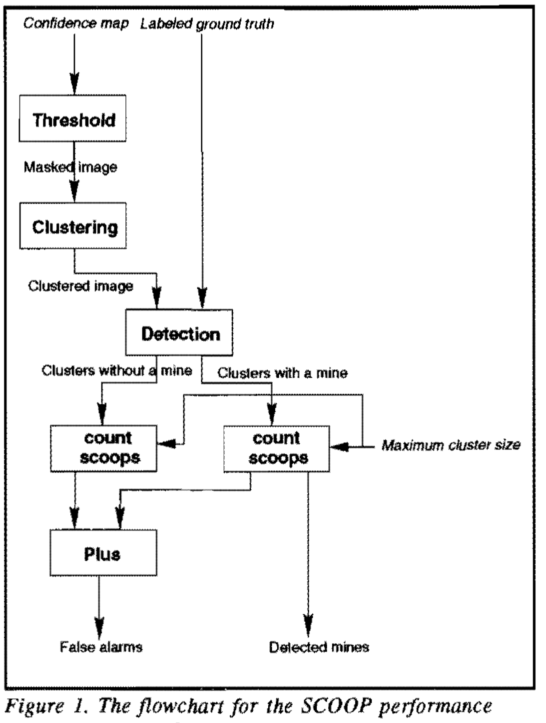

Figure 1. The flowchart for the SCOOP performance evaluation method.

4.1 Method 1

Method 1 is a sequence of resampling, blob search and contrast enhancement. It consists of the following processing steps:

1. resampling : reduce the size of the infrared image to GEODE standard grid size by resampling the image. The resampling is done by selecting the local maximum in the image data for each grid cell.

2. blob search : search in the resampled image for blobs with a positive contrast. Blobs are generated by applying all possible thresholds to the image. Select those blobs whose size is between $l \times l$ and $u \times u$. Optimal l and u on the GEODE dataset are found to be 9 and 9 respectively.

3. local contrast enhancement : calculate the local average intensity and local variance in intensity for every grid cell using a window size of 40 x 40 grid cells (one square meter). Normalize the intensity of each grid cell to its local mean and variance.

4. output : As output, give the maximum value calculated in step 3 for each blob found in step 2 to all grid cells in that particular blob.

The processing steps are visualized in Figures 2(a) to 2(d). The ground truth (mines) is shown in Figure 2(h).

4.2 Method 2

This method is an adaption of method 1. It outperforms the previous method for lower number of false alarms but is less good for higher number of false alarms. See also Figure 4(b) in Section 6. As such, depending on the required detection rate and number of false alarms, one can choose for one of the methods.

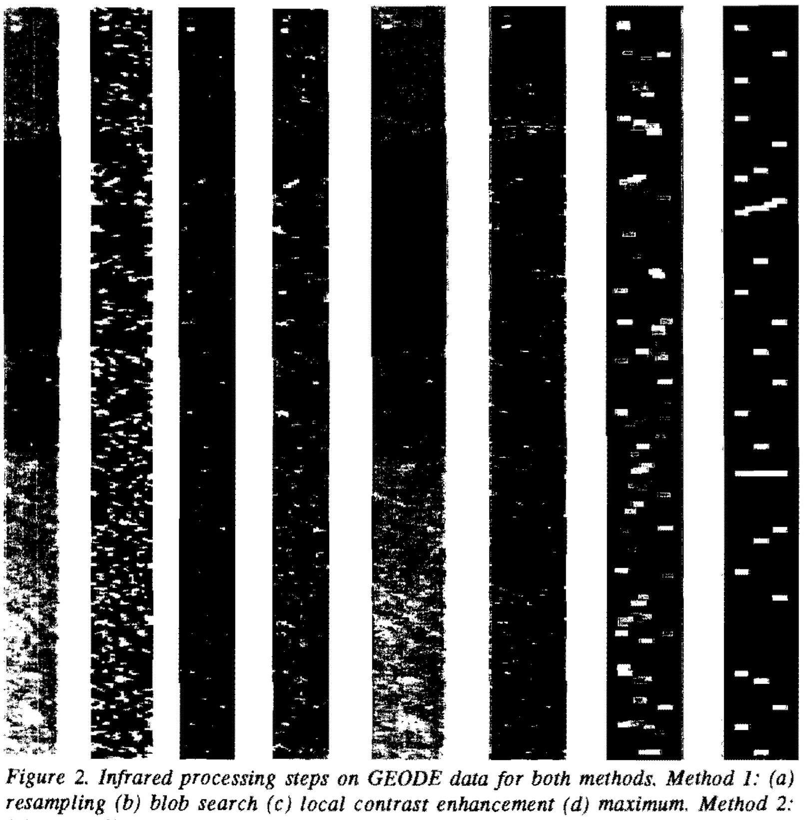

Figure 2. Infrared processing steps on GEODE data for both methods. Method 1: (a) resampling (b) blob search (c) local contrast enhancement (d) maximum. Method 2: (e) resampling (f) normalization (g) projection(h) Ground truth.

1. resampling : reduce the size of the infrared image to GEODE standard grid size by resampling the image. The resampling is done by selecting the local maximum in the image data for each grid cell.

2. local positive contrast enhancement : normalize the resulting resampled image to its local mean and local standard deviation (positive contrast). The window size used in the mean and standard deviation calculation is 40 × 40 grid cells, corresponding with one square meter.

3. multi-level thresholding : create for each threshold $t \in [0;255]$ a binary image of the resampled image. The result is a stack of binary images.

4. multi-level opening and closing : for each stack element (binary image) blobs are removed based on size and shape properties using image operators (binary openings and closings) from mathematical morphology [13]. The remaining blobs are reshaped into squares corresponding with the SCOOP size (8 × 8 grid cells).

5. projection of resulting levels on confidence grid : project all blobs in each stack element onto a confidence grid in which the confidence level is determined by the normalized intensity value of the blob.

The steps taken for method 2 are visualized in Figures 2(e) to 2(g). The false-alarm reduction is clearly visible as only a selected number of blobs remain present on the confidence grid.

5 Sensor-fusion methods

In this section we discuss our concept of decision-level sensor fusion. The advantage of decision-level fusion is that all knowledge about the sensors can be applied separately. Each sensor expert knows the most about the capabilities and limitations of their own sensor and can they can use this information to optimize the detection performance. The availability of this expert knowledge was the reason for choosing decision-level fusion for our application.

In our application, a fusion technique is considered to be a function that separates mines from background on the basis of the output of the different sensors. The output of each sensor is a measure of confidence in the presence of a mine and is called the confidence level.

The general layout of our concept of a sensor-fusion method is shown in Figure 3. The input of each sensor-fusion method is a confidence level per grid cell. A confidence level at a certain location expresses a confidence or belief in a mine detection on that position, but it is not necessarily a probability of detection

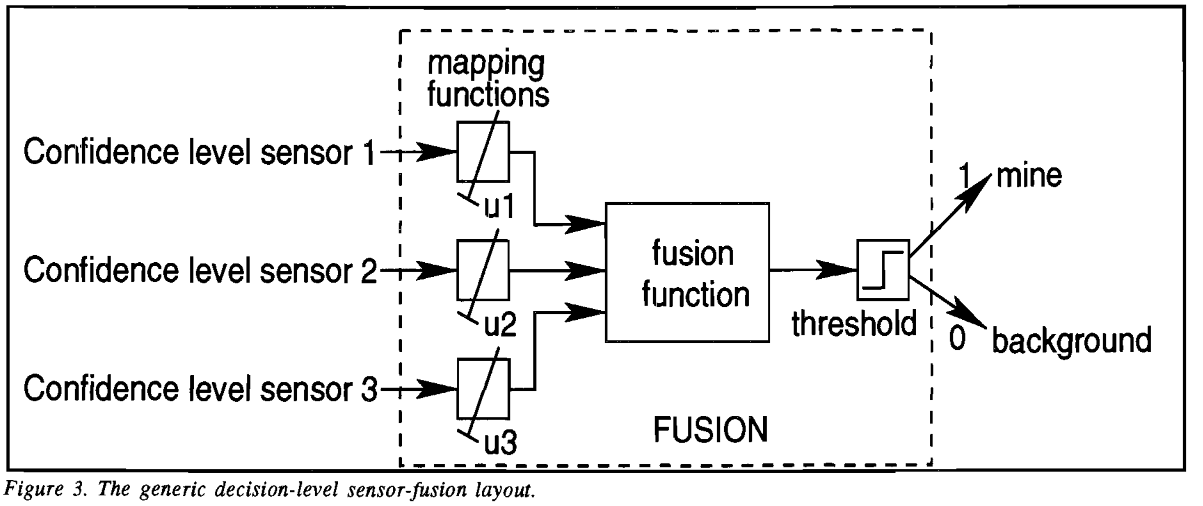

Figure 3. The generic decision-level sensor-fusion layout.

in a statistical sense. The confidence levels are used to indicate an order in probability of a detection of an object given a certain sensor. This means that a higher confidence level implies a higher probability of a mine, but these do not have to scale linearly.

The output of the fusion process is one for a detection and zero for no detection per grid cell. Each of the methods scales the influence of each of the sensors in a different way. This mapping requires one parameter (u_1; u_2; u_3) per sensor. This mapping may remove the differences in definitions of the confidence levels. The mapped inputs are combined in a fusion function to acquire a single value per grid cell. The mapping functions and the fusion function are given in Table 3. For a more detailed description of the mapping and fusion functions we refer to [3, 4, 9, 7, 5, 11].

6 Experiments

In this section we show results of experiments with both processing methods on the infrared (3-5 μm) dataset as recorded within the GEODE project. Furthermore, we show results of sensor fusion using the infrared camera, GPR, and metal detector. The results of both processing methods and sensor-fusion algorithms are evaluated with the SCOOP algorithm as described in Section 3 and [8]. The implementation of the SCOOP algorithm improves the ROC curves, as the false alarm surface and the number of false alarms are both taken into account.

method	mapping function	fusion function
best sensor	none	selection
naive Bayes	linear scaling	product
Dempster-Shafer	uncertainty level	Dempster's rule of combination
rules	linear scaling	summation
fuzzy probabilities	fuzzy membership	minimum
voting	threshold	summation

Table 3. The different functions for scaling the input and combining these into a single (fused) result.

6.1 Infrared processing

In Figure 4(b) we have shown the ROC curve of processing methods 1 and 2 for the infrared dataset of GEODE. The GEODE dataset has about 50 percent surface mines (see Tables 1 and 2) which can easily be detected without almost any false alarms. Additionally, the ROC curve in case of no processing (confidence levels are raw sensor data) is presented for comparison. Figure 4(a) gives the ROC curves of the other sensors on the same test lane, the ROC curve of processing method 1 is added for comparison.

From Figure 4 we may conclude that the infrared sensor outperforms the other sensors on this particular dataset. Only the metal detector has an operating point at 64% detection with one false alarm that is comparable in performance.

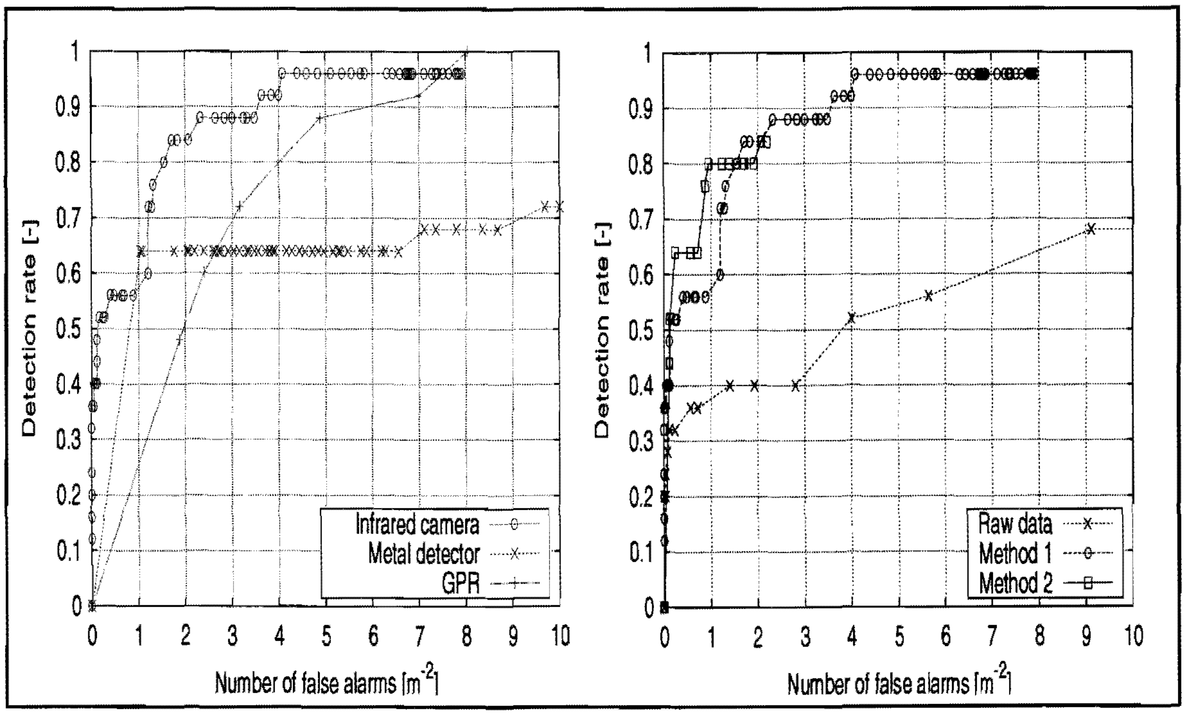

Figure 4. (a) ROC curves of the confidence levels of the infrared camera (processing method 1), metal detector and ground-penetrating radar. (b) ROC curves for infrared image processing of the GEODE dataset for no processing (global thresholding of raw sensory data) and methods 1 and 2.

6.2 Sensor fusion

For an unbiased comparison of sensor-fusion methods, with the limited data set we have, a leave-one-out evaluation method is used, see [14]. In the leave-one-out evaluation method, the parameters for each method are acquired on a training set, which contains all but one sample (a region containing one mine and on average 1 m^2). The acquired parameters from the training set are tested on the single sample left out (the evaluation set). This is repeated for all mines and their surrounding region as evaluation set. The results from the training and evaluation sets are summed and normalized to acquire a detection rate and number of false alarms per m^2.

The results of this leave-one-out evaluation in Figure 5 show that some of the sensor-fusion methods perform better than the best sensor on the evaluation set. Furthermore the method with most parameters, the rule-based method, performs best on the training set, but has the worst performance on the evaluation set. This performance loss is a confirmation of what we already expected, see [8]. The Dempster-Shafer implementation seems to be the most robust, while Fuzzy Probabilities gives very unpredictable results.

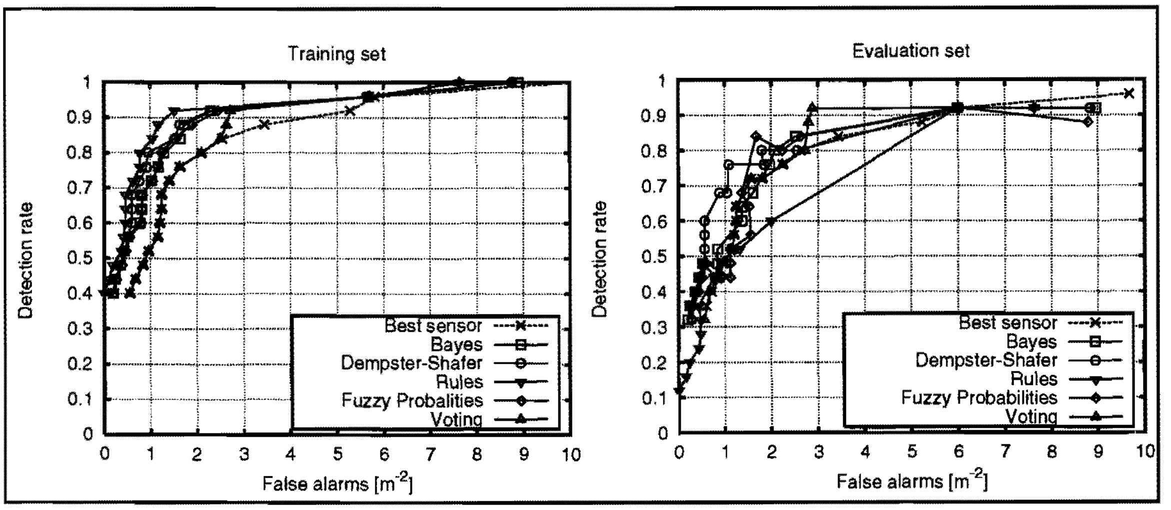

Figure 5. ROC curves for the different sensor-fusion methods evaluated with leave-one-out for the sensor combination low ground clearance GPR, metal detector, and infrared. The training set results are given in (a) and the evaluation set results are given in (b).

7 Conclusions

We have shown an increase of performance for the infrared processing for the GEODE dataset when compared with the original infrared processing. Our processing methods made the infrared sensor the best sensor for that particular dataset.

A point of concern is that the current implementations of processing methods are not computationally efficient and cannot, in their current state, perform in real time. We see, however, possibilities to increase processing speed by changing the implementation of the methods to an implementation based on DSP boards.

Another point of concern is the scenarios in which the infrared processing must operate. From the results of the GEODE and LOTUS [4] datasets we may conclude that infrared processing performs better for mines on the surface. We have the opinion that the processing may be optimized for different scenarios. Our design of the test lanes for the LOTUS trials is done in such a way that different scenarios and corresponding sketches can be used to determine the performance of infrared processing under different circumstances.

Concerning sensor fusion, the results of the independent training and evaluation sets, obtained by using a leave-one-out method, show that the Dempster-Shafer implementation performs better than the best sensor. The decrease in performance of the rule-based method is the largest, which is according to our expectations.

This method is clearly overtrained due to the many optimization parameters. The fuzzy probabilities method gives very unpredictable results. The voting fusion-method performs similar compared to the other methods.

The actual performance (if a very large data set is used) of these methods will be somewhere between the results of the training and evaluation sets. Our current experiments on the LOTUS datasets [4] can validate that assumption.

8 Acknowledgments

This research is partly funded by the European Union as ESPRIT project LOTUS, number 29812. The consortium consists of the following companies: Emrad limited, United Kingdom, Institute Dr. Förster, Germany,

THOMSOM-CSF DETEXIS, France and TNO Physics and Electronics Laboratory, The Netherlands.

9 References

[1] M. G. J. Breuers, P. B. W. Schwering, and S. P. van den Broek. Sensor fusion algorithms for the detection of land mines. In A. C. Dubey and J. F. Harvey, editors, *Proc. SPIE Vol. 3710, Detection and Remediation Technologies for Mines and Minelike Targets IV*, pages 1160–1166, Orlando (FL), USA, Apr. 1999.

[2] F. Cremer, E. den Breejen, and K. Schutte. Sensor data fusion for anti-personnel land-mine detection. In M. Bedworth and J. O'Brien, editors, *Proceedings of EuroFusion98. International Conference on Data Fusio*n, pages 55–60, Great Malvern, UK, Oct. 1998.

[3] F. Cremer, J. G. M. Schavemaker, E. den Breejen, and K. Schutte. Detection of anti-personnel land-mines using sensor-fusion techniques. In T. Windeatt and J. O'Brien, editors, *Proceedings of EuroFusion99. International Conference on Data Fusio*n, pages 159–166, Stratford Upon Avon, UK, Oct. 1999.

[4] F. Cremer, J. G. M. Schavemaker, E. den Breejen, and K. Schutte. Towards an operational sensor fusion system for anti-personnel landmine detection. In A. C. Dubey and J. F. Harvey, editors, *Proc. SPIE Vol. 4038, Detection and Remediation Technologies for Mines and Minelike Targets* V, Orlando (FL), USA Apr. 2000.

[5] B. V. Dasarathy. Decision fusion benefits assessment in a three-sensor suite framework. *SPIE Optical Engineerin*g, 37(2):354–369, Feb. 1998.

[6] W. de Jong, F. Cremer, K. Schutte, and J. Storm. Usage of polarisation features of landmines for improved automatic detection. In A. C. Dubey and J. F. Harvey, editors, *Proc. SPIE Vol. 4038, Detection and Remediation Technologies for Mines and Minelike Targets* V, Orlando (FL), USA, Apr. 2000.

[7] A. P. Dempster. Upper and lower probabilities induced by a multi-valued mapping. *Annals of Mathematical Statistic*s, 38:325–339, 1967.

[8] E. den Breejen, K. Schutte, and F. Cremer. Sensor fusion for anti personnel landmine detection, a case study. In A. C. Dubey and J. F. Harvey, editors, *Proc. SPIE Vol. 3710, Detection and Remediation Technologies for Mines and Minelike Targets IV*, pages 1235–1245, Orlando (FL), USA, Apr. 1999.

[9] K. Fukunaga. *Introduction to statistical pattern recognition*. Academic press, Inc., Boston, USA, 2nd edition, 1990.

[10] C. King, editor. *Jane's mines and mine clearance*, volume 98-99. Jane's Information Group, Surrey, UK, 3rd edition, 1998.

[11] L. A. Klein. A boolean algebra approach to multiple sensor voting fusion. *IEEE transactions on Aerospace and Electronic systems*, 29(2):317–327, Apr. 1998.

[12] P. B. W. Schwering, M. G. J. Breuers, and S. P. van den Broek. Sensor fusion algorithms for the detection of land mines. In *Proc. of Third NATO IRIS Joint Symposium*, pages 365–371, Quebec, Canada, Oct. 1998.

[13] J. Serra. *Image Analysis and Mathematical Morphology*. Academic Press, 1982.

[14] S. M. Weiss and C. A. Kulikowski. *Computer systems that learn*. Morgan Kaufmann

Publishers, 1991.

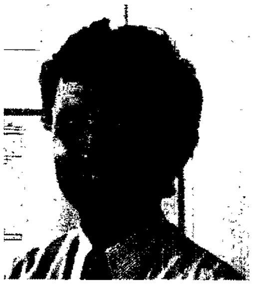

Biography

Ir. A. v.d. Stadt

Ir. Arend van de Stadt (1960) is the founder and managing director of Eagle Vision Systems bv. He received his M.Sc. in 1985 at the Department of Applied Physics of the Technical University of Delft. His thesis work was performed at the Pattern Recognition group in the area of 3D robot vision (at Philips' CFT Center for Manufacturing Technology in Eindhoven). After his study he joined the Robotics and Automation group of Philips Laboratories in Briarcliff Manor (NY, USA) were he worked in the research areas of robot vision, quality control and sensor development. This work resulted in a US Patent on his name. In 1991 he joined an industrial automation and engineering company in Utrecht, the Netherlands. Within this company he initiated and managed a growing number of machine vision related projects, resulting in a management buy out of all vision related activities in 1995. This marked the start of Eagle Vision, a technology company focussing on development and application of machine vision related technology for various markets. Mr. Van de Stadt's short term objective is to translate customer requirements into highly-advanced yet practical and industrial vision-based solutions. In the longer term, he wants to apply vision technology in other application areas as well (such as security and traffic).

Filled Bottle Inspector FBI™ for inspection of filled bottles

Ir A. v.d. Stadt
Eagle Vision Systems B.V.

1 Eagle Vision Systems B.V. overview

Eagle Vision develops, provides and maintains complete vision systems for consumer and manufacturing industries. These systems comprise colour video camera's, optics, illumination, processors and advanced image processing software. Multidisciplinary modules are integrated into an optimal total solution for the customer: from a robust industrial camera to self-learning sorting algorithms. A number of standard systems have been developed over the years, aiming mainly at the food industry. But since the systems are build-to-order in practice many times they are a variation on a theme. At anyway we provide a "turn key" solution, added with after sales service, parts and training possibilities.

The 5-year-old company is based in Naarden, and is employing around 20 people / FTE's like programmers, hardware and optical people, sales and service. There are –at this moment- 4 vacancy.

We are well known in the brewery industry for our innovative approach on automatic machine vision solution such as the FBI™ Filled Bottle Inspector, the MRI Mouth Rim Inspector, Scuffing inspection, SCOUT sorter for crates and label inspection etcetera.

Furthermore, according to the nature of these vision systems we often cooperate with OEM machinebuilders and general integrators in bigger projects where we take the responsibilities for what is often a keyfactor in the project: the automatic machine vision system.

2 Introduction and principle

Eagle Vision and GEI International Ltd. originally designed the system for Heineken and PA consultants with the objective to be capable of detecting (small) glass fragments in filled and capped bottles. This contamination causes a genuine consumer hazard whilst breweries are trying very hard to maintain the high quality image of a product packed in glass.

The working principle is that a bottle will be spinned (in the case of a typical beer bottle at around 1000 RPM) and stopped. In the vortex glass fragments have a different rotating momentum then beer (or other liquids) and "air" bubbles.

The bottles are transported in a carrousel mechanism with individually rotating tables. Per table position a camera and illuminator (to beam light in the bottom of the bottle) is mounted.

A great number of images are acquired during spinning and consequently stopping of the bottle. These images are compared (or rather: subtracted) in an intelligent way using unique software algorithm's. With this process the system is able to pinpoint contaminated bottles which are then led into a reject lane after the system.

In order to run at typical brewery and bottling line speeds of up to 60.000 BPH (bottles per hour) the system has currently 36 tables (with 36 camera's and illuminators). All these camera's generate some number of images and 6 IPP (Image processing PC's) systems plus 2 PC's (communication and backup) are integrated in one processor to accommodate high speed image processing. All the processing is done onboard, in the carrousel. The image processor therefore contains no moving parts (like harddisks). The illuminators and camera's are housed in rugged, specially designed "food-proof" IP 68 housings, whilst maintaining there modularity. In other words, should they defect they will be easily changeable for continuity of the process.

At this moment the system has proven it's capability of detecting 1 x 1 x 1 mm glass fragments minimum in lager type beers with green, brown or translucent glass bottles. Also thin neck fragments (typically called "Bird Swings") which sometimes occur at capping bottles are detected reliable.

The carrousel mechanism and bottle handling is manufactured by GEI Int. Ltd. The illuminators, cameras, software and PC's are made by Eagle Vision. In the current system (the first one has been installed at Heineken Zoeterwoude Holland over the last weeks) GEI is the main contractor.

Patents protect the system and its unique parts, the working principle and brandname.

2.1 (near) Future:

Clearly this first system is aimed at (and asked for as) high line throughputs of around 60.000 BPH. At this moment we are in discussion with our partner GEI on a "low end" system with the same functionality but with -for example- less camera positions. As the entire system is constructed modular this is possible. It could be used at smaller breweries and the wine and softdrinks industry.

Furthermore, Eagle Vision is also the Northern Europe distributor of DYLOG X-ray inspection systems (Dylog is the World's market leader in this field). By means of X-ray it is also possible to detect foreign bodies (such as glass, stone, metal, bone and some harder plastics, like PVC) in already closed containers or packages. Typical resolution of these X-rays in glass detection is 2 – 3 mm minimal parts. Dylog developed also the patented "double point of view" system, especially for babyfood- and liquid products.

Currently another new system is under development to inspect bottles under a 45° angle whilst turning the individual bottles upside down. The aim is to detect particles at 1.5 mm minimum at brewery speeds as well. Heineken, together with PA Consulting, has reviewed this option as well and consequently turned to a vision oriented system.

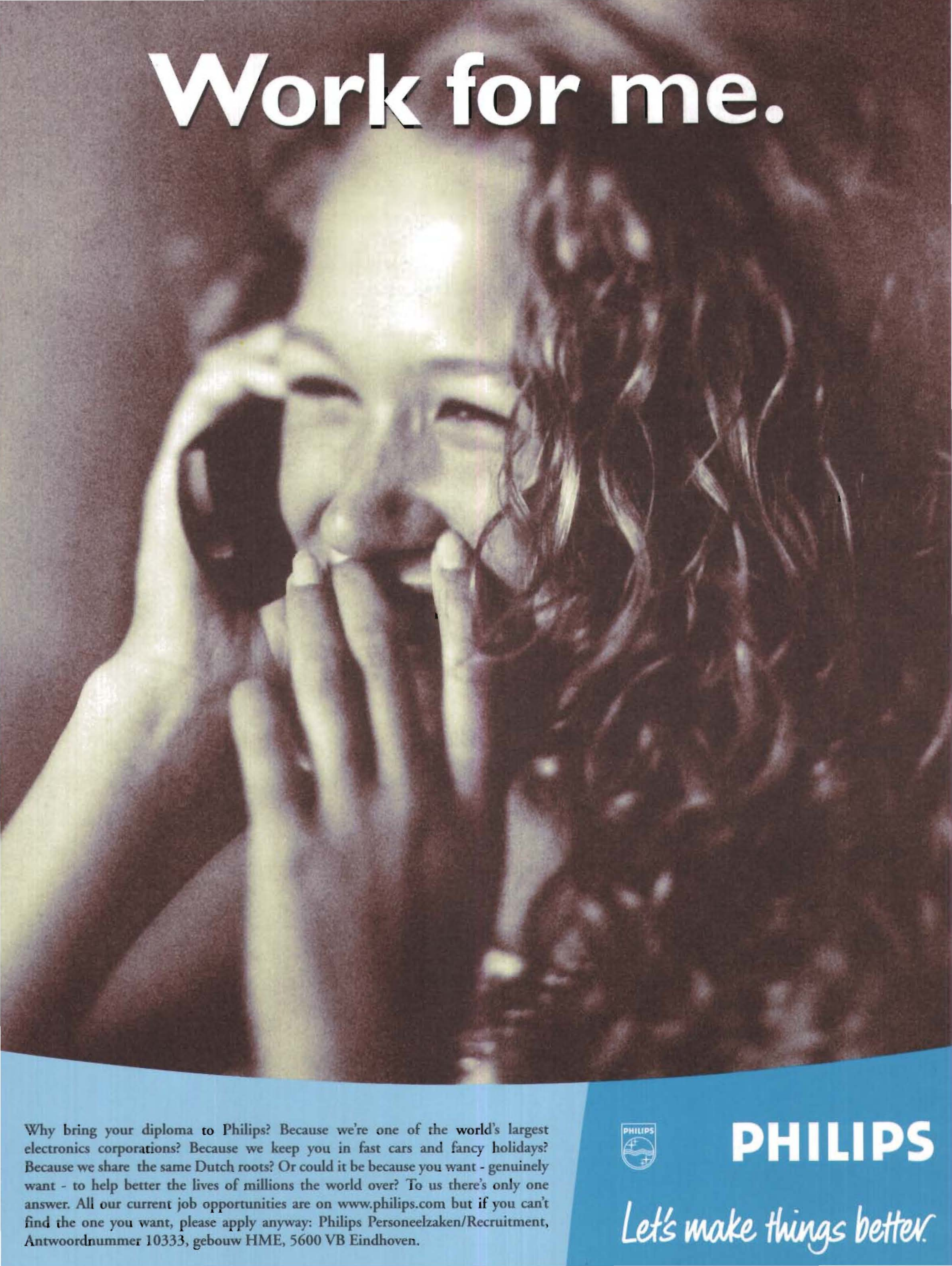
Work for me.
Why bring your diploma to Philips? Because we're one of the world's largest electronics corporations? Because we keep you in fast cars and fancy holidays? Because we share the same Dutch roots? Or could it be because you want - genuinely want - to help better the lives of millions the world over? To us there's only one answer. All our current job opportunities are on www.philips.com but if you can't find the one you want, please apply anyway: Philips Personeelzaken/Recruitment, Antwoordnummer 10333, gebouw HME, 5600 VB Eindhoven.
PHILIPS
Let's make things better.

Biography

Ir. C. Beumier

Charles Beumier was born in Mons, Belgium, in September 1964. He got the degree in electrical engineering from the Université Libre de Bruxelles (ULB) in July 1987. Since 1988, he has been working at the Signal and Image Centre (SIC) of the Electrical department of the Royal Military Academy of Belgium. He was first concerned with image acquisition and graphical user interfaces. Then he focused on Pattern recognition. From 1990, he was deeply involved in automatic face recognition, considering frontal, profile and volumetric approaches. Since 1999, he has been active in the field of humanitarian mine detection.

Automatic Face Recognition

Ir. Charles Beumier,
Researcher at the RMA/SIC
Beumier@elec.rma.ac.be

Abstract

This paper describes the activities of the RMA/SIC department in the field of Automatic Face Recognition, involving a frontal, a profile and a surface approach. After outlining the difficulties encountered while looking for robust lighting- and pose-invariant features in the frontal face analysis, a prototype for automatic profile identification is presented. This prototype benefits from the simplicity and quickness of contour analysis and allows to demonstrate real-time identification. This geometrical approach is further investigated by considering the capture and comparison of 3D facial surfaces. A cheap and fast 3D acquisition system has been developed and a recognition approach has been designed based on the extraction of planar profiles. From the presentation of the three approaches we conclude that a face recognition system should integrate 3D capabilities in order to benefit from the complementarity of the geometrical and gray-level information. Furthermore, the 3D analysis brings robust features and can help normalise a gray-level approach that would otherwise largely depend on illumination and point of view.

1 Introduction

Automatic face recognition has gained a large interest [Chellappa95,Samal92] this last decade for several reasons.

First, the ever increasing mobility of people raised the issue of improving security. Typical applications concern the access to buildings, networks or secured data.

Secondly, the computational power offered by nowadays computer makes possible to implement methods which were poorly tractable before.

Thirdly, although several biometrics solutions have been developed and commercialized, the face recognition advantage lies in the user acceptance. Unfortunately, its practical implementation is constrained by a wide variety of "real life" influences (pose, lighting, facial expression) so that the obtained performances are insufficient for most applications. Nowadays solutions are based on several modalities (image, speech, password or card) to cope with the current face recognition limitation.

2 Framework

We address the problem of face recognition in the context of access control. This leads to three simplifications.

The first one concerns the relatively high level of control during system installation. The camera can be positioned close enough to offer a good resolution of the acquired face, possibly with a simple background. Lighting conditions can be adapted to achieve good quality images.

The second simplification comes from the user cooperation. The user knows that he is checked and accepts the rules to be able to enter the building or to obtain the service. For example, he will adopt a correct attitude and pose and he will take care that disturbing artefacts like hat and scarf do not interfere.

Finally, the reference database used to check people identity is under control. This means that facial updates like beard, glasses or hair color can be handled easily thanks to the user cooperation.

3 Scenario

The typical scenario for a face recognition system consists of two steps.

The first one is the creation of a database of reference images or characteristics. This is done during the enrollment of each person to be recognized and with the supervision of a human operator.

The second step concerns the use of the system. An image of the person is taken and is compared with entries of the database, either in the form of images or subimages or thanks to the extraction of characteristics like the nose length, the distance between the eyes or the hair color. Based on the degree of resemblance, the person can be accepted, rejected or asked to supply further information in case of doubt.

Two different comparison approaches exist. In the first case, called verification, the person first declines his identity so that he can be compared with his own reference data in the database. The comparison issues a similarity measure which is compared with a threshold to decide for acceptance or rejection. In the second case, called identification, the comparison is made with the whole database in order to find the best match which is supposed to be related to the searched person if this match is good enough. Identification requires more comparison effort, especially for large database.

4 System Evaluation

Recognition systems can be evaluated according to several criteria [Jain99]. Let us mention the facility to extract information, the permanence of the extracted features, the user acceptability against the system and the recognition performances. The choice of a solution depends on the application and has to take into account the irritability of a person wrongly rejected and the penalty of accepting an imposter.

Scientific organizations often focus on the recognition performance. We decided to guide the research to achieve the best recognition performance, but keeping into account the time response, the hardware needs and the code simplicity.

The recognition performance is evaluated in terms of false acceptance (FA: the person is accepted although he should be rejected) and false rejection (FR: the person is not accepted, although he should be). Related to the number of tests and expressed as a percentage, we talk about False Acceptance Rate (FAR) and False Rejection Rate (FRR). Figure 1 depicts a typical 'ROC' curve, showing the operational points (FAR/FRR couples) for different values of the acceptance/rejection threshold. The curve expresses the natural compromise between a low FAR and a low FRR. Depending on the application and thanks to the threshold, one can choose to favour lower FAR, to reduce the risk of imposter accesses, or lower FRR, such as in forensic applications where we want to maximize the chance to identify a criminal. The Equal Error Rate (EER) is often given as an overall performance number. It corresponds to the operational point for which FAR equals FRR.

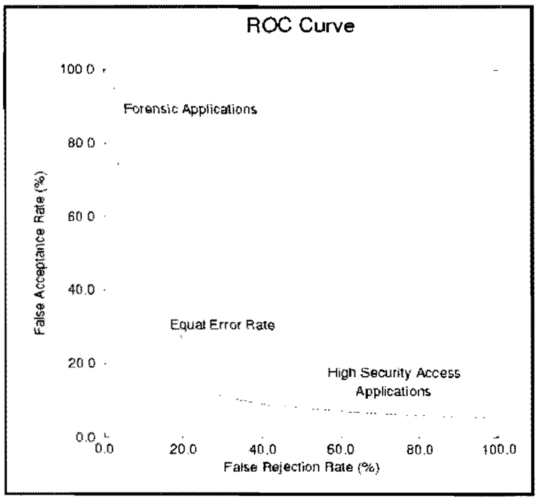

Figure 1. Typical ROC Curve showing the compromise FAR/FRR

5 Historic

The activities of the Signal and Image Centre in face recognition started in 1990 rather naturally with the study of frontal images. Although offering a fair success for a few persons, the frontal face analysis appeared to be much too dependent on head pose, lighting conditions and face changes (hairstyle or expression). Also, most of partial solutions to these problems implied high computational needs.

We thus started in 1992 a profile based study in order to develop a fast identification system, relying on the external contour of the profile, and little dependent on pose and illumination. The success of this geometrical analysis of the face made us consider in 1994 the facial surface as a 3D object, in order to get more geometrical information, independent from pose and illumination.

From 1995 till 1998, we participated to a European project of the ACTS programme (M2VTS: *Multi-Modal Verification for Teleservices and Security Applications* [Richard99]) which aimed at developing a multi-modal (speech and image) person verification system for teleservices and security applications. In this project, we realized a prototype for real-time profile identification [Beumier97] and we worked on the facial surface acquisition and analysis. We also studied the combination (fusion) of the different modalities.

Today, the activities in fusion are pursued with a study of the best combination of speaker and face recognition experts ([Verlinde00]).

6 Automatic Frontal Face Recognition

6.1 Motivations

Tackling the problem of face recognition from frontal images seems quite logical, as the frontal view is the normal presentation and offers many facial features. Cooperation from the user is natural. Two kinds of information can be exploited. On the one hand, each facial feature (eye, mouth, nose, hair, chin, ...) can be analyzed independently to look for discrepancies between test and reference images using criteria like length, area, shape or color. On the other hand, the spatial configuration of the different facial features leads to other personal characteristics.

6.2 Approaches

There are basically two different approaches to compare objects and in particular faces.

The first one, called global or 'holistic' considers the face image as a whole without trying to analyse its content. The utilized techniques encompass pixel correlation, artificial neural network with images as input pattern (see [Kohonen89,Stonham86]), or image transform such as the principal component analysis [Turk90], to name a few. The same techniques are advantageously applied to facial parts, usually rectangular areas around the nose, the eyes and the mouth ([Brunelli93,Beymer94]).

The second approach, called 'featural', looks for facial characteristics such as distance, area, shape or color measures. It typically analyses parts of the face such as the eyes, the nose, the mouth, the chin, and the hair. The comparison of the face is then translated into the comparison of the feature vector and classical classification techniques can be used to verify similarity (by techniques such as nearest neighbor, neural network or least mean squares).

The global approach has the advantage to process the whole image without a priori analysing its content. However, image computation is often heavy and important facial details relating to small areas collapse in front of large but non informative regions. The featural approach benefits from a more controlled strategy of analysis, although requiring more work from the developer and leading to application dependent solutions. Feature extraction also allows for information compression as a few features are expected to code most of the facial information. To be complete, let us mention the model-based approach [Mundy91, Yuille89, Wiskott96] which shares the advantages of the global and featural techniques. Global characteristics are present in the generic model. This model is adapted to a given image thanks to extracted features.

6.3 Difficulties

Several major difficulties complicate the frontal approach. First, the image quality largely suffers from the lighting conditions and the distance between the subject and the camera. Secondly, the 2-D image projection on the camera sensor of the 3-dimensional face depends on the relative orientation between the camera and the head ('point of view'). Thirdly, the person does not always adopt a neutral attitude (no emotion, with eyes opened and mouth closed). Finally, glasses, a hat and a scarf are likely to hide partial information and are not always easily handled. The last three difficulties can however be reduced thanks to the cooperation of the user.

6.4 Results

In our first experiments with Artificial Neural Network in 1990, a Kohonen map [Kohonen89, Perneel90] was tested with face images as input patterns. Although the recognition ability of the network was shown, this global approach revealed its limitations in dealing with illumination, rotation, scale and translation changes.

We then considered a featural approach about the configuration of facial components, where reference points were obtained from the vertical gray-level profile, horizontally centered around the nose region (see Figure 2). Although successful even with low resolution images, this implementation suffered from the limited number of available features.

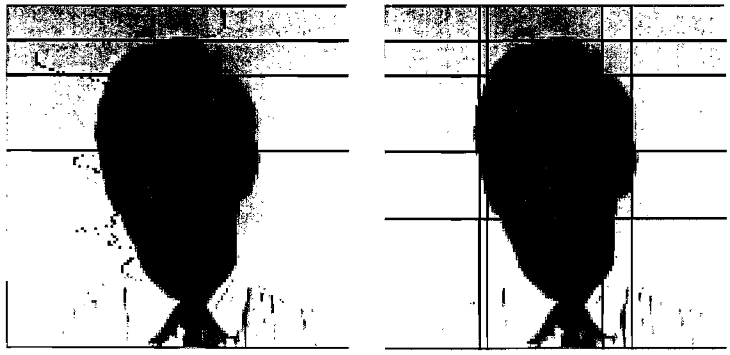

Figure 2. Vertical gray-level profile and vertical and horizontal references.

6.5 Conclusions

The problem of automatic frontal face matching is not easy to address, due to extrinsic (light, point of view) and intrinsic (emotion, changes, accessories) conditions. While basic features can be easily obtained (distances between facial parts, hair color, beard presence), their combination is not trivial as many features may be improperly measured or may vary significantly.

7 Automatic Profile Identification

7.1 Motivations

If a frontal image of a face can undergo large variations, a profile, on the contrary, remains rather stable in normal situations. The term profile used hereunder relates to the external contour of the head from side view and is composed of the forehead, the nose, the lips, the chin and the neck, most of which are rather rigid parts.

From the user point of view, the cooperation is easy. The user looks in a given direction, perpendicular to the camera, and preferably with his mouth closed.

Practically, the profile capture doesn't require illumination conditions which are difficult to satisfy and processing relates to a 1-Dimensional curve allowing for quick computation.

Figure3. a) Profile image b) contour extraction, nose and eye localization, feature extraction

7.2 Approach

The first step of profile recognition consists in extracting the external contour of the head profile. To simplify processing, we implemented a method based on a white background.

The second step is the extraction of characteristics. The contour is analyzed in terms of curvature and protrusion to localize the nose which is used as first reference point. The second reference point is the eye, obtained as the first concavity above the nose. These two reference points define a scale unit and a rotation reference. From the nose reference point, and at regular interval based on the reference scale, angle and curvature values are measured along the profile. Angles are given relatively to the direction nose-eye. The curvature values are derived from three neighbor points along the profile.

The third step is the profile comparison with reference profiles to identify the most similar person. We based our distance measure on the difference of angle and the difference of curvature values of corresponding points along the profiles. Using the very precise nose localization no translation adaptation has to be made.

The three steps have been designed and implemented to be very fast. On a Pentium 200 MHz, the acquisition, feature extraction and comparison with a database of more than 270 contour references take less than 250 msec. In continuous identification, the system delivers 4 identifications each second. For a natural pose of a few seconds, this allows to analyze more than ten system answers to reduce false rejections and false acceptances.

7.3 Results

A profile identification prototype has been developed with a PC, a camera, an acquisition board and a white wall as background. A database of 41 people with 5 to 10 shots per person has been acquired in a span ranging from a few days to a few months, depending on the availability of people. Considering half the entries as references and the other half for test, we reached a recognition rate of about 80 % (Equal Error Rate = 10 %). The same recognition rate was achieved with another database of 120 people containing one session used as reference and one as test, these sessions being acquired two months apart from each other.

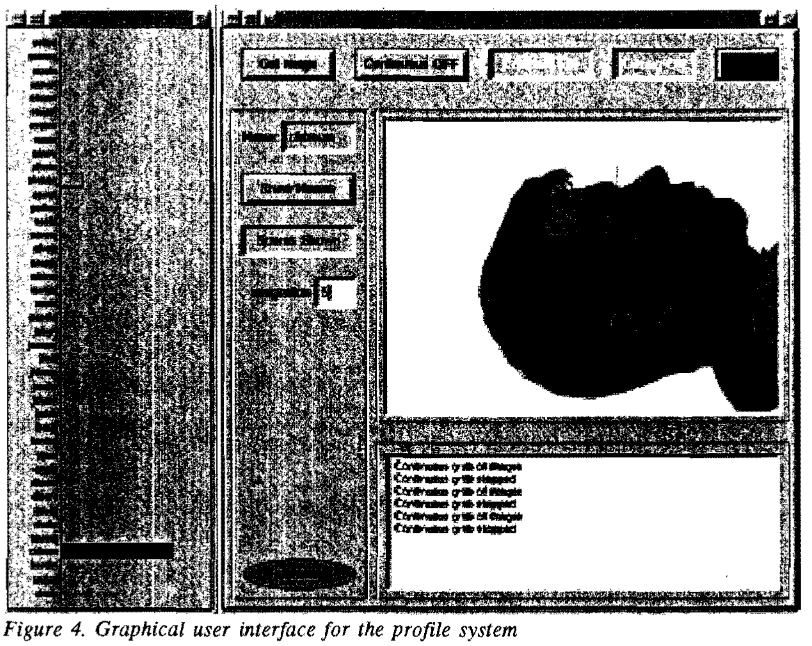

Figure 4. Graphical user interface for the profile system

As a second test, the available persons were asked to test the system in real time, considering all the entries of the database as references. For this a few seconds of presentation were necessary to obtain between 10 and 20 person identifications. If half or more of the identifications concerned the same person, this person was assumed to be identified (maybe wrongly). This temporal fusion reduced by far the false acceptance level (false acceptance occurs less often than right acceptance) and also false rejections because up to half of the identifications can be missed. After testing more than half of the persons present in the database and a few imposters, the EER achieved less than 4.0 %.

7.4 Conclusions

The developed profile prototype offers an easy and quick solution to the problem of automatic person identification. The user constraints are rather soft: looking in a general direction and taking glasses out, if any. The response latency amounts to a few seconds. The white background can be replaced by a static background if profile extraction is based on image difference.

One important conclusion to be drawn from the profile analysis is that geometric information is well suited to automatic face recognition. It weakly depends on illumination and is rather stable for a given individual although major differences exist between people.

8 Automatic 3D Head Verification

8.1 Motivations

The success of the profile approach motivated a facial surface analysis. This brings more information than the sole profile. The 3-D description allows for translation, rotation and scale normalization. As the volume information is looked for, the dependence on illumination can be kept small.

3-D acquisition has been traditionally reserved to expensive solutions with rather slow scanning devices. There has recently been an increase of developments of low cost 3D acquisition systems based on structured light illumination [Jarvis93, Proesmans97, Turing], and capturing the 3D scene in one or a few images. At video speeds, this results in quick solutions for which the subject is no more asked to stay still for a while.

Although 3D facial analysis is active in the field of image coding and synthesis [Saulnier94, Aizawa95], reported 3D facial recognition experiments are still rare [Lapreste88, Lee90, Gordon91, Achermann97].

8.2 Approach

The method is described in terms of its two components: 3D acquisition and 3D comparison. The 3D acquisition (see [Beumier99a]) of the facial surface is made by triangulation, thanks to a camera and a projector sending a specific pattern of light. The structured light consists in our case of parallel lines ('stripes') of two different thicknesses, arranged as a barcode in order to allow for the identification of each stripe when the thickness of a few neighbors are known.

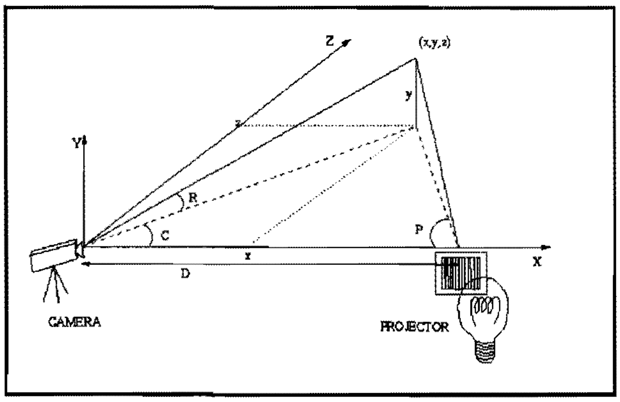

Figure 5. Structured light system

The system is cheap, involving a normal camera and a normal projector. The slide is made of glass to avoid thermal effects with the lamp heat. To work with lenses with small optical distortion, but to stay at reasonable distances, we chose a distance of work of 1.5 m. The corresponding volume of acquisition is 40x30 cm with a depth of focus of about 40 cm. It fulfils the needs of head capture for a sitting and cooperative person.

Figure 6. Images with and without stripes

The system is fast. A single image with projected stripes contains full 3-D information. At the speed of video cameras, no normal human motion impairs the integrity of the volume captured.

The striped image (see Figure 6) is first processed to detect vertical lines corresponding to the stripes. Line detection problems in dark areas appearing around the eyes, the eyebrows, the mouth and the nostrils have been reduced by turning the system so that the face is diagonally striped.

Each stripe is then classified as thick or thin based on the relative amount of dark and bright gray-levels present in the horizontal gray-level profile around the stripe. Based on a few neighbor thicknesses, each stripe is labeled by its number. The position in the image of points along each stripe and the stripe label allows to derive the xyz coordinates of these points. The intrinsic (CCD, acquisition board, lenses) and extrinsic parameters (camera/projector relative position) of this transformation are obtained during a calibration phase based on the capture of the corners of a reference planar square (Figure 7).

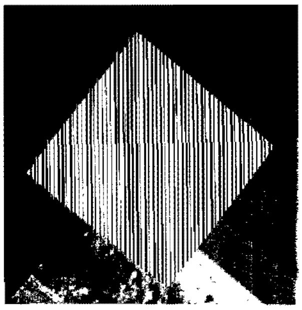

Figure 7. Calibration square

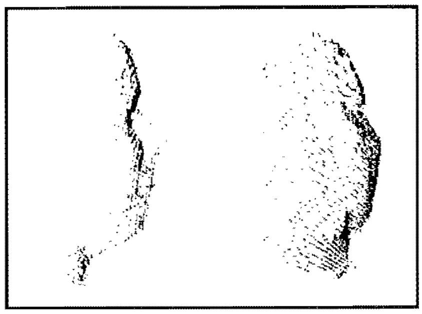

Figure 8. 3-D reconstruction

Perspective reconstructions are shown in Figure 8. The time spent to get the 3D coordinates from the image is about half a second on a Pentium 200 MHz.

The 3D comparison method adopted in our project considers planar cuts in the volume by parallel planes separated by 1 cm. Each planar cut delivers a 2D profile which is compared to its homologue of another facial volume (see Figure 9). This profile comparison outputs a distance equal to the area contained between the two profiles. The 3D comparison process minimizes the total distance of the plane cuts for the possible 3 translations and 3 rotations, no scale factor being considered as the system measures the true scale. This 6-dimensional minimization was successfully carried out by a 'iterative conditional mode' procedure where each parameter is recursively optimized on its own. Good approximation of initial values helped avoiding local minima and speeded up the process. A comparison between two facial surfaces on a Pentium 200 takes typically 1.0 second.

In order to further speed up processing, we also considered the comparison of the vertical profile passing through the nose augmented with the average of the two lateral vertical profiles at 3 cm from the nose (Figure 10). This choice was motivated by the fact that those vertical profiles can be extracted automatically from each volume independently, thanks to the horizontal symmetry of the head. The verification of a test surface requires the extraction of the 2D vertical profiles of that test surface (about 0.5 second) and their matching with the vertical profiles of the reference surfaces, extracted offline. This matching only involves 3 parameters and lasts less than 0.1 second on a Pentium 200.

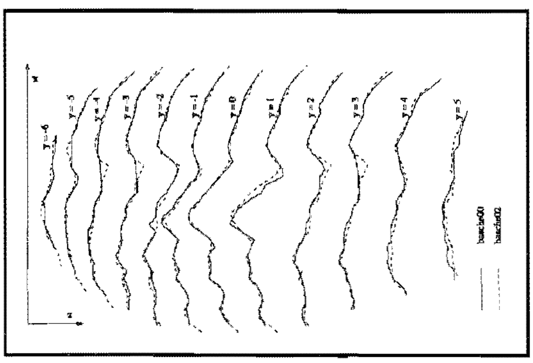

Figure 9. 3D comparison by parallel planar cuts.

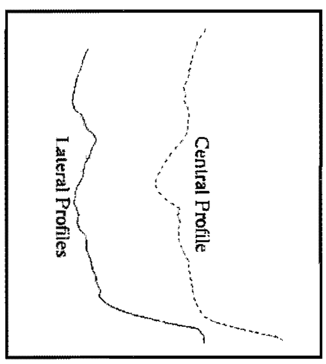

Figure 10. Central and Lateral profiles.

Finally, because the 3-D analysis allows to solve one of the main problems of frontal face analysis, the point of view, we considered the gray-level analysis normalized by the 3D information. First, the point of view can be obtained from the 3D information. Secondly, illumination influences can be compensated thanks to a model of the light projected and the captured facial volume. The ultimate goal is to combine gray and volume information which look to complement each other very well. On the one hand, gray-level features are localized in the mouth, eyes, hair and nose, precisely where a structured light system encounters acquisition problems. On the other hand, the forehead, cheeks and chin are poor in gray information although they are well captured by a 3-D system.

8.3 Results

A database has been acquired [Beumier99b] to test our 3D acquisition system and the face verification performances of the proposed methods. It consists of 120 people chosen for their probable availability in our premises. Three sessions have been organized in late 1997, early 1998 and mid 1999.

The automatic 3D acquisition program worked properly, especially regarding that no tuning was performed during the database collection. Common problems concerned the beard, moustache and spectacles while minor problems were found in the eyebrows, the nose and mouth.

The two methods presented in 8.2 offered similar results. [Beumier98, Beumier00b] give a precise description of the results. With fully automatic processing (acquisition and comparison, rejecting a few very bad acquisitions) the EER is about 10%. When manually refining the acquisition and the matching procedures, the EER falls at about 4%. Combining 3D and gray-level features on the same database led to a recognition rate higher than 95 %, as described in [Beumier00a].

Results could still be improved thanks to a better acquisition system, a better representativity of people, and a better matching procedure.

8.4 Conclusions

The whole chain of 3D processing, from acquisition to matching, offers a good performance relatively to the numerous disturbing factors mentioned above. An EER of 10 % has been obtained by two different comparison techniques, including normal acquisition errors, a lack of representativity and possible matching troubles. Manual intervention showed that the discrimative power of the 3D approach is higher, having reached 4% of EER when acquisition and matching were supervised.

A special care has been taken to keep the processing time below three seconds, from acquisition to decision. The integration is quick enough to verify the identity of one person in a few seconds on a Pentium 200.

At least four ways of improvement can be considered.

The first one concerns a better acquisition system, solving facial inconsistencies (thanks to a model) or cleaning regions which revealed to be too noisy. Secondly, the matching procedure could be accelerated and avoid local minima, possibly using gray-level features. A third improvement would take benefit of the acquisition speed to consider a better representation of people (more references) and to base the decision on a few captured surfaces. Finally, a gray-level analysis would complement the 3D processing. Gray-level clues can help the acquisition to deal with critical zones such as the beard, eyebrows or eyes. They can help in leading the matching procedure. They provide for complementary information, as shown in experiments [beumier00b], mainly in the eye, hair, nose and mouth, precisely where 3D capture is difficult.

9 Conclusions

The activities of the SIC in face recognition were presented. They were all conducted to meet practical constraints such as the time response, user cooperation and hardware cost.

Frontal face analysis appeared to be the most difficult to get good performances, considering the large influence of pose and lighting conditions.

The profile view offered a simple and quick automatic solution, based on the external contour consisting of rather rigid parts. The development of a prototype showed adequate system behaviour in realistic conditions, taking advantage of the overall speed to perform time fusion.

The 3D approach contained two challenges. The first one showed that 3D capture can fulfil system requirements about speed, cost and precision. The second challenge proved that facial surface analysis contains discriminative information, adequate for person verification.

An important and interesting future work lies in the further exploitation of gray information within the 3D approach. A system combining gray and volume information at all level of processing (capture, comparison and classification) appears to be a perfect example of fusion.

In order to increase the robustness of person identification, the activities of the SIC in expert fusion will be continued. They will lead to the development of a prototype implementing the fusion between speaker and face modalities.

10 Acknowledgements

This work has been partially supported by the European Programme ACTS.

11 References

[Achermann97] B. Achermann, X. Jiang, H. Bunke, Face Recognition Using Range Images, *In Proceedings International Conference on Virtual Systems and MultiMedia '97 (VSMM '97)*, Geneva, Switzerland, pp 129-136, September 1997.

[Aizawa95] K. Aizawa, T. Huang, Model-Based Image Coding: Advanced Video Coding Techniques for Very Low Bit-Rate Applications, In Proceedings of the IEEE, *Vol. 83, No. 2, Feb 1995.*

[Beumier97] C. Beumier, M.P. Acheroy, Automatic Profile Identification, In FIRST INTERNATIONAL CONFERENCE ON AUDIO AND VIDEO BASED BIOMETRIC PERSON AUTHENTICATION (AVBPA), *Crans-Montana, Switzerland, March 12-14 1997, pp 145-152.*

[Beumier98] C. Beumier, M.P. Acheroy, Automatic Face Authentication from 3D Surface, In British Machine Vision Conference BMVC 98, *University of Southampton UK, 14-17 Sep, 1998, pp 449-458.*

[Beumier99a] C. Beumier, M. Acheroy, 3D Facial Surface Acquisition by Structured Light, In International Workshop on Synthetic-Natural Hybrid Coding and Three Dimensional Imaging, *Santorini, Greece, 15-17 Sep, 1999, pp 103-106.*

[Beumier99b] C. Beumier, M. Acheroy, SIC_DB: Multi-Modal Database for Person Authentication, In Proceedings of the 10th International Conference on Image Analysis and Processing, *Venice, Italy, 27-29 Sep, 1999, pp 704-708.*

[Beumier00a] C. Beumier, M. Acheroy, Automatic 3D Face Authentication, In Image and Vision Computing, *Vol. 18, No. 4, pp 315-321.*

[Beumier00b] C. Beumier, M. Acheroy, Automatic Face Verification from 3D and Grey Level Clues, accepted by 11th Portuguese Conference on Pattern Recognition (RECPAD 2000), *Porto, Portugal, May 11th - 12th, 2000.*

[Beymer94] D. Beymer, Face Recognition Under Varying Pose, In IEEE Computer Vision and Pattern Recognition, *Seattle, WA, June 1994, pp. 756-761.*

[Brunelli93], R. Brunelli, T. Poggio, Face Recognition: Features versus Templates, In IEEE TRANSACTIONS ON PATTERN ANALYSIS AND MACHINE INTELLIGENCE, *Vol. 15, No. 10, Oct 1993, pp 1042-1052.*

[Chellappa95] R. Chellappa, C.L. Wilson and S. Sirohey, Human and Machine Recognition of Faces, In Proceedings of the IEEE, *The institute of electrical and electronics engineers, inc., Vol. 83, No. 5, May 1995, pp 705-740.*

[Gordon91] G. Gordon, Face recognition based on depth maps and surface curvature, In SPIE Geo-metric methods in Computer Vision, *Vol 1570, San Diego, 1991.*

[Jain99] In BIOMETRICS Personal Identification in Networked Society, *A. Jain, R. Bolle, S. Pankanti editors, Kluwer Academic Publishers, 1999.*

[Jarvis93] R. Jarvis, In Three-dimensional object recognition systems, *In K. Jain and P. J. Flynn, eds., Advances in Image Communication, Vol 1, (Elsevier, Amsterdam, 1993) pp 17-56.*

[Kohonen89] T. Kohonen, Self-Organization and Associative Memory, In Springer series, *3th edition, 1989.*

[Lapreste88] J.T. Lapresté, J.Y. Cartoux, M. Richetin, FACE RECOGNITION FROM RANGE DATA BY STRUCTURAL ANALYSIS, In NATO ASI series, Vol. F45, Syntactic and Structural Pattern Recognition, *Edited by G. Ferraté et al., Springer-Verlag Berlin Heidelberg, 1988.*

[Lee90] J.C. Lee and E. Milios, Matching Range Images of Human Faces, In Proc. IEEE Soc. 3rd Int. Conf. on Computer Vision, 1990, *pp 722-726.*

[Mundy91] J. Mundy, Model-based vision, an operational reality ?, In Applications of Digital Image Processing XIV, *SPIE Vol. 1567, pp 124-141.*

[Perneel90] C. Perneel and M. Acheroy, Face Recognition with Artificial Neural Networks, in IMACS Annals on Computing and Applied Mathematics, *Proceedings MIMS2 '90, Sept. 3-7, Brussels.*

[Proesmans97] M. Proesmans, L. Van Gool, Reading between the lines - a method for extracting dynamic 3D with texture, In ACM Symposium on virtual reality software and technology, VRST 97, *pp 95-102, Sept 15-17, 97 Lausanne, Switzerland.*

[Richard99a] G. Richard, Y. Menguy, I. Guis, N. Suaudeau, J. Boudy, P. Lockwood, C. Fernandez, F. Fernandez, C. Kotropoulos, A. Tefas, Ioannis Pitas, R. Heimgartner, P. Ryser, C. Beumier, P. Verlinde, S. Pigeon, G. Matas, Josef Kittler, J. Bigun, Y. Abdeljaoued, E. Meurville, L. Besacier, M.

Ansorge, G. Maitre, J. Luettin, S. Ben-Yacoub, B. Ruiz, K. Aldama, J. Cortes, Multi Modal Verification for Teleservices and Security Applications (M2VTS)", In IEEE International Conference on Multimedia Computing and Systems, ICMCS 1999, *Florence, Italy, 7-11 June, 1999, Proceedings, Volume I. IEEE Computer Society, pp 1061-1064.*

[Samal92] A. Samal and P. Iyengar, AUTOMATIC RECOGNITION AND ANALYSIS OF HUMAN FACES AND FACIAL EXPRESSIONS: A SURVEY, Pattern Recognition, *Vol. 25, No. 1, pp 65-77, 1992.*

[Saulnier94] A. Saulnier, M.-L. Viaud, D. Geldreich, Analyse et Synthèse en temps réel du Visage pour la Télévirtualité, Imagina 94, *pp 173-182.*

[Stonham86] T. Stonham, PRACTICAL FACE RECOGNITION AND VERIFICATION WITH WISARD, In Aspects of Face Processing, *Doordrecht, Netherlands: Martinus Nijhoff Publishers, pp 426-441, 1986.*

[Turing] http://www.turing.gla.ac.uk

[Turk90] M. Turk, and A. Pentland, Recognition in Face Space, In SPIE Vol. 1381 Intelligent Robots and Computer Vision IX: Algorithms and Techniques (1990), *pp 43-54, 1990.*

[Verlinde00] P. Verlinde, A contribution to multi-modal identity verification using decision fusion, Ecole Nationale Supérieure de Télécommunications, Paris, France, Sept 1999.

[Wiskott96] L. Wiskott, J.-M. Fellous, N. Kr\"uger, and C. von der Malsburg, Face Recognition by Elastic Bunch Graph Matching, Institut f\"ur Neuroinformatik, Universit\"at Bochum, FRG, Internal Report 96-08.

[Yuille89] A. Yuille, D. Cohen and P. Hallinan, Feature Extraction from Faces using Deformable Templates, In Proc. 1989 IEEE CS Conf. on Computer Vision and Pattern Recognition, *IEEE Computer Society Press, Los Alamitos, Calif., 1989, pp. 104-109, 1989.*

Sensaos: encounter the girl in the mummy

Rijksmuseum van Oudheden
Rapenburg 28
P.O.Box 11114, 2301 EC Leiden
phone: +31 71-516 31 63, fax: +31 71-514 99 41
info@rmo.nl, http://www.rmo.nl

TNO
http://www.tno.nl

1 Historical background

1.1 Sensaos: the girl, the mummy, the shroud, the coffin and the papyrus

Since 1829 the Rijksmuseum van Oudheden (National Museum of Antiquities) has housed the mummy of the Egyptian girl Sensaos, the shroud tied around her mummified body, the wooden coffin and the inscribed papyrus that was found in her coffin.

1.2 Sensaos: a girl in Ancient Egypt

Sensaos was the daughter of a high-ranking official in the provincial government of Thebes in Upper Egypt. She lived at the beginning of the second century A.D. In this period, at the time of Emperor Trajanus, Egypt was part of the Roman Empire. Sensaos and her family were members of a small Greek-speaking elite. The names of the members of Sensaos's family indicate that the family was of mixed Roman, Greek, Egyptian and Nubian origin. 'Sensaos' is the Hellenised form of the Egyptian name 'Tasjerytdjedhor'. Sensaos died in 109 A.D. at the age of sixteen. In those times women were at that age already adults and were often married.

1.3 Sensaos mummified

Despite the fact that her family belonged to the Hellenised elite, Sensaos was embalmed and mummified after her death, in accordance with Ancient Egyptian tradition. Cloths were wound around her embalmed body. Amulets were laid between the cloths to protect her during her journey to the underworld. Her eyes were covered with artificial eyes made of pottery and glass. The mummy was wrapped in a painted shroud and placed in a coffin in the family tomb in the mountains near Thebes.

1.4 Painted shroud

On the colour-painted shroud Sensaos is depicted in the form of the goddess Noet, surrounded by Egyptian gods and symbols. It was customary at that time to dress up women and girls on their deathbed as the goddess Noet or Hathor: with their hair flowing free in an 'old-fashioned' Egyptian style that was not customary for women during their lifetime. While she was alive, Sensaos most probably wore her hair gathered up in the Roman fashion. On the shroud she is depicted with her hair hanging free and wearing a long Egyptian robe. She has Hellenistic snake bracelets on her wrists. At her feet are two jackals of Anubis, the god of mummification, with the key to the Underworld, a motif from Greek-Roman art. The mummy was removed from its shroud in the second half of the nineteenth century. A drawing in the museum's archive shows the mummy of Sensaos in its original state.

1.5 The coffin
Sensaos's coffin is rectangular, with a convex lid and corner columns. This shape symbolises the vault of heaven, which was believed by the ancient Egyptians to be supported by the four corners of the world. The coffin is painted with images of gods and goddesses and with inscriptions and symbols designed to facilitate the resurrection of the body after death. The name 'Tasjerytdjedhor' (*'daughter of King Djedhor'*), which is the Egyptian form of the name Sensaos, is written on the coffin in hieroglyphics. The girl was named after Djethor, who was king of Egypt between 365 and 360 B.C.

A Greek inscription on the coffin says: 'Sensaos, daughter of Soter Cornelius, whose mother was Cleopatra (also known as Candace, daughter of Ammonius), died a virgin at the age of 16 years, two months and 9 days, in the twelfth year of the reign of Trajanus on the 21st day of the month of Epiphany'.

Depicted on the inside of the coffin lid is the goddess Noet in the midst of the signs of the zodiac, as a symbol of the everlasting cycle of the sun and the moon. Sensaos herself is depicted on the bottom of the coffin, wearing a sumptuous robe and sandals. The weighing of Sensaos's heart is represented on the outside of the lid. If her heart is as light as an ostrich's feather, the symbol of truth and justice, Sensaos will be admitted to the underworld, where she will live ever after. The sides of the coffin depict Sensaos, accompanied by four baboons, revering the sun-boat pulled by jackals. On the left-hand side of the coffin is the Ba, Sensaos's soul: a bird with a human head. On the inner sides twelve figures are depicted with a solar disc on their head, indicating the hours of the day and night. The coffin is decorated in accordance with centuries-old Egyptian tradition, but also shows innovations in style and motifs which in part come from Greek-Roman culture. The signs of the zodiac originally come from Mesopotamia, and made their first appearance in Egypt during the Hellenistic period.

1.6 Papyrus with words from the 'Book of Breathing'
On the right-hand side of the mummy a small papyrus was found in the coffin which contained a text from the 'Book of Breathing'. The text is written hieratically, i.e. in a simplified form of Egyptian hieroglyphics. It can be seen from the handwriting that a reed was used for writing on the papyrus. The 'Book of Breathing' was supposed to help Sensaos to overcome death. In the text, Thot, the god of writers, is called upon to protect her from danger on the way to the underworld. The text also mentions Sensaos's Egyptian name.

1.7 The family tomb in Thebes
Sensaos was buried in the family tomb in the Theban mountains in Egypt. In 1820 the tomb was discovered by grave robbers. The tomb was emptied by Antonio Lebolo from Piedmont, who was working for his compatriot Drovetti, a dealer in Egyptian antiquities. The mummies and mummy coffins from the tomb finally found their way to several museums. The mummy of Sensaos and her shroud, the wooden coffin and the papyrus in her coffin became the property of Giovanni D'Anastasy. His collection, and with it the mummy of Sensaos and its attributes, has been part of the collection of the Dutch Rijksmuseum van Oudheden since 1829. The mummies of the father of Sensaos, Soter, and of her sister Cleopatra, are in the British Museum in London, together with the mummy of the child of one of her brothers, Tphous. The mummy of her other brother, Petamenophis, is in the Louvre in Paris. The mummies of Takoedja and Sensaos, the young younger sisters of Sensaos and a nephew, Phaminis, are in the collection of the Egyptian Museum in Berlin.

2 From mummy scan to a new face for Sensaos

2.1 CT scan of the mummy

The mummy of Sensaos was scanned by Philips Medical Systems in Best under the direction of Margriet Hendrix, head of Computer Tomography, and Professor Dr. F. Zonneveld, senior Clinical Scientist CT. A three-dimensional Computer Tomography scan (CT scan) was made, using an advanced machine, the Tomoscan AV Expander. The machine made 558 cross-sections of the mummy with a thickness of 3 millimetres, and 190 of the head with a thickness of 1 millimetre. The cloths, the outer layers of the skin, the skeletal system and the skull could be seen. The information yielded by the scans was then processed into a three-dimensional computer image of the skull and the body.

2.2 Scientific result

The scan data yielded new knowledge about Sensaos, for instance about her state of health, skeletal system, teeth and the way in which she was mummified. It emerged that Sensaos is approximately 1.45 metres tall, has long, flowing hair and that her body was completely filled with resin.

The brain appears to have been removed from the skull via the nose. A few remnants of bone and hardened tissue were left. As a result, the interior of the skull was badly damaged. Her head slopes forward from the cervical vertebrae, almost resting on the breast.

It appears from the collapsed state of the pelvis that Sensaos's body was already in an advanced state of decomposition when she was mummified. The Greek writer Herodotus states in his 'Histories' that leading Egyptian families sometimes waited before having female members of the family mummified, so as to prevent embalmers from violating the corpses. Perhaps because it was already decomposing, Sensaos's body was filled with resin and wrapped in cloths saturated with resin. This explains the considerable weight and the plump exterior of the mummy. Some of the resin escaped from the corpse. That is why it looks on the scan as if she is lying in a 'bath' of resin.

It can also be seen on the scan that Sensaos's eyes were covered with decorative artificial eyes made of glass. They now appear to have slid off her eyes. In the cloths next to one of the lower legs there is a thin metal object, and at the level of the hips a ceramic object can be seen. Presumably these are amulets.

At the place of the heart there is a small packet of linen. This is not surprising, since it was customary to wrap the embalmed bowels in linen and replace them in the corpse. Embalmed bowels were formerly preserved in Ancient Egypt in canopic vases, which were interred with the dead person.

2.3 The skull

The data from the CT scan were processed under the direction of ir. Edith Groenewolt (Ingenieur Prototyping Division Product Manufacturing) and Niek Dijkshoorn (Projectmanager Division Product Manufacturing) of TNO Industrie of Delft into a three-dimensional model of the skull. The skull was constructed with wax-like material, using a process known as 'Multi-Jet Modelling'. The apparatus used - actually a computer-controlled printer - builds up the skull layer by layer. The whole process took 36 hours. To support the skull, its cavities were filled with 'supports' made of the same material. The supports were later removed.

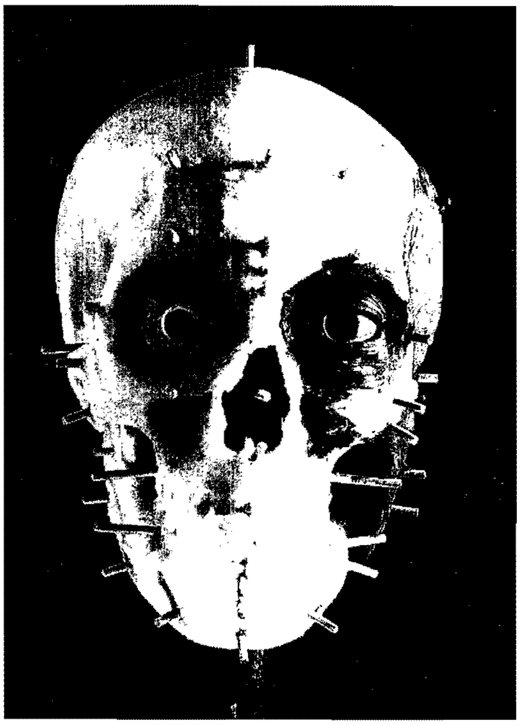

Figure 1. The reconstructed skull of Sensaos including the first muscle layer. The sticks placed in the skull indicate the thickness of the muscle tissue and skin.

2.4 A new face

Richard Neave then moulded the girl's face onto the skull. The skull provides a lot of information about the original facial exterior. On the basis of the skull, Neave determined the proportions of the eyes and the space between them, the approximate proportions of the nose, the width of the face, the width of the jaw and the position of the ears.

On the basis of the thickness and the shape of the skull and using a database containing scientific measurements of facial muscles and skin according to age, Neave was able to calculate the thickness of the muscle tissue and the skin. Measurements carried out on other mummies provided a lot of data on the facial structure of people in Ancient Egypt.

2.5 Skin and muscles

Neave drilled 24 holes in the reconstructed skull. In these he placed small sticks which indicate the thickness of muscles and skin. For the eyes, ears and nose he made marking points which can be found when the skull is covered with clay. The nose opening in the skull determines the shape of the nose. Sensaos was given a small, graceful nose. The skull was covered with muscle groups in clay, starting with the large muscle groups, followed by the smaller ones. For this Neave used the visible points by which the muscles are attached to the skull. Muscle groups which could be deduced, such as those of the mouth and the tip of the nose, were estimated by Neave. The size of the mouth and the distance between nose and upper lip can, however, be deduced from the skull. As it is known that Sensaos was partly of Nubian descent, she was given a full mouth. The position of the ears was determined by the hole in the skull through which the ear nerve enters the brain. The original shape of the ears cannot be deduced, however. Neave made the ears and mouth harmonise with the rest of the face. He then applied the top layer (the skin) over the muscles in strips of clay of different thicknesses. This 'basic face' was given a clay neck that matches the anatomical proportions of the skull.

2.6 Make-up and hair

The face thus created did not yet have an identity, as complexion and hair are lacking. Make-up could not be applied, however, as the clay would then develop cracks. So a wax model was made of the basic face. Tracy O'Brien, a specialist in historical make-up, added make-up, eyebrows and lashes to the face. The facial exterior was determined by the age, the prosperity and the stated health of Sensaos. The facial colour was applied in lots of thin layers. The face was given a light brown complexion and brown eyes, like those of contemporary Egyptians, and eyebrows and lashes of black human hair. Sensaos's hair was supplied by The London Wig Company. The wig is made of black human hair. Sensaos's forehead is framed with curls.

Figure 2. Muscles are deposited in clay layer by layer on the reconstructed skull of Sensaos. The sticks placed in the skull indicate the thickness of the muscles and the skin.

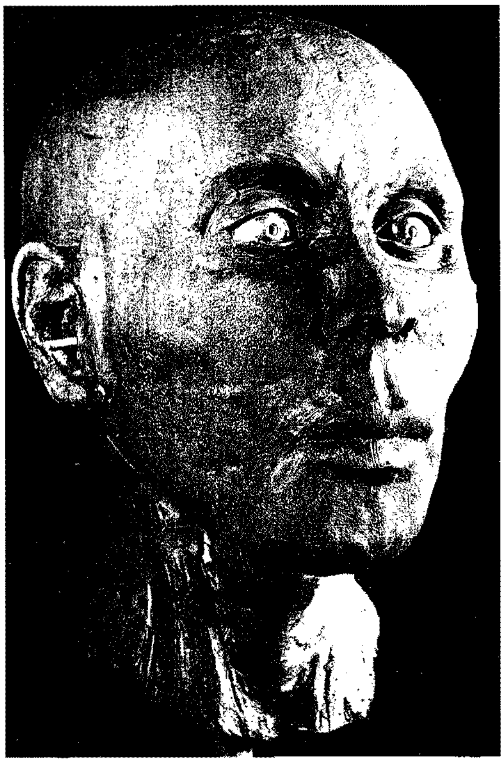

Figure 3. The reconstructed skull of Sensaos is entirely covered with muscle tissue and skin made from clay. A model was made of the head, which then was made up and given hair.

2.7 Fact and fiction

The reconstruction of Sensaos's face is partly based on fact, but is also fiction. The clay face reconstructed by Neave is a close approximation of Sensaos's actual appearance. A test reconstruction of the face of a living person showed that Neave's approach produces results that come very close to reality.

The make-up and the hair are partly fictitious. Both are based on mummy portraits from the corresponding period of Roman Egypt. The make-up is discreet. The hair is gathered up in a style that was typical of the reign of Emperor Trajanus. It can be seen on the CT scan that Sensaos has long, flowing hair. This is connected with a funeral ritual. It was customary in Ancient Egypt to dress up women and girls on their deathbed as the goddess Noet or Hathor, with flowing hair, an 'old-fashioned' Egyptian hairstyle such as was not worn by women during their lifetime.

Figure 4. The reconstructed face of an Egyptian girl called Sensaos, who died 109 AD at the age of sixteen.

3 A skull of wax

3.1 Sensaos and TNO

TNO Industry in Delft manufactured the skull, on which Richard Neave's reconstruction of the face of Sensaos is based. For TNO the research project concerning the mummy of the Egyptian girl Sensaos was en excellent opportunity to demonstrate that modern techniques can be applied in diverse ways and to many different products.

3.2 'Multi-Jet Modelling'

The data of the computer tomography scan, made by Philips Medical Systems in Best, were transformed into a three-dimensional skull by TNO using wax-like material. The transformation process is known as 'Multi Jet Modelling' (MJM). The high-speed MJM machine has a head with 96 individual jets. The head moves back and forth across a production platform, spraying the wax-like material layer by layer. A computer, which is controlled by a format, determines when a jet has to deposit the material. The data from the CT scan are stored in this format. Spots not covered by material receive support from thin threads. These support threads are later removed. It took 36 hours to manufacture the skull of Sensaos.

3. 3 'Rapid prototyping'

'Multi Jet Modelling' is one of the 'rapid prototyping' systems that TNO uses to process computer data into a three-dimensional model. The technique selected depends on the requirements that are made of the model. The rapid prototyping systems are controlled via 3D CAD (Computer Aided Design). The 3D CAD model is translated into STL files (Standard Triangulation Language): a mesh of triangles that completely describes the surface. A printed three-dimensional model of a product is used in the idea and concept stage of the product development process. This is used to assess the shape and appearance of the product and to test initial market response. A computer image usually is insufficient for this task.

In the next production stage of the production process, models are manufactured using different techniques to gain insight into the production and assembly techniques. This makes it possible to trace problems in the joining of different parts of a product at an early stage.

IEEE

IEEE (the Institute of Electrical and Electronics Engineers) is an international organization operating in the sciences related to electrical, electronics and computer engineering. With more than 330.000 members worldwide, IEEE is the largest organization in its kind. IEEE publishes technical papers, defines standards and organizes congresses as its main technical activities.

IEEE Student Branch Eindhoven

Through student branches, IEEE serves the needs of electrical and computer engineering students. IEEE Student Branch Eindhoven is the student branch at the Eindhoven University of Technology, which like most branches is run by students. The branch is involved in activities such as symposiums, study tours and company visits, thus giving students the opportunity to meet potential employers and make valuable contacts. IEEE SBE gives students the chance to find out about the numerous opportunities in electrical and computer engineering, and actually see the type of projects engineers are working on.

Another aspect of IEEE SBE is the social environment it provides for students. Within IEEE SBE, students can meet other students, discuss common interests, voice concerns, and generally become more informed about issues that affect engineers and students alike. Informal activities such as contests and social evenings together with other branches contribute to a pleasant working climate and good cooperation with colleagues abroad.

By becoming involved in IEEE SBE, students can also get a head start on their careers as electrical or computer engineers. IEEE SBE members can subscribe to technical periodicals of all IEEE societies at student discount prices. Periodicals cover topics such as computer graphics, biomedical engineering, microprocessors, light wave technology and robotics. Not only will students be more informed about their chosen field, but they will also be able to present themselves to future employers more professionally.

Acknowledgements

The 2000 Symposium Committee would like to thank the follwing persons for their cooperation and dedication that allowed us to organize the symposium "Imaging"

Dr. ir. J.B.O.S. Martens (IPO)

Murat Eyuboglu, Ph. D., (Middle East Technical University)

Dr. E.A. Hendriks (Delft University of Technology)

Dr. ir. F.A. Gerritsen (Philips Medical Systems)

Dr. ir. P.J.M. Cluitmans (Eindhoven University of Technology)

Dr. A.M.J. Paans (PET-Center, Groningen University Hospital)

Dr. ir. V. Rasche (Philips Medical Systems)

Dr. ir. J.M.L. Engels (Philips Medical Systems)

Dr. J.G.M. Schavemaker (TNO Physics and Electronics Laboratory)

Ir. A. v.d. Stadt (Eagle Vision Systems)

Ir. C. Beumier (Royal Military Academy)

The Symposium Committee would also like to thank the board of IEEE for their useful comment and support, the Committee of Recommendation and all those who contributes to our ymposium. A special thanks goes out to the advisory committee for their indispensable support.

Committee of recommendation

Dr. ir. M.J. Bastiaans (Associate Professor at Technische Universiteit Eindhoven and Counselor of IEEE SBE)

Prof. dr. ir. W.M.G. van Bokhoven (Dean of the Department of Electrical Engineering, Technische Universiteit Eindhoven)

C. Boonstra (President of Royal Philips Electronics N.V.)

Dr. W. Boontje (CEO of the Technology Foundation STW)

Prof. dr. ir. P.P.J. van den Bosch (Professor of Electrical Engineering, Technische Universiteit Eindhoven)

Prof. dr. ir. W.C. van Etten (Professor University of Twente and president of the NERG)

C. Groutars (communication manager The Industree)

Ir. H.J.A. van Helden (CEO KEMA)

Prof. ir. G.D. Khoe (Professor of Electrical Engineering, Eindhoven University of Technology)

Prof. dr. ir. P.C.T. van der Laan (Professor of Electrical Engineering, Technische Universiteit Eindhoven)

Prof. dr. J.K. Lenstra (Dean of the Department of mathematics and computing science, Technische Universiteit Eindhoven)

Ir. R.M. Lutje Schipholt (member board of management TNO)

Ir. B. van Nederveen (president Royal Institution of Engineers in the NetherlandsKIvI)

Dr. A.M.J. Paans (head Biophysica PET-Center, Groningen University Hospital)

Prof. dr. M. Rem (Rector Magnificus Technische Universiteit Eindhoven)

Ir. P. Smits (member board of management KPN Nederland N.V.)

Dr. ir. A.B. Smolders (project manager Astron)

N.M. van der Spek (alderman city of Eindhoven)

Prof. ir. M.P.J. Stevens (Professor of Electrical Engineering, Technische Universiteit Eindhoven)

Dr. J. Systma (Group leader Projection Lenses ASML)

Prof. dr. F. van Vught (Rector Magnificus University of Twente)

Prof. ir. K.W. Wakker (Rector Magnificus Delft University of Technology).

List of sponsors

Aragorn Computers B.V.

ASML

Capaciteitsgroep ICS

Department of Electrical Engineering, Technische Universiteit Eindhoven

Ellips B.V.

Ericsson

Hollandse Signaalapparaten

IEEE SBE

Logica

Philips

TNO-FEL

Turpin Vision

Twinning Centre Eindhoven

The 2000 Symposium Committee

Thank you for joining "Imaging - making the invisible visisble", the 10th symposium of IEEE Student Branch Eindhoven. With a great deal of fun and excitement, we have worked on the preparation of this symposium; we hope that our enthusiasm has inspired you also and made this day worthwhile!

The 2000 Symposium Committee consists of six people, students and engineers of the Technische Universiteit Technology and all member of the IEEE Student Branch Eindhoven.

From the left to the right:

Jan van Gurp, treasurer

Davy Verstraeten, secretary

Emiel Nuyten, vice chair

Johan van Berkel, committee member

Paul Lokkart, committee member

Suzanne Jongen, chair

Proceedings of the symposium "Imaging - making the invible visible", held at the Technische Universiteit Eindhoven, Thursday 18 May 2000.

Publisher IEEE Student Branch Eindhoven
Eindhoven University of Technology
P.O. Box 513, EH 6.29
5600 MB Eindhoven
the Netherlands

Tel.: +31 (0) 40 247 3433
Fax.: +31 (0) 40 247 3661
E-mail: ieeesb@tue.ele.nl
WWW: http://www.ele.tue.nl/ieeesb

Editor / Layout Johan van Berkel

Cover design Paul Lokkart

Printed by Van Meurs, Ridderkerk

New Technological Development in 3D Medical Imaging

Dr. ir. V. Rasche (Philips Medical Systems)

Non-nuclear medical imaging is currently undergoing some major changes, the three most important of them being a transition from a couple of 2D slices to true 3D imaging preferably at high isotropic resolution, the extraction of physiological information instead of pure anatomy, and the trend to realize real-time image acquisition and display. Techniques capable of significantly contribute to these trends are Ultrasound (US), Magnetic Resonance Imaging (MRI), Computer Tomography (CT), and recently introduced 3D Rotational X-Ray Imaging (3D-RX). Currently, technical developments are undertaken for each of these modalities for improving their performance in the above-mentioned fields. The new capabilities of the different modalities produce an enourmous amount of data and information during a single exam. This causes a tremendous need for faster reconstruction and visualization platforms and for the development of user-interaction concepts supporting the physician during diagnosis.

Magnetic Resonance Imaging Technique, Application and Perspective

Dr. ir. J.M.L. Engels (Philips Medical Systems)

The growth of Magnetic Resonance Imaging (MRI) as a diagnostic modality in the hospital has been explosive in the past 15 years and is still going on. MRI is fully accepted in the clinical routine practise. It applies the original Nuclear Magnetic Resonance technique, whereby in addition to the static magnetic field of the magnet, additional dynamic magnetic gradient fields are applied for the localisation of the signal. The MRI signal is the result of the relaxation of the protons in the human body after excitation by RF energy. The contrast in the MR images is the result of the different values for the relaxation times (the spin-lattice relaxation time T_1 and the spin-spin relaxation time T_2) and the proton density in healthy or sick human tissue and organs. In more recently developed applications other effects such as stationnary or moving protons, chemical shift effects, susceptibility effects and optimized synchronization with the cardiac and respiratory motions of the body are used for the creation of better contrasts and higher resolution. As a result new applications such MR Angiography, MR Cardiology, funcional MRI are possible on the latest generation of MRI scanners. Also the speed of the data acquisition is improved dramatically, resulting in applications for interactive and interventional studies.

In short, the basics of the MRI technique will be explained and the current and future applications will be discussed and illustrated.

Sensor-fusion for anti-personnel land-mine detection

Dr. J.G.M. Schavemaker (Electro-Optical Systems, TNO Physics and Electronics Laboratory)

The requirements placed upon automatic detection systems for humanitarian demining cannot be met by a single-sensor system. Common choices for sensors include ground-penetrating radar, metal detector, and infrared cameras. The combination of different sensors is called sensor fusion. Sensor fusion is one of the topics of Dutch (HOM 2000) and European (GEODE and LOTUS) projects in which TNO-FEL participates.

Filled Bottle Inspector

Ir. A. van de Stadt (Eagle Vision Systems)

Recently, Eagle Vision has developed with Heineken, GEI International and PA consulting the Filled Bottle Inspector (or FBI). This revolutionary system detects glass particles in glas bottles filled with beer. Even tiny glass fragments are detected reliably at line speeds of up to 60.000 bottles per hour. In order to obtain a throughput of 17 bottles per second, the system needs to look at several bottles in parallel. This is achieved by using a caroussel machine with 36 heads. Each head is equipped with a camera and illuminator. The 36 camera's are connected to 8 PC's via a video multiplexer. On the PCs the image series are processed with blob analysis software and several advanced algorithms. Some images of the working FBI system will be shown at the presentation.

Automatic Face Recognition

Ir. C. Beumier (Signal and Image Center, Royal Military Academy)

The activities of the RMA/SIC department in the field of Automatic Face Recognition are presented. After having outlined the difficulties for lighting, pose and stable features in the frontal face analysis, a prototype for automatic profile identifaction is presented. This geometrical approach is further investigated by considering the capture and comparison of 3D facial surfaces.

Symposium

IMAGING

Making the invisible visible

Thursday 18 May 2000

Eindhoven University of Technology

Introduction

On Thursday the 18th of May IEEE Student Branch Eindhoven organises the symposium 'Imaging'. The purpose of this symposium is to show you the world of Imaging and its applications. Imaging is the aspect of gathering and processing an "image" of a certain object, which can be many things, for example a human being or a bottle of beer. Because of the wide scope of uses for imaging technologies, this symposium stresses on the medical and industrial applications of Imaging. The symposium is meant for students, academical staff and people from the trade of industry. Because this sympoium is held in the lustrum week of the IEEE Student Branch Eindhoven, a large group of IEEE students from our colleague branches around the globe will also attend the symposium. For this reason the symposium will be in English.

Organisation

IEEE is the Institute of Electrical and Electronics Engineers, Inc. It's the greatest (330.000 members) international organisation for electrical, electronics and computer science engineers and engineerings students, for which it organises conferences and publishes technical literature as its main activities. To improve the interaction between both engineers and engineering students many Student Branches were founded. Our Student Branch in Eindhoven organises symposia, lectures, excursions and study tours. By becoming active in a Student Branch students get the opportunity to develop their leadership skills. For this symposium, the "SymCo 2000" was called into existence by the Student Branch Eindhoven. This committee exists of (Phd.) students, who want to be active on their own profession.

Committee of recommendation

Dr. ir. M.J. Bastiaans (TUE), Prof. dr. ir. W.M.G. van Bokhoven (TUE), C. Boonstra (Philips Electronics N.V.), Dr. W. Boontje (Technologiestichting STW), Prof. dr. ir. P.P.J. van den Bosch (TUE), Prof. dr. ir. W.C. van Etten (NERG), C. Groutars (Industree), Ir. H.J.A. van Helden (KEMA), Prof. ir. G.D. Khoe (TUE), Prof. dr. ir. P.C.T. van der Laan (TUE), Prof. dr. J.K. Lenstra (TUE), Ir. R.M. Lutje Schipholt (TNO), Ir. B. van Nederveen (KIvI), Dr. A.M.J. Paans (PET-Center, Groningen University Hospital), Prof. dr. M. Rem (TUE), Ir. P. Smits (KPN Nederland N.V.), Dr. it. A.B. Smolders (Astron), N.M. van der Spek (municipal Eindhoven), Prof. ir. M.P.J. Stevens (TUE), Dr. J. Systma (ASML), Prof. dr. F. van Vught (University of Twente), Prof. ir. K.W. Wakker (Delft University of Technology).

Program

9.00 Reception with coffee

9.30 Welcome
Dr. ir. J.B.O.S. Martens (IPO)

9.45 Opening lecture
Ph. D. Murat Eyuboglu
(Middle East Technical University)

10.30 Coffeebreak

11.00 Introduction lectures

11.00 "Digital Imaging and Image Processing, what is it all about."
Dr. E.A. Hendriks (Delft University of Technology)

11.40 "Virtual Reality in Medical Imaging-Guided Surgery"
Dr. ir. F.A. Gerritsen (Philips Medical Systems)

12.20 Lunch and Informationmarket

13.30 Parallel Sessions

Parallel Session 1: Medical Applications

Parallel Session 2: Industrial Applications

16.10 Forum

17.00 Drinks

Parallel Session 1

Medical Applications conducted by dr. ir. P.J.M. Cluitmans

13.30 "Positron Emission Tomography"
Dr. A.M.J. Paans
(PET-Center, Groningen University Hospital)

14.20 "New Technological Developments in 3D Medical Imaging"
Dr. ir. V. Rasche (Philips Medical Systems)

15.00 Coffeebreak

15.30 "Magnetic Resonance Imaging Technique, Application and Perspective"
Dr. ir. J.M.L. Engels (Philips Medical Systems)

Parallel Session 2

Industrial applications conducted by dr. ir. J.B.O.S. Martens

13.30 "Sensor-fusion for anti-personnel land-mine detection"
Dr. J.G.M. Schavemaker (Electro-Optical Systems, TNO Physics and Electronics Laboratory)

14.20 "Filled Bottle Inspector"
Ir. A. v.d. Stadt (Eagle Vision Systems)

15.00 Coffeebreak

15.30 "Automatic Face Recognition"
Ir. C. Beumier
(Signal and Image Center, Royal Military Academy)

Summary

Virtual Reality in Medical Imaging-Guided Surgery

Dr. ir. F. A. Gerritsen (Easy Vision Advanced Development, Philips Medical Systems)

This presentation discusses relatively recent advances in the use of techniques from medical imaging and simulation to facilitate minimally invasive surgery. The descriptions in the paper are based on original work done in the EC-sponsored project "European Applications in Surgical Interventions". During the symposium also more recent advances by others will be explained for tutorial purposes.

Positron Emission Tomography

Dr. A.M.J. Paans (PET-Center, Groningen University Hospital)

Positron Emission Tomography (PET) is a method for determining biochemical and physiological processses in vivo in a quantitative way by using radiopharmaceuticals labeled with positron emitting (short lived) radionuclides as carbon-11, nitrogen-13, oxygen-15 and fluorine-18. Image formation is established by measuring the annihilation radiation using a coincidence technique. PET is increasingly used for measuring deviations of normal metabolism as well as evaluating the effect of therapy in medicine.

Digital Imaging and Image Processing, what is it all about.

Dr. E.A. Hendriks (Department of Information Technology and Systems, Delft University of Technology)

Due to the rapid progress of video and computer technology, digital imaging and digital image processing has undergone a large growth in possibilities and applications in the last two decades. Nowadays digital imaging is playing a more and more important role in the broadcast world (digital television), medical world, consumer market (computer games), industry (inspection, control) and surveillance, among others.

In this introduction the basic concepts of digital imaging and image processing will be discussed. We will address the formation and representation of digital images, the type of operations we can perform and what the goals of these operations can be.

Organized by:
IEEE Student Branch Ei
Technische Universiteit
Department of Electrical Engineering
Den Dolech 2, EH 6.29
5612 AZ Eindhoven, The Netherlands
Tel: +31 (0) 40 2473433
Fax: +31 (0) 40 2473661
E-mail: IEEESB@tue.nl